PE&RS

December 2024 Volume 90, Number 12

The official journal for imaging and geospatial information science and technology

PHOTOGRAMMETRIC ENGINEERING & REMOTE SENSING

asprs THE IMAGING & GEOSPATIAL INFORMATION SOCIETY

ASPRS MEMBERSHIP

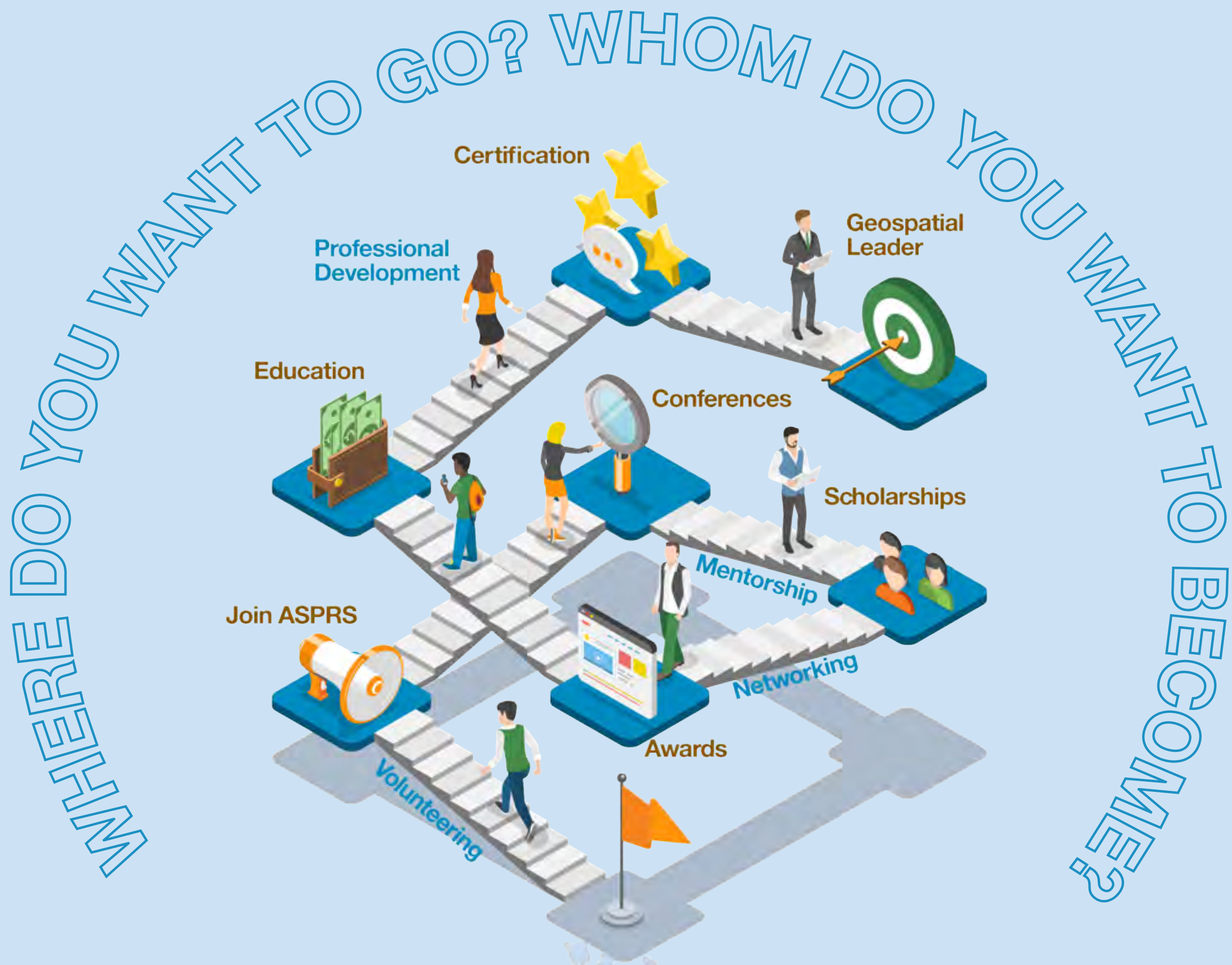

Joining ASPRS is a great way to boost your resume and learn valuable life lessons

WHY GET INVOLVED WITH ASPRS?

- Develop leadership skills
- Experience working on a team
- Gain valuable soft skills
- Network
- Learn about yourself
- Have fun!

Scholarships

The many ASPRS scholarships are only available to student members

Certification

The ASPRS certification program for mapping scientists, photogrammetrists and technologists is the only fully Accredited certification program in the geospatial sciences

Continuing Education

Earn professional development hours and CEUs by attending workshops at our conferences and on-line as well as our monthly on-line geobytes series

PE&RS

Our monthly journal, is packed with informative and timely articles designed to keep you abreast of current developments in your field. Now available in e-format.

Get Connected

facebook.com/ASPRS.org

linkedin.com/company/asprs/about/

twitter.com/ASPRSorg

youtube.com/user/ASPRS

Image and text courtesy the ASPRS Florida Region

asprs FLORIDA REGION THE IMAGING & GEOSPATIAL INFORMATION SOCIETY

To have your press release published in *PE&RS*, contact Rae Kelley, rkelley@asprs.org.

INDUSTRYNEWS

ANNOUNCEMENTS

Geospatial Leaders in the U.S. Assign New Grades on the Nation's Spatial Data Infrastructure

The Coalition of Geospatial Organizations (COGO) is pleased to release its third Assessment from its ongoing review of the U.S. National Spatial Data Infrastructure (NSDI). This Assessment serves as a periodic evaluation of the condition of the nation's geospatial data infrastructure, which, like other forms of public works, is essential for our economy, health, safety, and activities of daily life.

This 2024 report leveraged the expertise from teams of subject matter experts from the public and private sectors with knowledge in each of the eight national Framework data themes: addresses, cadastral, elevation, geodetic control, governmental units, hydrography, orthoimagery, and transportation. Each team assessed the developments and advances within their respective themes since the 2018 Report Card and engaged with the Federal Geographic Data Committee for guidance and feedback as they determined new individual scores. The cumulative score for the NSDI data themes is B, indicating an improvement since the last evaluation. The NSDI as a whole also received its own grade, a C-, reflecting a lack of significant improvement over the last six years relative to the other aspects of the NSDI, which include technologies, policies, organizations, and people. The NSDI is intended to be an interconnected system that supports the nation's broad and significant need for spatial data.

Shelby Johnson, State Geographic Information Officer of Arkansas and a former COGO Chair, notes, "Our country relies on these systems and data every day. It helps us in so many ways. It makes us more efficient and prosperous. The challenge is maintaining the themes where we are doing well, then finding the will and the means to improve on the rest. Our hope is this Assessment will assist government agencies in collaboratively completing and maintaining the NSDI. We still have a long way to go."

The organizations comprising COGO are leaders in the geospatial field. Collectively they represent over 170,000 individual members and speak with a unified voice on national geospatial policy initiatives. COGO's previous NSDI Report Cards were a wake-up call for Congress to take action in this important area, and contributed in part to the Geospatial Data Act of 2018. This new assessment follows the same arc and is intended to encourage continued and critical improvements in our national geospatial infrastructure.

The full 2024 Report Card on the U.S. National Spatial Data Infrastructure and its Executive Summary can be found at the COGO website.

- American Association of Geographers (AAG)
- American Association for Geodetic Surveying (AAGS)
- American Society of Civil Engineers (ASCE)
- American Society for Photogrammetry and Remote Sensing (ASPRS)
- Cartography and Geographic Information Society (CaGIS)
- Geographic Information Systems Certification Institute (GISCI)
- International Association of Assessing Officers (IAAO)
- Management Association for Private Photogrammetric Surveyors (MAPPS)
- National Society of Professional Surveyors (NSPS)
- National States Geographic Information Council (NSGIC)
- United States Geospatial Intelligence Foundation (USGIF)
- University Consortium for Geographic Information Science (UCGIS)
- Urban and Regional Information Systems Association (URISA)

The GIS Certification Institute (GISCI), www. gisci.org is thrilled to announce **Pickett and Associates**, LLC (Pickett), www.pickettusa.com, a multidisciplinary engineering firm specializing in transmission line engineering, surveying, and GIS & geospatial services, as the latest organization to join its Endorsing Employer Designation Program.

Pickett has extensive experience providing GIS services for various utility, municipal, and commercial clients, spanning spatial analysis, data visualization, asset management, and geospatial technology integration. Pickett's GIS team, comprised of eight GISPs, leverages a variety of tools and in-house expertise to support informed decision-making, facilitate communication, and ensure efficient project delivery. With the designation as a GISCI Endorsing Employer, Pickett reaffirms its dedication to deliver effective and quality GIS services across their range of clients.

"Pickett is honored to be recognized as a GISCI Endorsing Employer and believes this is an emblem of our commitment to GIS and geospatial excellence," says Director of GIS and Innovation Michael Jensen. "We're always looking for top talent to continue to deliver best in class service, and we are excited for the recruitment opportunities and national recognition this will bring," Jensen continues.

The GISCI Endorsing Employer Designation Program was established to enhance the value of the GISP® certification, promoting its adoption across the geospatial profession. This designation is available to organizations in the public, private, and commercial sectors dedicated to upholding professional standards in GIS and fostering the continuous growth of their teams' expertise.

New Landsat Science Team Request for Proposal Now Open. The **U.S. Geological Survey (USGS)** and NASA have officially opened a Request for Proposal (RFP) for the 2025-2029 Landsat Science Team. This team will play a pivotal role in shaping the future of the Landsat program, supporting the ongoing operations of Landsat 8 and 9 while contributing to the development of Landsat Next, which is set to launch in 2030/2031.

Interested applicants should submit their proposal by December 17, 2024. For more information and submission guidelines, visit www.usgs.gov/landsat-missions/news/new-landsat-science-team-request-proposal-now-open.

NOAA, Coast Guard, USACE, and **Woolpert**, www.woolpert.com, Collaborate to Reopen Navigation Channels in Tampa Bay. The teams quickly coordinated the collection, processing, and delivery of bathymetric data to ensure navigation channels were clear and could reopen after Hurricane Milton.

The National Oceanic and Atmospheric Administration's Office of Coast Survey, the U.S. Coast Guard, the U.S. Army Corps of Engineers, and Woolpert mobilized Friday, October 11, 2024, to conduct emergency response surveys of federal navigation channels to support the reopening of Port Tampa Bay following Hurricane Milton.

The Woolpert survey team worked from Friday evening to Saturday morning to survey and map a wide swath of the Tampa Bay entrance channel up to the Sunshine Skyway Bridge. This enabled the Tampa Bay entrance channel to reopen at noon ET Saturday.

Port Tampa Bay is Florida's largest port, with about 70 miles of channels, and ranks 12th in the U.S. by trade volume. It is responsible for 7 billion gallons of fuel, or nearly half the fuel the state relies on daily, for residents, businesses, military bases, and airports across the state each year.

For a major hurricane to make landfall Wednesday, and the state's largest port to reopen Saturday, the USCG has made clear their appreciation and commendation to the NOAA response and the recognition of each individual member of the Navigation Response Teams and Woolpert survey team. NOAA also commended the collaboration and quick work of the team.

"NOAA appreciates the quick action of our contract partners to assist in these emergency response efforts," said Rear Adm. Ben Evans, director of NOAA's Office of Coast Survey. "These relationships and mechanisms allow NOAA to accelerate the resumption of maritime commerce in the Tampa Bay area."

NOAA Navigation Manager Tim Osborn echoed Evans. "The Woolpert team worked through the night in coordination with NOAA, USCG, and USACE to provide critical data to decision-makers in regard to channel conditions," Osborn said. "Through these efforts, the port was able to reopen the inbound corridor of the Tampa Bay entrance channel at noon on Saturday, and fuel barges were able to continue moving critical resources through the channels."

Woolpert Vice President and Maritime Market Director Dave Neff said that this collaboration illustrates the shared focus of these teams and the value they place on public safety and disaster recovery.

"When a storm of this magnitude impacts a commerce-rich environment like Tampa, there is a high likelihood that it will drag debris into the navigation channels, which are important economic lifelines to these regions," Neff said. "In addition to clearing the way for emergency supplies, this work provides a critical service to quickly reopen shipping and commerce that equates to millions of dollars for the local economy."

Xtensible Solutions Joins SAM! **SAM**, www.sam.biz, the Managed Geospatial Services™ Company for utilities, transportation, and infrastructure-focused clients, announced its acquisition of Xtensible Solutions, an innovative leader of semantic-based integration and information data management solutions to the utility industry worldwide. Semantic integration permits the sharing and interoperability of data and systems across different platforms, applications, and stakeholders so utilities can more easily apply advanced analytics, machine learning, and automation across their organizational data streams and operational footprint to improve decision-making. This acquisition extends SAM's consulting capabilities, enriches its technology offerings, and brings a connected and integrated Managed Geospatial Service™ portfolio to the utility industry.

Xtensible Solutions has been at the forefront of standards-based consulting for the utility industry for over two decades. It is renowned for its Model-Driven Integration (MDi) and Model-Driven, Data-Driven Integration (MD3i) software architectural frameworks. SAM is poised to leverage these innovative solutions to deliver greater value to its clients.

The acquisition of Xtensible will help us accelerate our expansion and enhance our expertise in data analytics and system integration while, strengthening our reputation as a trusted partner for clients seeking comprehensive Managed Geospatial Services™

"Xtensible has been instrumental in developing industry standards and providing innovative system integration and data management solutions. Our commitment to excellence and innovation in this space is solidified by joining SAM. We're excited for future, groundbreaking work," said Xtensible's President, Greg Robinson.

Upon acquiring Xtensible Solutions, SAM becomes the exclusive commercial partner to the North American utility industry for Affirma, a subscription-based single solution for enterprise semantic modeling and metadata management.

PE&RS
PHOTOGRAMMETRIC ENGINEERING & REMOTE SENSING
The official journal for imaging and geospatial information science and technology
December 2024 Volume 90 Number 12

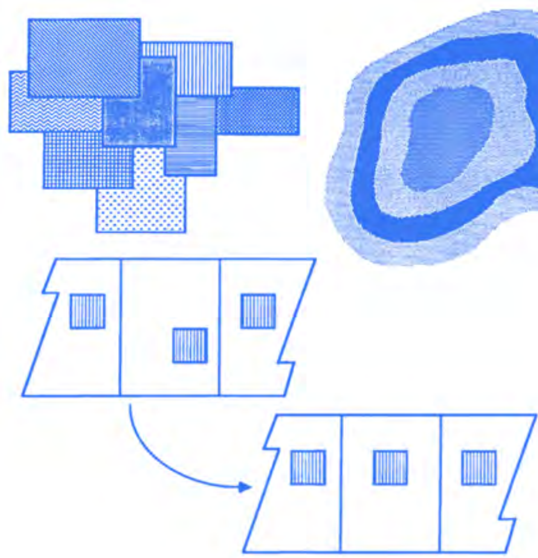

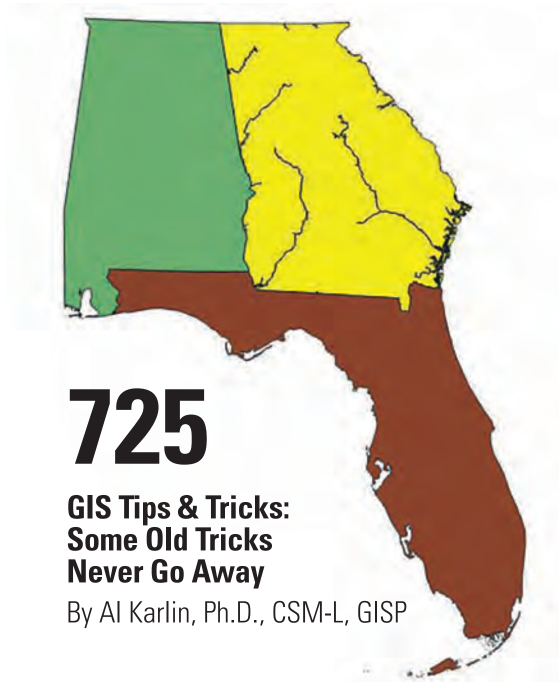

HIGHLIGHT ARTICLE

COLUMNS

ANNOUNCEMENTS

DEPARTMENTS

See the Cover Description on Page 716

COVER DESCRIPTION

Pine Island Glacier, along with neighboring Thwaites Glacier, garners attention as one of the main pathways for ice flowing from the West Antarctic Ice Sheet to the Amundsen Sea. It has also been one of the fastest-retreating glaciers in Antarctica, and ice on its seaward edge regularly fractures and calves off icebergs—some large enough to be named. In October 2024, however, it was the atmosphere above the ice that stole the show with a display of blowing snow and "sea smoke."

Satellites are usually unable to capture clear images of these near-surface atmospheric phenomena because clouds tend to be present when they occur, said Christopher Shuman, a University of Maryland, Baltimore County, glaciologist based at NASA's Goddard Space Flight Center. This was not the case on October 10, 2024, when the OLI (Operational Land Imager) on Landsat 8 acquired this image. It illustrates "the power of the wind," in this case racing out to the edges of the continent from the cold interior, he said.

In this image, "sea smoke" appears to form at the very edge of the glacier's terminus, as well as over open water along its northern edge, Shuman said. This phenomenon occurs because of a stark difference in temperature between the ice and the water surrounding it. Here, winds are pushing water and sea ice away from the ice front, driving an upwelling of relatively warm water to replace it from below. Sea smoke forms when cold air moves across the warmer water, and when the cold air cannot hold the water vapor it encounters, it quickly condenses into small ice crystals.

The wind is also kicking up snow from the surface of the adjacent West Antarctic Ice Sheet, accounting for more streams of white across the scene. The origins of some of these plumes are particularly visible near the jumbled shear zone along the south side of Pine Island Glacier, shown in the detailed image on the Landsat website at https://landsat.visibleearth.nasa.gov/view.php?id=153509.

The two phenomena seen here are a testament to the strength of springtime winds over Antarctica. "One really shouldn't be surprised to see winds coming out of the interior with all the cold winter air that's been isolated there for months," Shuman said. The ice sheet's mass of cold air sets the stage for katabatic winds, which develop when that relatively cold, dense air flows downslope and rushes out toward the coast.

In parts of Antarctica, including the area around Pine Island Glacier, strong winds can transport and sublimate enough snow to have significant influence on the surface mass balance of polar ice sheets. However, the extent to which blowing snow contributes to the loss of surface mass is not fully understood due to the difficulty of collecting ground-based data at these sites and gaps in satellite observations.

References

American Museum of Natural History Katabatic Winds. Accessed October 25, 2024.

Gerber, F. et al. (2023) CRYOWRF—Model Evaluation and the Effect of Blowing Snow on the Antarctic Surface Mass Balance. *Journal of Geophysical Research: Atmospheres*, 128(12), e2022JD037744.

NASA Earth Observatory (2019, April 9) The Wide View of a Shrinking Glacier: Retreat at Pine Island. Accessed October 25, 2024.

NASA Earth Observatory (2020, February 14) Pine Island Glacier's Newest Iceberg. Accessed October 25, 2024.

NASA Earth Observatory images by Wanmei Liang, using Landsat data from the U.S. Geological Survey. Story by Lindsey Doermann.

asprs
THE IMAGING & GEOSPATIAL INFORMATION SOCIETY

PHOTOGRAMMETRIC ENGINEERING & REMOTE SENSING

JOURNAL STAFF

Publisher ASPRS
Editor-In-Chief Alper Yilmaz
Director of Publications Rae Kelley
Electronic Publications Manager/Graphic Artist
Matthew Austin

Photogrammetric Engineering & Remote Sensing is the official journal of the American Society for Photogrammetry and Remote Sensing. It is devoted to the exchange of ideas and information about the applications of photogrammetry, remote sensing, and geographic information systems. The technical activities of the Society are conducted through the following Technical Divisions: Geographic Information Systems, Photogrammetric Applications, Lidar, Primary Data Acquisition, Professional Practice, Remote Sensing Applications, and Unmanned Autonomous Systems. Additional information on the functioning of the Technical Divisions and the Society can be found in the Yearbook issue of *PE&RS*.

All written correspondence should be directed to the American Society for Photogrammetry and Remote Sensing, PO Box 14713, Baton Rouge, LA 70898, including general inquiries, memberships, subscriptions, business and editorial matters, changes in address, manuscripts for publication, advertising, back issues, and publications. The telephone number of the Society Headquarters is 225-408-4747; the fax number is 225-408-4422; web address is www.asprs.org.

PE&RS. *PE&RS* (ISSN0099-1112) is published monthly by the American Society for Photogrammetry and Remote Sensing, 8550 United Plaza Blvd, Suite 1001, Baton Rouge, Louisiana 70809 . Periodicals postage paid at Bethesda, Maryland and at additional mailing offices.

SUBSCRIPTION. *PE&RS* is available as an e-Subscription (single-site and multi-site licenses) and an e-Subscription with print add-on (single-site license only). PE&RS subscriptions are on a calendar-year, beginning in January and ending in December.

The rate for a single-site e-Subscription for the USA/Non-USA is $1040 USD, for Canadian* is $1092 USD.

The rate for a multi-site e-Subscription for the USA/Non-USA is $1040 USD plus $250 USD for each additional license, for Canadian* is $1092 USD plus $263 for each additional license.

The rate for e-Subscription with print add-on for the USA is $1546 USD, for Canadian* is $1637 USD, and for Non-USA is $1596 USD.

*Note: Subscription prices for Canada includes 5% of the total amount for Canada's Goods and Services Tax (GST #135123065). **PLEASE NOTE: All Subscription Agencies receive a 20.00 USD discount.**

POSTMASTER. Send address changes to PE&RS, ASPRS, PO Box 14713, Baton Rouge, LA 70898. CDN CPM #(40020812).

MEMBERSHIP. Membership is open to any person actively engaged in the practice of photogrammetry, photointerpretation, remote sensing and geographic information systems; or who by means of education or profession is interested in the application or development of these arts and sciences. Membership is for one year, with renewal based on the anniversary date of the month joined. Membership Dues include a 12-month electronic subscription to *PE&RS*. Annual Individual Membership dues are $175.00 USD and Student Membership dues are $50.00 USD. A tax of 5% for Canada's Goods and Service Tax (GST #135123065) is applied to all members residing in Canada.

Case for a Qualitative Geospatial Revolution

Jeffrey M. Young

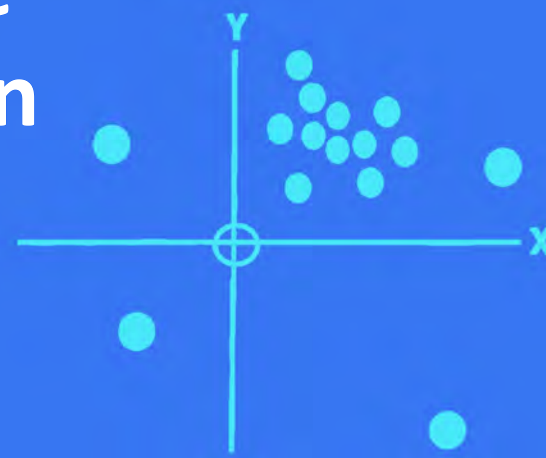

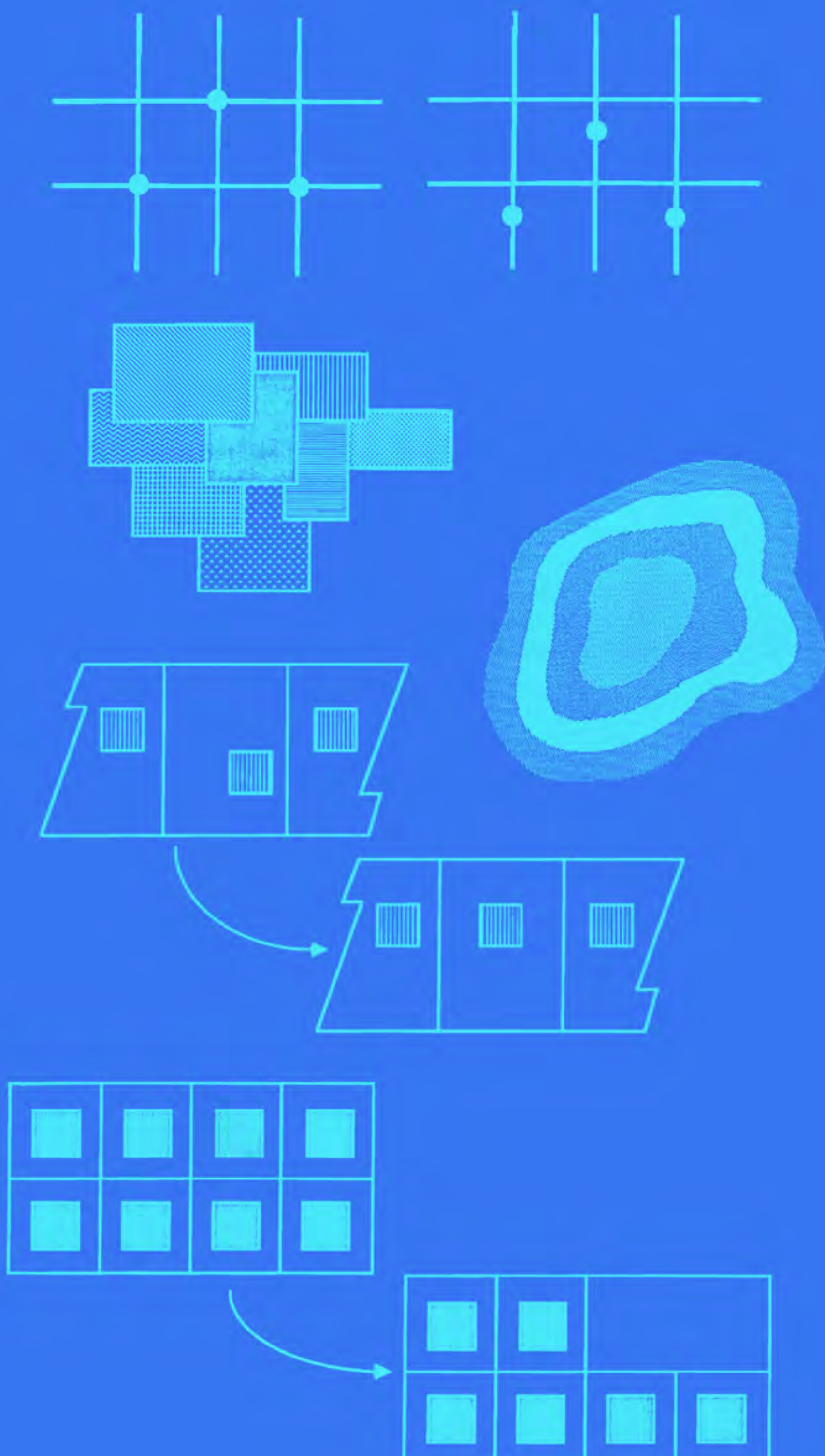

Author's Preface

ASPRS is a thought leadership professional society in everything geospatial including measures of positional accuracy. We serve the needs of our individual and corporate members by being persistent innovators and advocates of the diligent and ethical application of geospatial technologies. As geospatial technologies expand into almost all facets of human endeavor, there is a need for standards, professional certifications, procurement guidelines, exchanges of best practices and innovations achieved through regular interactions and agreements of peer professionals. The Imaging & Geospatial Information Society, ASPRS, has been, and is, a world class foundry for global geospatial innovation. Precise and accurate definition of position, representative descriptions of locations, and robust characterizations of places are at the core of our skill set. Perpetual geospatial innovation and persuasive advocacy imperatives serve as ASPRS' heartbeat and truly differentiate ASPRS from other geospatial member organizations. We collect and manage massive data sets and comprehensively model landscapes to address local to global natural hazards and human-induced problems facing our Earth and its inhabitants. As a professional society we shed passé methods and techniques with keen eyes on the horizon for continued refinement of current best practices and early adoption of geospatial technological innovations. This brief commentary is intended to acknowledge other geospatial quality measures beyond accuracy that we face in the real world every day.

Historic Perspective on Soil Allocation, Measurement and Geospatial Data Quality

Since ASPRS has recently adopted new positional accuracy guidelines, I feel some discussions of quality is merited. To understand quality is to understand error. Let's leave room for professional judgment, interpretation, and critical examination of data gathered. Mapping professionals, and for that matter, national governments, have been concerned with spatial quality measures for centuries, if not millennia. Interestingly, Herodotus (c. 484 to c. 425 BC.) the noted Greek historian and geographer, documented a very early, if not the first, division of "soil" and tax assessment in the form of a rent paid year by year. Lots were divided into squares and values were adjusted if flooding or significant erosion occurred. The Egyptian King Sesostris, who ruled almost 2000 years before Christ, is credited by Herodotus with instituting this land tenure system, a systematic use of land measurement and the first application of geometry (surveying) for subdividing "soil" (land). In the case of the United States, our founding planters and surveyors like George Washington and Thomas Jefferson were keen on accurate land surveys for both political and personal reasons. Both lived full lives and enjoyed comfortable living conditions, no doubt, enabled by enslaved African Americans. Washington and Jefferson resided on relatively expansive estates as the result of their personal achievements and economic status tied in no small part to their successful land management. However, each dealt with geospatial error and the need for a standard framework for measuring the earth and resulting economically motivated land transactions. In Washington's case, in 1791 he called upon Congress to establish a scientific basis for measures and weights (Linklater, 2002). Jefferson was very much a measures and weights reformer, so much so that he became a metric advocate and supported the "Latitude of Paris" in 1791 (See Figures 1 and 2 below … the residences of Washington and Jefferson).

Ever-present Error

Even with all the recent advances in Geospatial Information science, surveying, and engineering, error remains ever present, particularly macro-geospatial errors related to land settlement in flood-prone areas, earthquake zones, exposure of the built environment to extreme meteorological and climatic occurrences; wasteful use and inefficient distribution of water; environmental contamination, and generally our inability to inhabit safe geographies. Preston James also characterizes the persistence of error in geographic research (James, 1966) which undoubtedly introduces error and bias into research conclusions. James does offer a set of conditions where avoidable errors in geographic research can occur:

- Inexact use of words
- Uncritical use of statistical data
- Failure to indicate the reliability of data
- Failure to distinguish between different kinds of spatial distributions

The history of geospatial error and error reduction over time lends itself to many worthy research topics. Immanuel Kant, who lived from 1724 to 1804 (the same time period as Washington and Jefferson), was a regular lecturer on Physical Geography and wrote extensively about the "universal principle of right" and the linked notion of "What is Truth." Kant wrote about the cognitive faculties of understanding, judgment, and reason. In his *Critique of Judgment*, Kant further described judgment as a middle term between understanding and reason (Kant, 1790). Perhaps with all our technological advances to measure and monitor the earth we have lost touch with applying judgment through achieving understanding of the world around us and reasoning accurate models to describe the current state and what might happen in the future … sea level changes, droughts, slope failures, high volume precipitation events … and on and on.

Figure 1. George Washington's Mount Vernon (photo by J. M. Young).

Figure 2. Thomas Jefferson's Monticello (photo by J. M. Young).

A Quality Model for the Qualitative Geospatial Revolution

Early in my career, under an EPA Research contract assignment, I was directed to follow a laboratory-oriented QA methodology (see Young et al, 1985). After some intellectual struggle, I adopted the following Quality Model. The Model has survived the test of time and remains quite relevant today (See Figures 3, 4, 5, and 6 below):

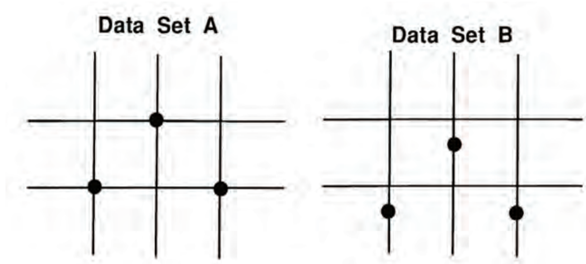

Figure 3. Precision – Agreement between data sets, methods, and or technologies.

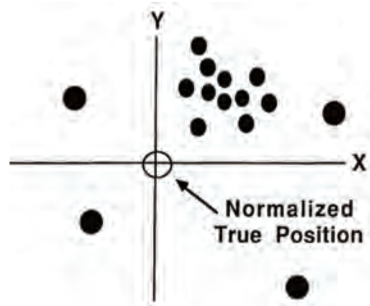

Figure 4. Accuracy – Conformity to a correct value or set of values. Also, Bias can be detected.

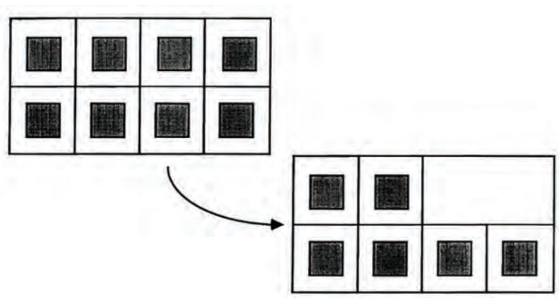

Figure 5. Completeness -– Measure of the transformation and/or capture omissions of a set of points, lines, or areas.

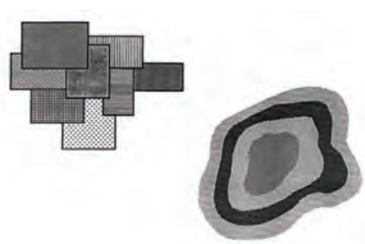

Figure 6. Representativeness -– measure of a subset of data which is statistically representative of an area, feature, or condition.

- Comparability – Measure of factual, temporal, positional, or areal sampling interval agreement.

Error Diagnosis encompasses consideration of both systematic and random error types and bias, including the following (See Figures 7, 8, 9, and 10 below).

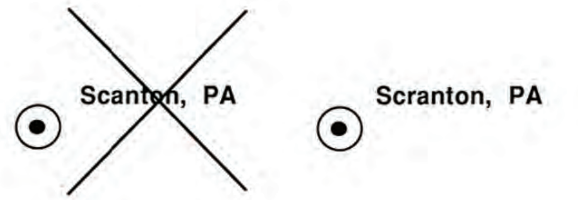

Figure 7. Factual Error.

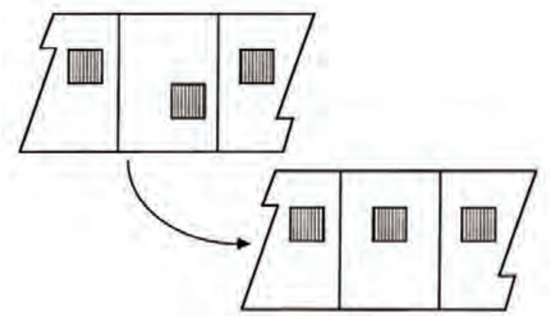

Figure 8. Positional Error.

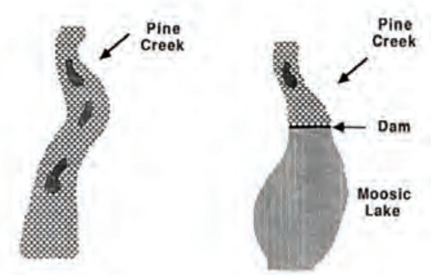

Figure 9. Temporal Error.

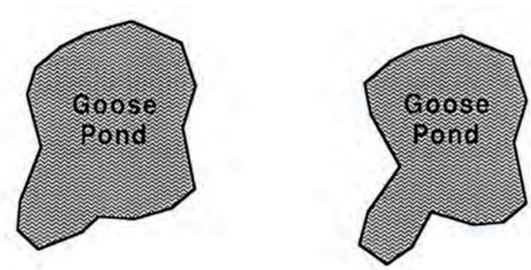

Figure 10. Areal Error.

- Compound Error – a combination of any of the errors described above
- Conceptual Error – related to generalization of position, location, or subjective descriptions of place

Remember that according to the Romans, one-foot equals 16 fingers, so why are we all so confused (Linklater, 2002)?

Indeed, it is time for a Qualitative Geospatial Revolution. As always, I welcome your questions and comments.

Jeffrey M. Young
Managing Director
Geographic Imperatives LLC-- A Colorado Company –ASPRS Sustaining Member
5793 S. Hannibal Way
Centennial, CO 80015
Cell 303-815-2254
Jeffreymyoung@msn.com

References

Herodotus. *The History of Herodotus*. Translated by George Rawlinson, Encyclopaedia Britannica, 1952.

James, P., 1967. “On the Origin and Persistence of Error in Geography,” *Annals* 57: 1–24. Washington DC: AAG Published Honorary Presidential Address in 1966.

Kant, Immanuel. *The Critique of Judgement*. Translated by James Creed Meredith, Encyclopaedia Britannica, 1952.

Linklater, A., 2022. *Measuring America*, New York: Walker.

Young, J., R. Dulaney, S. Wright, and J. Scholl, 1985. *Field Test and Evaluation of a Method for Estimating Time-Weighted Urban Population Distributions*. Las Vegas: United States Environmental Protection Agency.

Brief Biographical Sketch

Jeffrey M. Young has over 30 years of sales, program, project and channel management experience, including more than 25 years in senior management of geospatial corporations in various capacities. Mr. Young’s educational background is as follows: Master of Arts, Geography—specializing in Land Use Analysis and Environmental Hazards, (National Science Foundation supported); Arizona State University, Bachelor of Science, Geography, cum laude; Lock Haven State College, Pennsylvania. Young was an ASPRS-RMR President and was a member of the ASPRS Executive Committee for several years. Currently Young is a Managing Account Executive with 1Spatial USA.

RONGJUN QIN

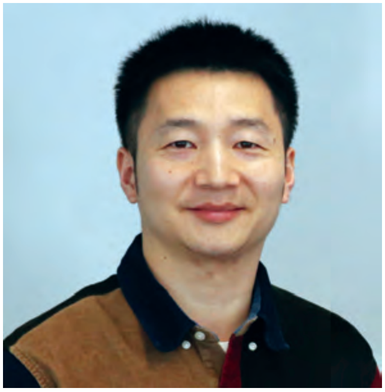

Rongjun Qin is a tenured Associate Professor of Photogrammetry and Remote Sensing (P&RS) at The Ohio State University (OSU). Dr. Qin earned a Ph.D. in Photogrammetry and Remote Sensing from ETH Zurich in 2015. He also spent time as a visiting scientist in the Department of Photogrammetry and Image Analysis at the German Aerospace Center. His research interests include both the theoretical foundations and practical applications of photogrammetry, remote sensing, computer vision, and geospatial sciences.

At OSU, he leads a research group of over 15 members, including research scientists, Ph.D. students, Master's students, and undergraduates. Their work spans diverse subfields within P&RS and computer vision, including satellite photogrammetry, UAS and mobile mapping, image-based localization, semantic segmentation, land-cover change analysis, 3D modeling, scene representation, structure from motion, and object detection.

What motivated you to become the Editor-in-Chief of *PE&RS*?

PE&RS has been a renowned journal since 1934, and has published many influential papers that are transformative and impactful even till today. As a researcher specializing in Photogrammetry and Remote Sensing, serving for *PE&RS* not only offers a great opportunity for me to contribute to the geospatial community, but also allows me to advocate its unique values across different disciplines. In addition, *PE&RS* is a journal that is of significant personal value to me, because it published my first ISI-indexed research paper. The constructive comments I received from the journal board while in the process of publishing this research paper partly shaped my scientific rigor and career path going forward. I would like to continue this standard of value and ensure that *PE&RS* fosters the growth of young researchers.

What are your short- and long-term goals for *PE&RS*?

My short-term goal is to refocus the journal's scope by making sure it captures both what it has been famous for and what is currently needed in the field, make *PE&RS* more accessible to researchers, and expand its impact and visibility. In the long-term, make sure *PE&RS* is a highly recognized brand for the geospatial research community in providing high-quality scientific and applied research articles, and guiding researchers and professionals in their research and industry practice.

What are your plans to enhance the value of *PE&RS* to the members, subscribers, and the geospatial community?

PE&RS has been a crucial resource fueling the geospatial community with solid foundation of knowledge. Given the highly competitive publication landscape today, *PE&RS* needs to stand out by leveraging its unique niche in its technical competency and application relevancy in geospatial science and engineering. My immediate plan is to establish a supporting editorial board and a series of courses of action, to make sure we select quality articles that are of the highest value to the community; enhance the reach of the content to readers both within this community and beyond; provide a smooth and rewarding submission experience; significantly reduce the manuscript processing time to allow for timely publication; and most importantly, support the readers with original and highly relevant content that is key to their success.

How do you plan to keep *PE&RS* relevant and exciting to readers?

Under the leadership of Dr. Yilmaz, *PE&RS* has been very relevant to the geospatial community. To continue this momentum, my plan is to encourage original research articles that are not only relevant to geospatial science and engineering, but also those that hold practical implications for relevant applications. I would also advocate for code and dataset sharing to allow readers to reproduce results and transfer these into their own practice.

ASPRS serves members in private industry, government and academia, how do you see *PE&RS* balancing the needs (some unique and some shared) of these three areas?

Photogrammetry and Remote Sensing by itself has an entire industry behind it. Therefore, research frontiers in this field are of core value for these three tightly connected sectors. I see *PE&RS* contributing to these sectors at different levels: research articles in *PE&RS* provide novel technical concepts and solutions to both classical and modern research problems in academia; the benchmarking of algorithms and approaches at the geospatial scale would provide practical implications to the industry and government sectors, which further provide guidance to geospatial standards. It could also benefit other fields that heavily rely on geospatial engineering and data science, such as ecology, urban science and forestry etc. Overall, *PE&RS* holds a valuable blend of knowledge that supports the needs of these sectors and many others.

NETROnline completes scanning of the challenging first half of the Edgar Tobin Aerial Survey film archive using GeoDyn's PromptScan

NETROnline, the producers of www.historicaerials.com, have successfully completed the scanning of the first half of the 1.2 million frames of the Tobin aerial film archive that dates back to the 1930's. This archive documents in detail the massive changes that took place across the southern United States during the first half of the 20th century.

University of New Orleans – Orthomosaic

The scanning was performed using GeoDyn's PromptScan M2 photogrammetric scanner. To date, NETROnline has scanned over 600,000 frames at a resolution of 13 microns, accurately capturing and preserving the full detail from this important archive.

The initial phase of the project has been the most challenging as it included many rolls of film from the 1930's that are primarily nitrate-based, as well as over thousand frames that had been previously cut out of the rolls and which required careful handling. Without scanning, these films would soon have deteriorated beyond scannable condition, risking a significant heritage loss.

"Digitizing these historical aerial images presented a significant challenge due to the age and diversity of the film types," said Brett Perry, President of NETR. "GeoDyn's PromptScan M2 scanner proved to be instrumental in meeting our stringent time and quality standards, delivering exceptional results with each scan." Said Jeff Teasley, Director of Historic Aerials at NETR.

Scanning represents just the initial phase of the process. To fully leverage scanned imagery, the imagery needs to be georeferenced and then accurately orthorectified. This was also a very significant challenge, as only a few of the original flight records existed and those that did, were sketches drawn by navigators often flying in wooden biplanes. Finding even the approximate location of the images across the southern US for a terrain that has changed beyond recognition, has been an immense challenge.

NETROnline is utilising GeoDyn's PromptGeoref service to enable georeferencing, aerial triangulation and accurate orthorectification of the imagery. These services include

Sanders Beach, Florida – Orthomosaic

extensive machine learning assisted searches to identify the possible image locations and then identification of the very few locations that had not changed. The processes then use ArcGIS based aerial triangulation and orthorectification procedures to create the seamless orthoimage mosaics that form temporal basemaps. These can be used to quickly identify what was where and when, determine change, and identify trends.

"We are proud to partner with NETROnline on this groundbreaking project," said Roger Thomas , GM at GeoDyn. "The successful completion of digitizing such a vast collection of historical aerial images underscores our commitment to providing cutting-edge solutions that meet the evolving needs of archival preservation."

For more information about GeoDyn's advanced scanning and georeferencing solutions, visit www.geodyn.com.

About GeoDyn
GeoDyn provides full-service aerial film conversion and rapidly digitizes films using advanced PromptScan photogrammetric aerial film scanners. Highly automated processes then accurately georeference the imagery to create temporal ortho image basemaps and oriented imagery that can be efficiently served, visually interpreted and analyzed in ArcGIS. As an Esri Gold Partner, GeoDyn assures full integration with ArcGIS.

About NETROnline
Historic Aerials by NETROnline (owned by NETR) is a comprehensive platform offering access to public records across the United States, specializing in property records, deeds, and mortgages. Beyond standard records, it features a unique repository of historical aerial imagery, enabling users to explore changes in landscapes and properties over time, making it a valuable resource for researchers, analysts and historians alike.

GeoDyn Technology
www.geodyn.com

GIS Tips & Tricks

By Al Karlin, Ph.D., CSM-L, GISP

Some Old Tricks Never Go Away

It is hard to believe that Microsoft Windows™ celebrated its 39th anniversary in November 2024. That first edition and the subsequent upgrades, along with all of the applications that followed the Windows™ "standard", changed the way we used personal/desktop computers by standardizing a several keystroke combinations, such as saving a file with <CTRL+S>, or removing a selected item with <CTRL+X>. While in previous columns I focused on GIS software-specific, specialized "keyboard shortcuts", for this column, I would like to revisit two Windows™ "standard" keyboard shortcuts, the copy <CTRL+C> and paste <CTRL+V> functions and how they operate in the GIS environment.

In most non-GIS Windows™ applications, using the Copy/Paste function requires, (1) selecting some object(s), such as a word (word processing), or group of cells (in a spreadsheet), or a picture object (in image editing), (2) placing those objects into the computer memory <CTRL+C>, and then (3) inserting those objects <CTRL+V> into some other place within the document or some other document. The workflow is much the same in a GIS environment; (1) you select features from one feature class/layer (a donor), (2) copy those features into memory, and then (3) paste the features into another feature class/layer (a recipient). The only GIS-centric constraint is that the recipient feature class must be of the same geometry as the donor feature class, i.e. point-to-point, line-to-line, polygon-to-polygon. With that as a constraint, below is the workflow for copying/pasting two polygon features into a third, different polygon feature class.

Important note: Copying raster cells from one raster to another raster requires an entirely different workflow; the subject of a future column.

Tip #1 — The ArcGIS Pro Copy/Paste Workflow

The ArcGIS Pro workflow follows the general workflow of selecting features, copying those features to memory, and pasting the features into a comparable feature class. In Figure 1, I have separate feature classes for each of the three state outlines, Florida, Georgia, and Alabama. My goal is to copy/paste the outlines for Georgia and Alabama into the Florida feature class to make a Southeast Region of States feature class containing the three state outlines. Of course, if you have a feature class containing several features that you want to copy into another feature class, you can select multiple features and copy them into the other feature class using the same workflow.

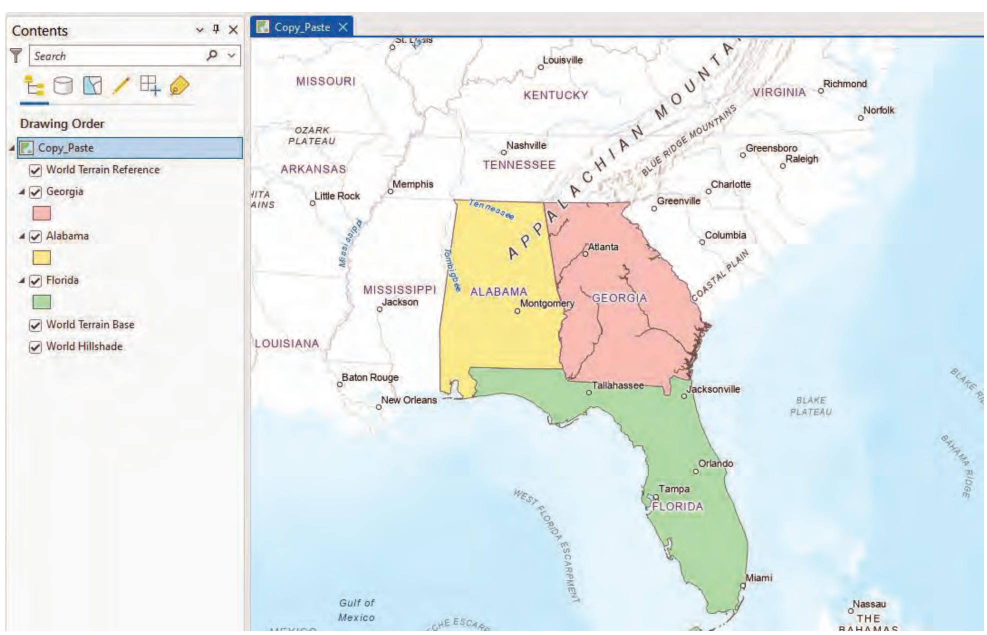

Figure 1. An ArcGIS Pro Map containing three feature classes.

Step 1

Select the State of Georgia Outline. Using the SELECT tool (I like using the Lasso tool), select the State of Georgia outline (Figure 2).

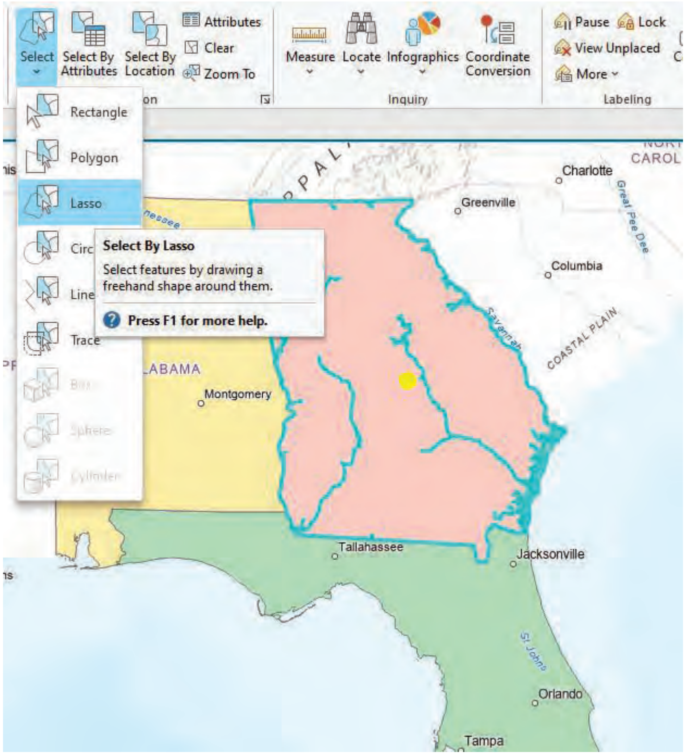

Figure 2. Selecting the feature(s) in the donor feature class; in this case, the outline of the State of Georgia.

Step 2

With the current map active (Map tab is blue) and the Georgia feature selected, use <CTRL+C> or in the Contents pane, select the Georgia feature class and right-click (Figure 3) to activate the options, and choose "Copy" (Figure 3), note that either method activates the "Paste" icon in the Clipboard group on the ribbon.

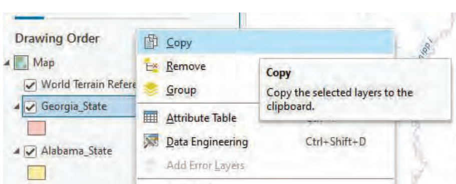

Figure 3. To copy the selected features into the computer memory use the key combination <CTRL+C> or select Copy on the feature class's option menu.

Or, as yet another alternative, select (highlight) the feature class in the Contents pane and select the COPY icon (Figure 4) in the Clipboard group. As with most GIS features, there are multiple options to accomplish the same task.

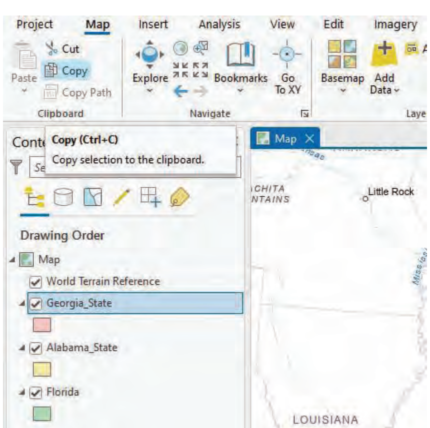

Figure 4. Using the ribbon to copy a feature class to memory.

Step 3

Use the down arrow under the Paste Icon on the Clipboard group (Figure 5) to activate the "Paste Special" option or use key combination <CTRL+ALT+V>.

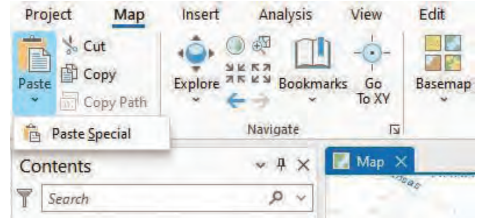

Figure 5. The "Paste Special" option on the Paste icon on the ribbon is used to open the Paste Special dialog box.

This will open the Paste Special dialog box (Figure 6). Change the "Paste into" option to **Layer** (Template is the default, and we never just accept the defaults without thinking!). In most cases, you will want to paste the copied features into a layer rather than a template.

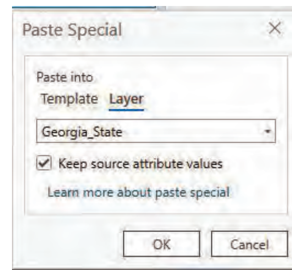

Figure 6. The Paste Special option dialog box. Note: the defaults "Template" and "Keep source attribute values" may need to be unchecked if the attributes of the donor and recipient feature classes are not identical.

Use the arrow to dropdown the available feature classes (layers), and scroll to the recipient feature class (layer) to copy the selected feature into (Figure 7).

If the selected feature's attribute from the donor feature class **do not match** the attributes in the recipient feature class, make certain to **uncheck** the "Keep source attribute values" box, again a default to change (Figure 8), and press "OK" to copy the feature class.

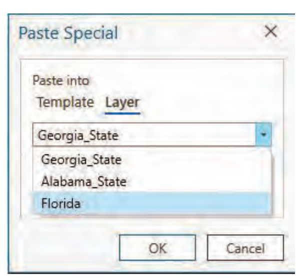

Figure 7. Available recipient feature classes (layers) for pasting the selected features.

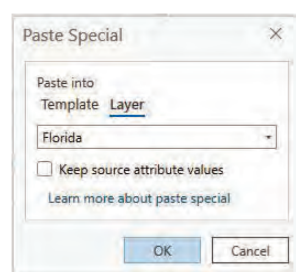

Figure 8. The Paste Special option dialog box. Note: the defaults "Template" and "Keep source attribute values" have been changed from their default values.

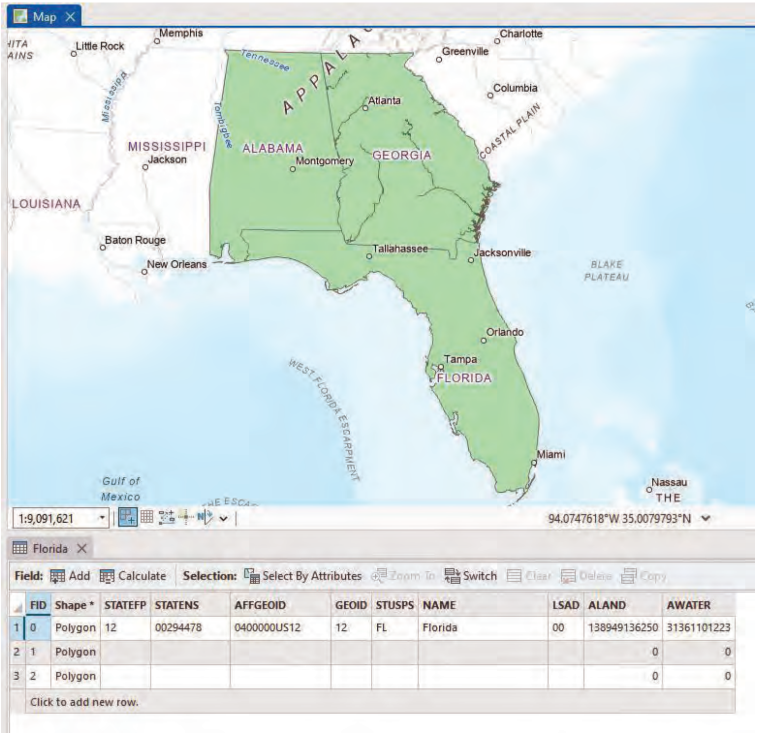

Figure 9. Map showing the three state outlines in a single feature class. Note that the attributes are blank for the features copied into the Florida feature class.

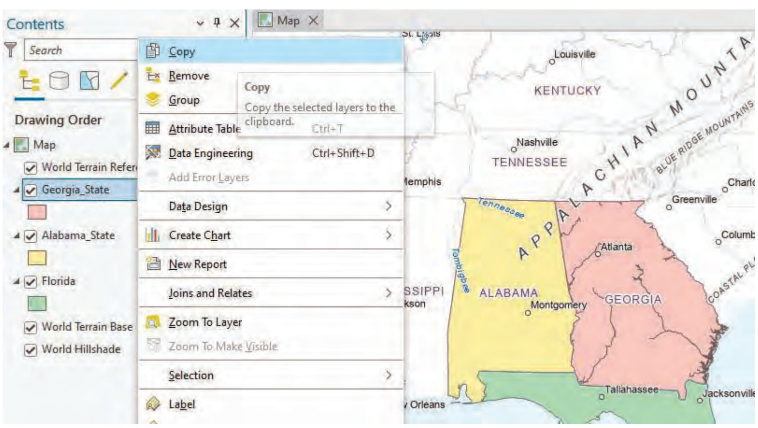

Figure 10. Selecting a feature class in the Contents pane for copying to computer memory.

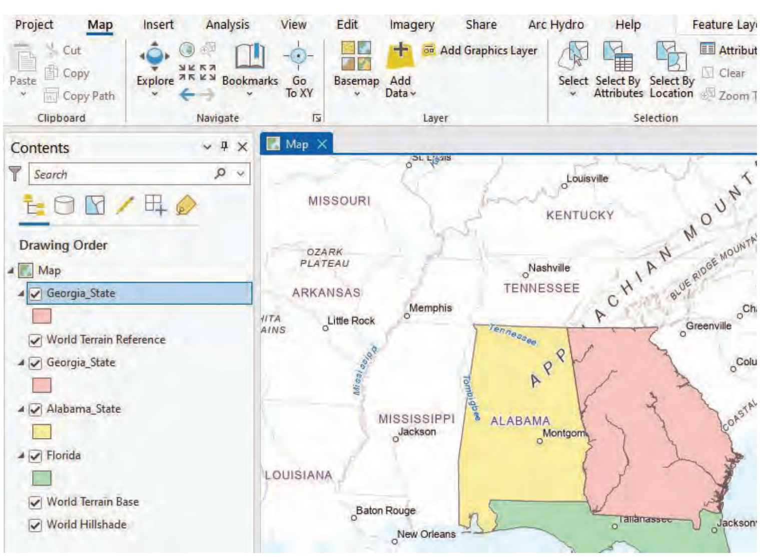

STEP 4

Repeat the workflow to add the Alabama State outline to the Florida feature class.

STEP 5

Finally, In the Edit group on the ribbon, Save the results in the Florida feature class. The end result is a single feature class with three records (Figure 9).

TIP #2

In ArcGIS Pro, you need to be VERY careful as the Copy/Paste can also function to add another copy of a feature class to the map. In this example, I used the Copy/Paste (not Paste Special) to add a copy of the Georgia outline to the map.

STEP 1

Select the feature class in the Contents pane, right click to activate the options, and select "Copy" (Figure 10).

STEP 2

Paste the feature class into the map (Figure 11). Note that the duplicate feature class has the symbology of the original feature class.

Figure 11. Pasting the feature class in computer memory into the Contents pane.

TIP #3 — The QGIS Workflow

The QGIS workflow, as the ArcGIS Pro workflow, will copy/paste between layers of similar geometry and requires first selecting the features from the donor layer, copying them to the clipboard (computer memory), then making the recipient layer editable, and pasting the features. Starting with the same three layers (Figure 12), the state outlines for Florida, Georgia and Alabama:

Step 1

Select (highlight) the Georgia layer in the Contents and use the Edit | Select all features tool to select the features (Figure 13).

Step 2

Copy the selected feature to the clipboard using the Copy tool on the Edit Menu (Figure 14).

Step 3

Highlight the recipient layer (Florida in this case), right-click and "Toggle Editing" to make the layer editable. Note the pencil in the layer's symbology in the menu (Figure 15).

Step 4

With the recipient layer highlighted (and the donor layer selected), use the Paste Features icon on the Edit menu to paste the features into the recipient layer (Figure 16).

When the features are pasted into the recipient layer, it will look like Figure 17.

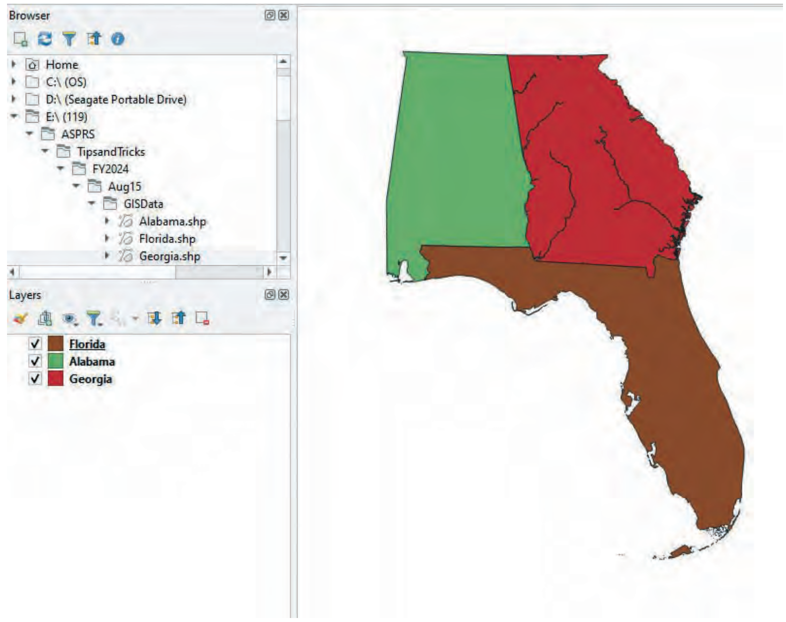

Figure 12. The QGIS map frame showing Florida, Alabama, and Georgia state outline feature classes.

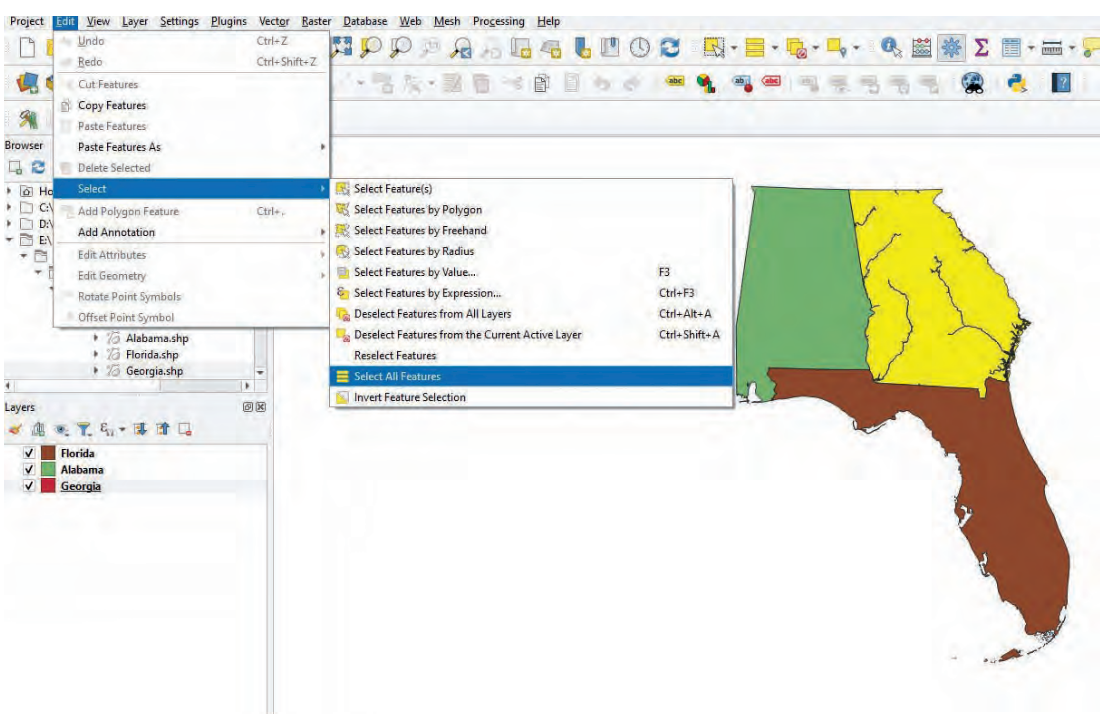

Figure 13. The Georgia state outline selected in the QGIS map

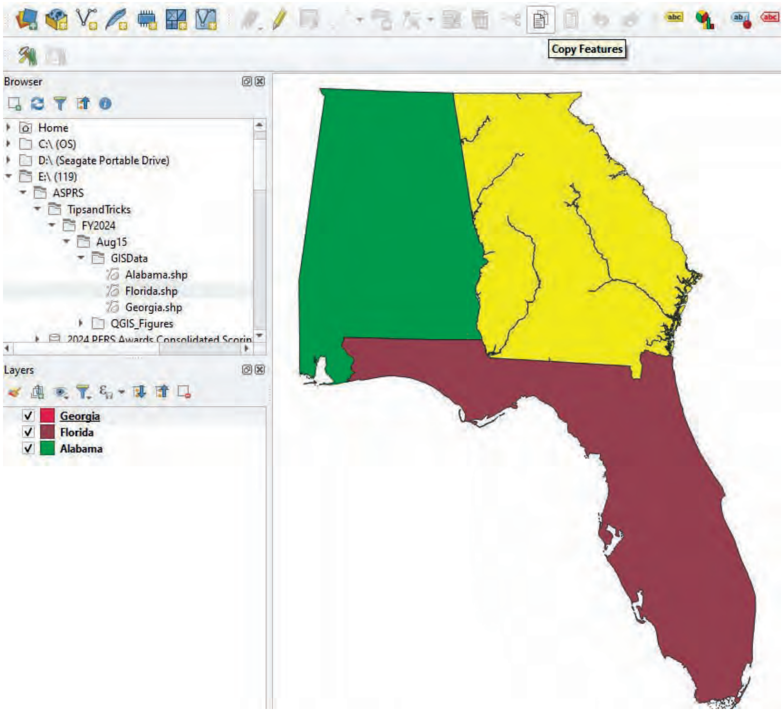

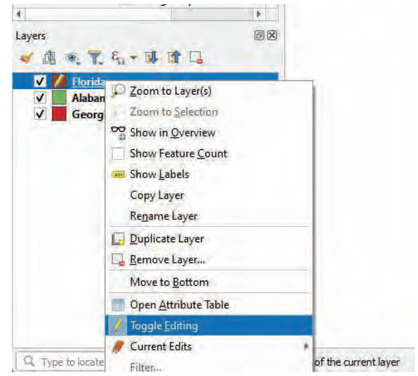

Figure 15. Setting the Recipient feature class to editable. Note that the symbol now contains a pencil to indicate that the feature class is editable.

Figure 14. The Copy Features icon on the QGIS Toolbar to copy the features to the Clipboard (computer memory).

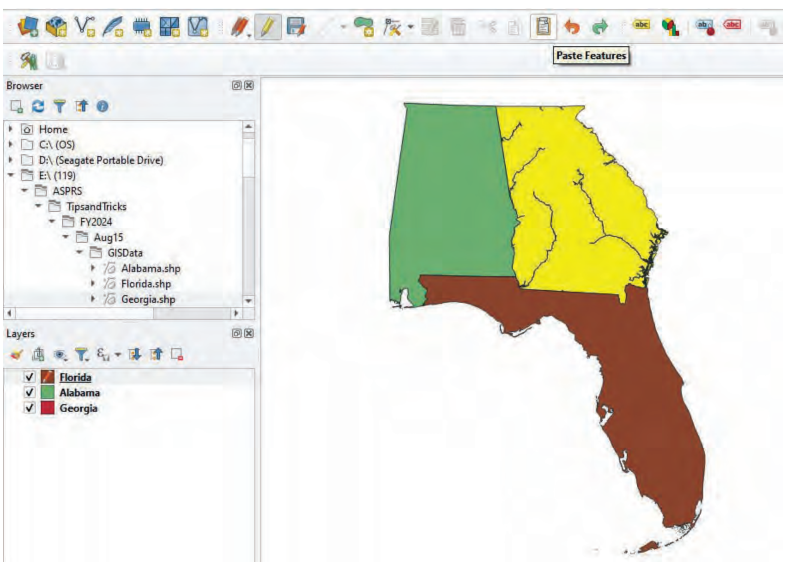

Figure 16. Using the Paste Features icon on the QGIS toolbar to paste the donor features into an editable recipient feature class.

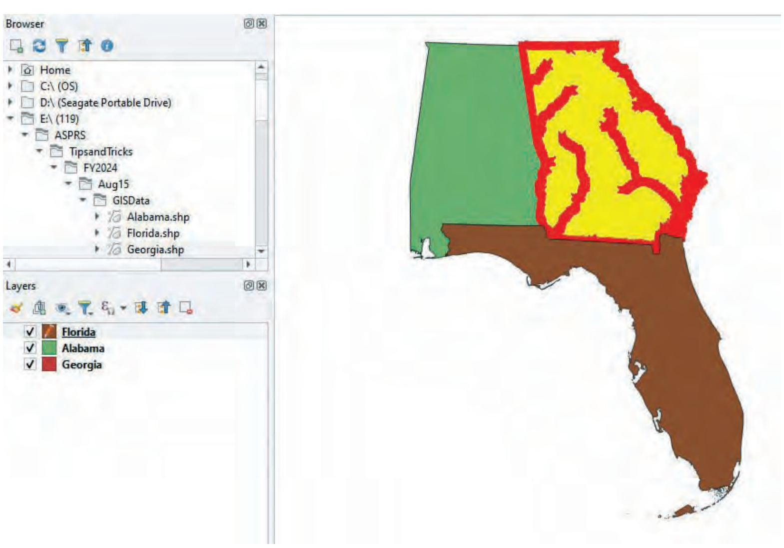

Figure 17. Map with features pasted into recipient feature class.

Step 5 — OPTIONAL

Deselect all the selected features by using the Edit | Select| Deselect Features from All Layers (or CTRL+ALT+A; Figure 18).

Step 6

Finish by right-clicking on the recipient layer and "Toggle Editing", this time to turn off the editing and save the edits (Figure 19).

You can also Copy/Paste symbology, annotation, and several other feature objects in both ArcGIS Pro and QGIS. Here are a few web-links for additional information:

https://pro.arcgis.com/en/pro-app/latest/help/editing/copy-and-paste-using-the-clipboard.htm.

https://gis.stackexchange.com/questions/20942/copy-a-geometry-from-one-feature-to-another-without-attributes.

Send your questions, comments, and tips to GISTT@ASPRS.org.

Al Karlin, Ph.D., CMS-L, GISP is with Dewberry's Geospatial and Technology Services group in Tampa, FL. As a senior geospatial scientist, Al works with all aspects of lidar, remote sensing, photogrammetry, and GIS-related projects.

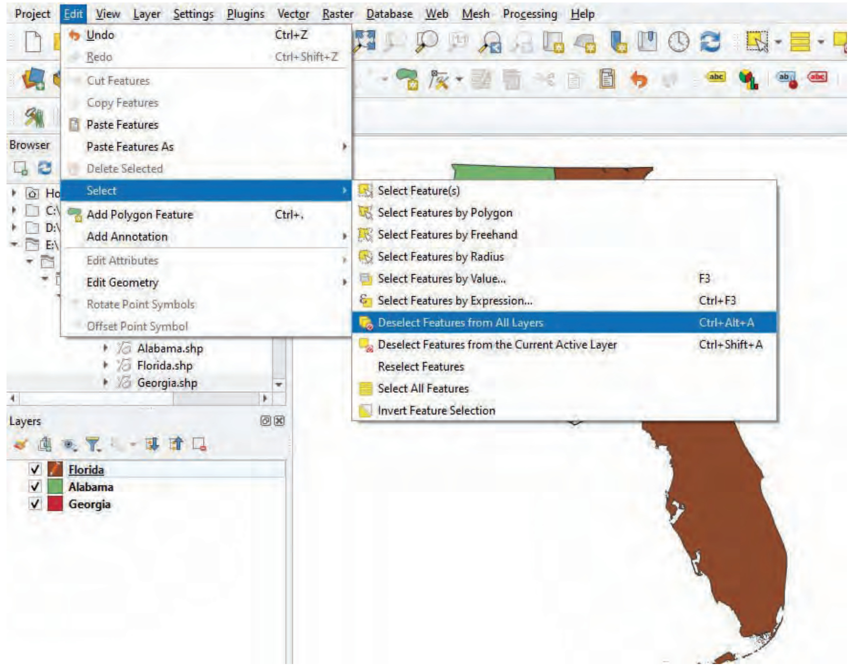

Figure 18. Clearing (Deselecting) selected features in QGIS.

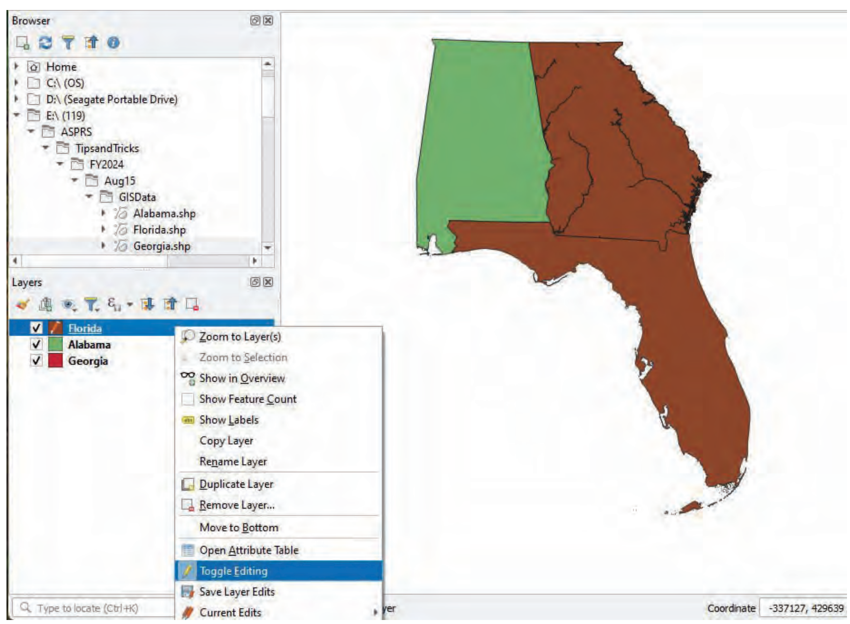

Figure 19. Toggling off editing following the copy/paste workflow in QGIS.

ASPRS THE IMAGING & GEOSPATIAL INFORMATION SOCIETY
STUDENT ADVISORY COUNCIL

Signatures

Introducing the new editorial committee for Signatures, the PE&RS Column for the Student Advisory Council. Adedayo Akande, Bruce Markman and Rajneesh Sharma will discuss topics relevant to students in the geospatial community. Contact the Signatures Editorial Committee directly to submit column ideas, ask questions, or to discuss a column, SignaturesColumn@asprs.org.

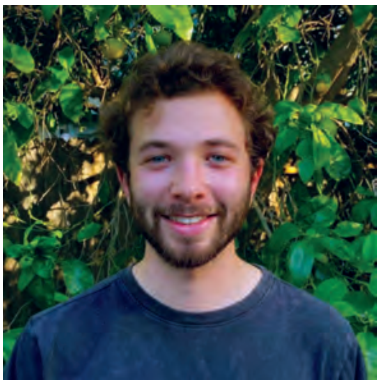

BRUCE MARKMAN

President — ASPRS Student Chapter at the San Diego State University, SAC Column Editor

Bruce Markman is a second-year MS student at San Diego State University studying GIS and Remote Sensing. He is the president of the American Society of Photogrammetry and Remote Sensing (ASPRS) Student Chapter located at the San Diego State University. Bruce holds a B.S. from UC Davis in Conservation Biology and has experience conducting geospatial research in academia, industry, and city/state government. Bruce's research interests lie at the intersection of conservation biology and GIScience, with a particular interest in applying novel remote sensing methods to solve problems that aid in the conservation of threatened lands. Currently, Bruce is collaborating with The Nature Conservancy to understand how UAV lidar and hyperspectral imagery can be used to quantify biomass across rangelands for fire fuel monitoring and grazing management. Bruce is very excited to be one of this year's SAC Column Editors and is looking forward to engaging with student chapters nationwide. In his spare time, Bruce enjoys playing guitar, mountain biking, and learning about the latest trends in the geospatial industry.

RAJNEESH SHARMA

Treasurer — ASPRS Student Chapter at the University of Georgia, SAC Column Editor

Rajneesh Sharma is a Ph.D. candidate in the Department of Geography at the University of Georgia, specializing in remote sensing, soil science, machine learning (ML), and coastal wetlands. He is also pursuing a master's degree in Artificial Intelligence from the Institute for Artificial Intelligence at the University of Georgia. His research employs a multi-layer approach using ground soil sensors, drones, and satellite data to map soil organic carbon in coastal wetlands, aiming to advance the understanding of carbon dynamics in these critical ecosystems. By integrating these diverse data sources, he aims to develop precise ML models that can capture the intricate interactions between soil carbon and bio geophysical drivers in wetland soils. This work has significant implications for advancing carbon sequestration strategies, informing conservation practices, and supporting climate resilience in coastal environments. Rajneesh's work highlights the transformative potential of geospatial technologies in environmental conservation and sustainable land management.

Outside of his research, Rajneesh enjoys reading books, watching anime and following the latest marvel movies/series. He also loves hiking, camping, and traveling to experience new cultures and landscapes. He also enjoys expressing his thoughts and experiences through poems and stories, tapping into his love for writing. He is excited to serve as a SAC Column Editor this year and can't wait to connect with fellow student chapters nationwide.

ASPRS THE IMAGING & GEOSPATIAL INFORMATION SOCIETY
STUDENT ADVISORY COUNCIL

Signatures

ADEDAYO AKANDE

Secretary — ASPRS Student Chapter at the Oregon State University ASPRS, SAC Column Editor

Adedayo Akande is a third-year Ph.D. student in the Department of Geomatics at Oregon State University, specializing in GNSS, geodesy, GIS, and atmospheric corrections. With a B.Tech. in Surveying and Geoinformatics from Bells University of Technology in Nigeria, Adedayo has a strong foundation in geospatial science and a keen interest in understanding ionospheric dynamics and variability.

Adedayo's research has included comprehensive analyses of GNSS Total Electron Content (TEC) data, providing valuable insights into ionospheric behavior. Currently, she is investigating the ionospheric response to the March 2023 geomagnetic storms at high and mid-latitudes, motivated by the need to understand how such storms impact TEC, which is critical for GNSS positioning, satellite navigation, and radio communication. She is also experienced in flood mapping, coastal resilience, and community engagement, contributing to a National Science Foundation-funded project focused on climate impact and community preparedness in coastal regions.

In addition to her research, Adedayo has practical experience in GIS, web app design, flood and sea level analysis. She has served as a Graduate Teaching Assistant at Oregon State University, where she enhanced student engagement in GIS and surveying courses, and she is the Secretary of the American Society for Photogrammetry and Remote Sensing (ASPRS) Student Chapter at OSU. Beyond her academic and professional pursuits, Adedayo enjoys traveling and exploring new ideas.

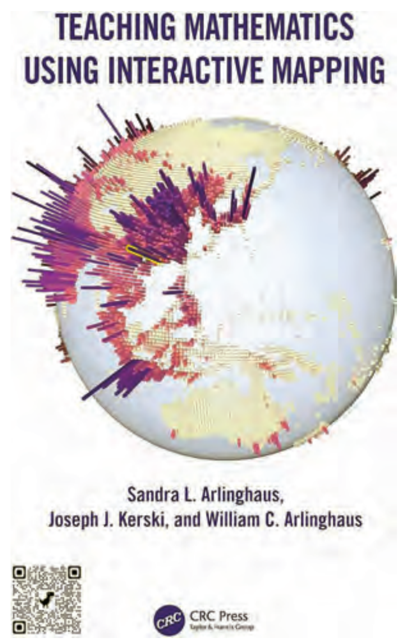

Teaching Mathematics Using Interactive Mapping

Sandra L. Arlinghaus, Joseph J. Kerski, and William C. Arlinghaus. CRC Press: Boca Raton, FL. 2023. xxiii and 225 pp. Softcover. $61.99. ISBN 978-1-032-30533-2.

Reviewed by Isaiah Ditmer, CMS-Lidar, Kodiak Mapping Inc; Adjunct Instructor, Department of Geomatics, University of Alaska Anchorage

In *Teaching Mathematics Using Interactive Mapping*, the authors propose to illustrate "novel ways to learn basic math topics … through customized interactive mapping activities." Throughout the book, web-based GIS tools are utilized to demonstrate applied concepts from various mathematical fields using step-by-step exercises. The overall tone and format suggest the content is geared towards educators with a specific need for real-world examples of otherwise abstract mathematical principles. Indeed, at one point it is suggested that the exercises described are meant to provide an outline that a motivated instructor could use to develop further materials.

This book begins with simpler topics like numeric representations of data and basic statistics. Later sections examine foundational topics such as trigonometry and topology in relation to geospatial problems. While the book's primary audience is educators, the interested student of mathematics or geospatial sciences (or professional in either field) may find the examples in this book instructive. A highly detailed outline of the topics covered is included in both the table of contents and at the beginning of each chapter. While some material builds on previous chapters, the exploratory nature of the book allows readers to select a topic of interest from virtually any section.

The authors have done an excellent job making use of tools that are freely available, primarily the ArcGIS Online platform. A handful of other tools, like those provided by Gapminder and the EPA, are used to develop alternative visuals of complex data. Exercises utilize publicly available data at every scale, with direct links included at each relevant step. In the physical edition reviewed, the specificity of the links leads to very long URLs which may hinder readers from following along efficiently. QR codes for the primary exercise links are included in an appendix. For those who value ease of navigation while reading, the eBook edition may be preferred.

Portions of this book read like a formal mathematics textbook, listing axioms and definitions. These sections are brief, however, and the mathematics is presented within the context of a specific application. One notable discussion along these lines is that of variance and correlation in the third chapter, where the use of spatial data and supporting plots allows readers to visualize concepts that are often abstract when first approached.

Each topic addressed begins with a descriptive introduction, often including anecdotal or historical narratives illuminating the need for a new tool or mathematical method. Some of the gems in this book are found in this portion of key chapters, as they provide insight into the high degree of overlap between mapping and mathematics. Examples include the relationship between graph theory and urban navigation, and the rise of fractal concepts from quantifying coastlines.

Concrete examples in the form of worked problems are included in the discussion that follows. These may include computations demonstrating the application of relevant equations. The concepts are further illustrated and reiterated through step-by-step interactive examples. The length and depth of this portion of each section varies with the complexity of the topic. In follow up discussions, the authors compel the reader to ask questions about why certain results arose, encouraging critical thought about the data and tools used. Some examples suggest additional fieldwork or classroom activities to further solidify the concepts.

While this book covers some underlying relationships between mathematics and the geospatial sciences, it is by no means a comprehensive elucidation of them. Its primary goal is to provide examples that encourage the reader to investigate these relationships using modern web-based tools. The software used and the format of the examples throughout this book support its utility as a teaching aid – not an in-depth tutorial for the purposes of production or research. Educators in mathematics and geospatial sciences may find this book to be a useful supplement to their own classroom activities and discussions.

NEW ASPRS MEMBERS

ASPRS would like to welcome the following new members!

AT LARGE
Isaac Frimpong Darko
Paul Odewale

CASCADIA
James T. Dietrich, Ph.D.
Jordan Grosser
Najiba Rashid
Austin Shute
Trevor Spahr
Wes Williams

EASTERN GREAT LAKES
Pranali Talla

FLORIDA
Emmanuel Junior Budukumah
Chloe Eaton
Luke Ryan Griffis
Ximena Mesa
Samantha Rae Morton
Briar Zealand Pierce

GULF SOUTH
Vladimir Serkov
Christie Marie Tregre
Martin Vargas

HEARTLAND
Khadijah Noura Audu
Aser Eissa
Adeyinka Michael Olusanya
Brett Ver Ver Helst

MID-SOUTH
David Layton Fawcett
Lander Stone

NORTH ATLANTIC
Lucas Carpenter
Summer Weidman

NORTHEASTERN
Travis Evans
Allyson Kitchens
Susmita Lamichhane
Bernardo Niati
Fredericus Darwin Setyawan
Austin J. Swanson
Aiyin Zhang
Dr. Fei Zhang

PACIFIC SOUTHWEST
Sergio Danilo Andrade
Eva Coleman
Nathan Lu
Joshua Monsanto
Erin Reilly
Paige Ilah Rohwer
Shane Vincent Santos
William Jon Witsell
Cohen Riley Woster
Alexander Zasso

POTOMAC
Rachel Caron
Adrian Oliver Croland
Quentin Cummings
Dr. Bradley Grinstead
Becc Hernandez-Lopez
Nivedita Priyadarshini Kamaraj
Nitheshnirmal Sadhasivam
Nichole Seward
Joyce Xu

ROCKY MOUNTAIN
Adrian N. Marziliano

WESTERN GREAT LAKES
Ehsan Chatraei Azizabadi
Mirmajid Mousavi Choobeh

FOR MORE INFORMATION ON ASPRS MEMBERSHIP, VISIT
HTTP://WWW.ASPRS.ORG/JOIN-NOW

Ad Index

Remote Sensing Tailing Pond Image–Detection Method Based on YOLOv8-RVSW

ZhengJun Dang and Kun Li

Abstract

This study proposes an automated tailings pond-detection method based on the YOLOv8-RVSW model to address the limitations of traditional surveys. A tailings pond dataset was created using high-resolution satellite images, and data quality was improved through data augmentation techniques. In the model, YOLOv8's backbone feature network was replaced with RepViT to effectively capture global and local information. Additionally, the C2f module was enhanced to QuadraSE_C2f to focus on essential feature channels, and WIoUv3 was used as the loss function to improve object localization and detection accuracy. Experimental results indicate that compared with the original model, accuracy increased by 3.9% to 97.4%, recall improved by 4.9% to 96.3%, and mean average precision rose by 2.4% to 98.5%. This method significantly enhances the automation and intelligence of tailings pond monitoring, providing an effective tool for emergency monitoring.

Introduction

Tailings ponds serve as reservoirs for storing the byproducts generated from ore processing, primarily comprising fine-grained solid residues, gravel, ore fragments, and chemicals (Islam and Murakami 2021). Tailings often contain heavy metals, chemicals, and other pollutants, posing a threat to the surrounding environment and water sources if not adequately managed. The accumulation of tailing sand in these ponds could result in catastrophic consequences, endangering the lives and properties of nearby residents in the event of dam failure or leakage (Halabi *et al.* 2022; Piciullo *et al.* 2022). Moreover, applying appropriate treatment techniques offers the potential to recover valuable minerals from tailings, thereby promoting resource efficiency and recycling. In summary, the management of tailings ponds is crucial for environmental safety, social stability, economic development, and ecological preservation, demanding comprehensive and effective strategies (Dong *et al.* 2020).

Remote sensing technology, which encompasses methods such as aerial photography and satellite imaging, proves invaluable for acquiring surface information across vast distances, facilitating the identification of tailings ponds even in regions with intricate or inaccessible terrain. Numerous scholars have used remote sensing imagery for monitoring and statistically analyzing tailings pond dynamics. One study examines the potential of multispectral interpretation of *Sentinel-2* remote sensing satellite imagery to prevent tailings pond failures (Cacciuttolo and Cano 2023). The approach is based on the analysis of real-life cases and is similar to another investigation (Bian *et al.* 2021). Analysis of decant ponds at tailings dams in South Africa using hyperspectral data received from the *Sentinel-2* satellite used high-resolution remote sensing data to conduct a comprehensive analysis of the structural, distributional, spectral, and textural characteristics of tailings ponds (O'Donovan *et al.* 2022).

Although the use of remote sensing imagery offers advantages in terms of comprehensiveness, timeliness, and cost-effectiveness over traditional methods based mainly on field surveys, it remains a visual inspection method. The lack of automation in this method frequently precludes the possibility of large-scale detection, thereby maintaining the challenge of accurately extracting tailings ponds on a large scale.

In recent years, the rapid advancement of artificial intelligence, with deep learning emerging as a pivotal element, has garnered considerable interest. For instance, a study from Balaniuk *et al.* (2020) showed more than 95% accuracy in detecting mining and tailings dams in satellite maps using deep learning. Similarly, an investigation by Yan *et al.* (2021) showed detection of tailings ponds in multispectral remote sensing images using the Faster *R* convolutional neural network (CNN) model with 85.9% AP, (Average Precision) with 71.9% recall in a separate study (Li *et al.* 2021). Identification of tailing ponds in the Beijing-Tianjin-Hebei region used the SSD (Single Shot MultiBox Detector) model,with a 93.3% recall rate. Collectively, these studies underscore the growing emphasis on applying deep learning for efficient automatic identification of tailings ponds, showcasing its potential to swiftly and accurately identify such features across expansive areas.

Although existing methods can automatically detect and identify tailings impoundments, they fall short in terms of precision and overall accuracy. To address this, a deep learning model based on the YOLOv8-RVSW architectural framework is proposed, aimed at high accuracy in recognizing tailings dams. This model was validated using the tailings dam dataset from Henan Province, provided by the China Scientific Data Resource Repository. Validation results indicate that the proposed model can accurately identify tailings dams with a high degree of precision.

Data and Methods

Data

This study assesses the effectiveness of the proposed YOLOv8-RVSW model for the detection of tailing ponds in remotely sensed imagery. To this end, the study uses the publicly available target detection dataset for tailing ponds, which was curated by J. Li *et al.* (2023) and made available on the China Scientific Data website (Li, et al,, 2022). The dataset encompasses four distinct time-phase remote sensing images situated between lat. 31°23'–36°22' N and long. 110°21'–116°39' E within the Henan Province of China. Imaging data were collected in 2016, 2018, 2020, and 2021, respectively; images were obtained from domestically manufactured civil land observation satellites, including panchromatic and multispectral images with a spatial resolution of 2 m.

Following the completion of the data stretching and enhancement steps, control point acquisition, leveling, ortho-rectification, fusion, mosaic preprocessing, and image mosaic preprocessing, a true-color mosaic image with a geometric positioning accuracy of more than 10 m was obtained. The shape, size, texture, hue, and other characteristics of the tailing ponds were analyzed to construct deciphering markers for the tailing ponds. These markers were then used with the ArcGIS vector editing tool (https://desktop.arcgis.com/en/index.html) to sketch the minimum

ZhengJun Dang and Kun Li are with the Department of Information Engineering and Automation, Kunming University of Science and Technology, Kunming 650550, Chenggong District, Yunnan, China.

Corresponding author: Kun Li (12309058@kust.edu.cn)

Received May 24, 2024, accepted Aug 14, 2024

Photogrammetric Engineering & Remote Sensing
Vol. 90, No. 12, December 2024, pp. 735–744.
0099-1112/22/735–744

doi: 10.14358/PERS.24-00065R2

**PEER-REVIEWED CONTENT
IS ONLY AVAILABLE TO
ASPRS MEMBERS AND SUBSCRIBERS**

**FOR MORE INFORMATION VISIT
MY.ASPRS.ORG**

PEER-REVIEWED CONTENT
IS ONLY AVAILABLE TO
ASPRS MEMBERS AND SUBSCRIBERS

FOR MORE INFORMATION VISIT
MY.ASPRS.ORG

PEER-REVIEWED CONTENT IS ONLY AVAILABLE TO ASPRS MEMBERS AND SUBSCRIBERS

FOR MORE INFORMATION VISIT MY.ASPRS.ORG

PEER-REVIEWED CONTENT IS ONLY AVAILABLE TO ASPRS MEMBERS AND SUBSCRIBERS

FOR MORE INFORMATION VISIT MY.ASPRS.ORG

PEER-REVIEWED CONTENT
IS ONLY AVAILABLE TO
ASPRS MEMBERS AND SUBSCRIBERS

FOR MORE INFORMATION VISIT
MY.ASPRS.ORG

PEER-REVIEWED CONTENT
IS ONLY AVAILABLE TO
ASPRS MEMBERS AND SUBSCRIBERS

FOR MORE INFORMATION VISIT
MY.ASPRS.ORG

**PEER-REVIEWED CONTENT
IS ONLY AVAILABLE TO
ASPRS MEMBERS AND SUBSCRIBERS**

**FOR MORE INFORMATION VISIT
MY.ASPRS.ORG**

PEER-REVIEWED CONTENT
IS ONLY AVAILABLE TO
ASPRS MEMBERS AND SUBSCRIBERS

FOR MORE INFORMATION VISIT
MY.ASPRS.ORG

PEER-REVIEWED CONTENT
IS ONLY AVAILABLE TO
ASPRS MEMBERS AND SUBSCRIBERS

FOR MORE INFORMATION VISIT
MY.ASPRS.ORG

Monitoring LULC Changes in Babil Province for Sustainable Development Purposes Within the Period 2004–2023

Hayder Hameed Jassoom and Rabab Saadoon Abdoon

Abstract

Land use and land cover studies are fundamental to achieving sustainable development goals by providing the information necessary for informed decision-making in social and economic development and natural resource management. This study relied on remote sensing data to analyze and assess land use and land cover changes in Babil Province, Iraq, over the past two decades. The study focused on identifying the patterns and factors influencing these changes, using Landsat satellite imagery to create digital maps classifying land into four main categories: urban lands, bare soil lands, water bodies, and vegetation lands. The results showed a noticeable expansion of urban lands at the expense of bare soil lands, primarily attributed to population growth, economic development, and improved security conditions. This study underscores the importance of sustainable land management and urban planning in Babil Province. These results highlight the importance of sustainable land management in Babil Province, including sound urban planning considering urban expansion's environmental, social, and economic effects. The classification was implemented using a maximum likelihood classifier, and the accuracy assessment yielded satisfactory results with an overall accuracy of 93.5517%. This study encourages using artificial intelligence to track and analyze land use changes in Babil.

Introduction

Classification of land use and land cover provides nations with the knowledge to make well-informed decisions using remote sensing data. Understanding and identifying land change is critical in conserving, managing, and planning for development. Knowledge of the changes in environmental dynamics is also beneficial for formulating policies that maximize these lands' use and ensure sustainable development. The classification of land use and land cover is essential for determining the relationship between human activity and the environment (Singh *et al.* 2021). It investigates the distribution of various land uses within a given area. Extensive applications of this analysis include urban planning, nature conservation planning, and disaster management. The significance of land use and land cover has escalated in tandem with the global population expansion and depletion of resources. Classification of land use and land cover entails identifying and categorizing various land use categories within a specified geographical region. Satellite imagery, field surveys, and remote sensing are all viable approaches for gathering data. The aggregation and hierarchical organization of the data can subsequently facilitate making the appropriate decision. The principal aim of a classification system is to determine the land cover and type of land use in a given region. The land use and land cover classification can be used to assess the effect of human activities on the environment and make sustainable land use decisions.

Traditional visual interpretation is the most commonly used land use and land cover classification method. An expert in the field must traverse the pertinent terrain while collecting exhaustive reports on the state of the land cover. The expert is tasked with conducting an impartial assessment of the area, encompassing its vegetation cover and bodies of water. Although this visual analysis aids in gaining a comprehensive comprehension of a particular area, it is unsuitable for large-scale land use and land cover analyses and may require additional reliability. Object-based image analysis is an alternative to visual interpretation. In this approach, an image is partitioned into discrete entities according to their physical attributes, including texture and shape, and each entity is allocated a distinct land use and land cover category. This method is advantageous for land use and vegetation classification on a large scale because it can efficiently and precisely process vast quantities of image data. Traditional visual interpretation could be more reliable and demand more user intervention than object-based image analysis.

Increasing applications use artificial intelligence and machine learning to classify land use and cover. Artificial intelligence and machine learning are gaining increasing attention as an emerging approach to land use and land cover classification. This approach relies on training a computer model to identify land use and land cover classes in satellite images by learning from labeled training data. This can be accomplished using various models, including support vector machines (Aslami *et al.* 2015; Rezaei Moghaddam *et al.* 2015; Kadavi and Lee 2018; Hamad 2020), convolutional neural networks (Balarabe and Jordanov 2021), deep belief networks (Lv *et al.* 2015; Vignesh and Thyagharajan 2019), and other models. Machine learning offers the benefit of efficiently processing vast quantities of data while delivering outcomes of superior accuracy compared with conventional methods of land use and land cover classification.

Population growth and socioeconomic recovery have pressured local land uses, resulting in unplanned and uncontrolled changes; thus, this research is crucial. Babil Province is a vital historical, cultural, and economic region located in central Iraq on the banks of the Euphrates River. It is one of the oldest civilizations in the world, having been the capital of the ancient Babylonian civilization. Babil Province faces increasing pressure from population growth and economic development, leading to rapid and widespread land use and land cover changes. Using geographic information systems (GIS) and remote sensing, the study of land use and land cover of Babil Province seeks to produce a cartographic representation of land use and land cover that classifies the two. This map will provide a reliable and effective tool for monitoring and managing the province's land use and cover changes.

Hayder Hameed Jassoom is with the Department of Physics, College of Science, University of Babylon, Babil, AL-Hilla, 51002, Iraq.

Rabab Saadoon Abdoon is with the Department of Physics, College of Science, University of Babylon, Babil, AL-Hilla, 51002, Iraq.

Corresponding author: Hayder Hameed Jassoom (hayder.hameed.jassoom@gmail.com)

Received March 11, 2024, accepted August 13, 2024.

Photogrammetric Engineering & Remote Sensing
Vol. 90, No. 12, December 2024, pp. 745–753.
0099-1112/22/745–753

doi: 10.14358/PERS.24-00027R3

This study is significant because it contributes to advancing sustainable conservation of resources and land use, facilitating efficient land management procedures and guidelines, and providing critical information to decision-makers in urban, agricultural, and biodiversity protection planning. Some additional details on the importance of the study include the fact that Babil Province plays a vital role in the Iraqi economy. To promote economic growth, it is essential to ensure the sustainable use of land in the province. Babil Province has a rich historical and cultural heritage, including many important archaeological sites. Protecting these sites from the negative effects of land use and land cover changes is essential. Overall, the study of land use in Babil Province is a critical study that contributes to achieving sustainable development in the province.

Related Work

Many studies have used remote sensing and GIS technology to classify and update land use and land cover data in various regions, with varying degrees of success (Dibs *et al.* 2020; Kaya and Gorgün 2020; Saddique *et al.* 2020; Bhattacharya *et al.* 2021; Ghayour *et al.* 2021; Sang *et al.* 2021; Darem *et al.* 2023). Abdallah *et al.* (2019) classified land use, land cover categories, and land cover variations in the Dam of Jizan, Kingdom of Saudi Arabia, using three cloud-free Landsat images. The study successfully classified five distinct land categories: urban areas, sand areas, rock areas, vegetated areas, and water of bodies, with an overall accuracy of 86.67%. Alqurashi and Kumar (2014) used maximal likelihood classification and object-oriented classification techniques to categorize Makkah and Al-Taif cities as desert cities in the Kingdom of Saudi Arabia. They delineated five distinct categories: vegetation, urban landscape, stony terrain, dunes, and desolate territory. In 1986, 1990, 2000, and 2013, the overall likelihood classification achieved an average accuracy of 88.9%. In contrast, the object-oriented classification maintained an average accuracy of 92.5% during the same period. Approximately 17.4% and 11.3% of urban areas in Makkah and Al-Taif expanded due to variations in average precipitation. Building on the success of traditional methods like maximum likelihood and object-oriented classification, recent advancements in deep learning offer powerful tools for detecting land use and land cover changes. Naik *et al.* (2024) applied deep learning techniques to detect and predict land use and land cover changes in the southwestern coastal region of Goa, India. A new change detection framework, the Self-Attention Temporal-Spatial Decoder-Encoder Network (STEDSAN), has been proposed. The two-branch architecture of STEDSAN works like this: the encoder uses progressively dilated convolutions with down-sampling to pull out features, and the decoder uses transposed convolutions with up-sampling to reconstruct space. This design allows the network to effectively analyze dual-temporal images (images from two time periods). Self-attention mechanisms play a crucial role by capturing complex spatial-temporal interactions across both space and time. This results in more discriminative features for Land use and Land cover Change (LULCC)analysis. Each branch of the STEDSAN model accepts land use and land cover (LULC) maps from two years as inputs. This enables the model to identify both binary changes (presence/absence) and multi-class changes between dual-temporal images. Through data analysis from 2005 to 2018, STEDSAN successfully identifies patterns, trends, and transitions among different LULC types during the study period. The binary change maps generated by STEDSAN were compared with existing state-of-the-art change detection methods, achieving an impressive overall accuracy of 94.93%. A long short-term memory network was used to predict LULCC changes for 2025. The analyses revealed significant trends over 13 years (2005–2018), with built-up areas, rabi crops, and double/triple crops experiencing net increases, while deciduous forests and fallow lands showed net decreases. These changes represent prevailing trends in land use change within the study area. Mahmoud and Alazba (2016) used the Surface Energy Balance Algorithm for Land model and field observations to figure out how actual evapotranspiration was spread out in the western and southern parts of Saudi Arabia from 1992 to 2014. In his study, Salih (2018) classified land use and cover using various image preprocessing techniques and the maximum likelihood classifier. Additionally, Khwarahm (2021) modeled and analyzed land use and land cover change trends in the Sulaimani region of Iraq using the maximum likelihood classifier. Using Landsat-7 data and a CA-Markov synergy model, Khwarahm *et al.* (2021) predicted and mapped land use and land cover variations in the province of Erbil, Iraq. Rahman (2016) employed Landsat imagery to quantify the extent of urban development, land use, and land cover alterations in Al Khobar, Kingdom of Saudi Arabia, over 23 years. Between 2001 and 2013, urban development experienced a significant rise from 17% to 43.51% between 1990 and 2001. Furthermore, between 1990 and 2001, vegetation cover grew by 11%, and from 2001 to 2013, it increased by 52%. Several investigations have analyzed land use and land cover using remote sensing and GIS. As an illustration, Alawamy (2020) employed a series of time data from Landsat from 1985 to 2017 to identify and analyze land use and land cover fluctuations in Al-Jabal Al-Akhdar, Libya. Wijitkosum (2016) illustrated the effect of spatial and land use changes on the desertification risk in deteriorated regions of Thailand. According to the study, using remote sensing and GIS technologies for detecting and classifying land use and land cover has been shown to be an accurate and efficient process. Remote sensing data-driven classification technology is increasingly used to obtain accurate and timely land use and land cover mapping data.

Methodology used

The steps of the work are summarized in the block diagram in Figure 1.

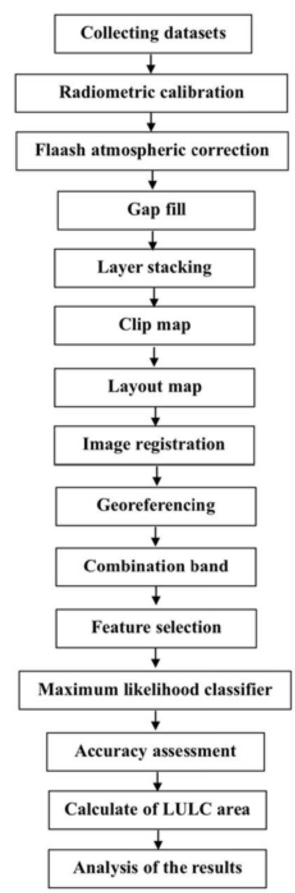

Figure 1. Fundamental steps in satellite image analysis for land cover determination. This figure presents a simplified overview of the critical stages of analyzing satellite imagery to ascertain land cover. Understanding these steps is vital for comprehending environmental alterations and making well-informed land and natural resource management decisions.

Study area

The province of Babil is situated in the center of Iraq. It is surrounded by five provinces: Baghdad Province borders it to the north, Wassit Province to the east, Holy Karbala and Al-Anbar Provinces to the west, and Al-Najaf Al-Ashraf and Al-Qadissiya Provinces to the south. It is situated latitudinally between 43°58′10″ and 44°38′35″ east of Greenwich and north of the equator between 32°7′25″ and 33°0′35″. The province has a land area of about 5335 km² and a population of approximately 2 065 042 people as of 2018. The province of Babil consists of seven administrative regions: Al-Hillah, Al-Muhawwil, Al-Musayyib, Al-Hashimiya, Al-Kifil, Kuthe, and Al-Hamza Al-Gharbi. The province of Babil has an arid climate, with summertime temperatures surpassing 50°C. Between April and November, precipitation is scarce, averaging 100 mm annually. Agriculture holds significant economic value in the province of Babil due to the region's substantial production of cereals, vegetables, and fruits. Many plantations and orchards in Babil Province are watered by an extensive network of canals (Hashim *et al.* 2022). Emphasizing the province's borders, Figure 2 illustrates the geographic location of Babil province.

Collecting datasets

Only cloud-free sequences were used when compiling the dataset from 2004 to 2023: Landsat 7 (+ETM) and Landsat 8 (OLI) data from multiple sources, including Google Earth Pro and the United States Geological Survey website (https://earthexplorer.usgs.gov). The dataset comprises remote sensing images of Babil Province, Iraq. The United Nations Office for the Coordination of Humanitarian Affairs provides a shape file of the administrative boundaries of Iraq. The shape file is available for download at the following link: https://data.humdata.org/group/irq. Table 1 presents the date/time of acquisition from Landsat 7 (+ETM) and Landsat 8 (OLI).

Preprocessing stage

In land use and land cover classification, primary data processing is crucial because it directly influences the precision of the resultant classifications. This procedure aims to enhance the preliminary data before classification by implementing spatial filtering, data enhancement, and radiometric corrections. To analyze remote sensing data, radiometric and geometric errors must be rectified during the acquisition, scanning, and transmission phases. This process includes a set of steps as follows: (i) Clip map: A clip map is an image where specific regions of interest are extracted by removing extraneous background data, allowing for more precise image analysis. (ii) Image registration matches comparable features by aligning pictures from distinct locations. It can even merge the coordinate systems of two images captured at the same spot (Ramdani *et al.* 2021). The study area within Google Earth Pro was defined, and four control points possessing known geographic coordinates were identified at its corners. The image of the study area was saved in JPEG format, alongside the four points with geographic coordinates saved in KML format. Employing ArcMap 10.8, each control point was linked to its corresponding location on the image. Subsequently, the image was saved in TIF format. After that, the geometrically corrected image was used to rectify satellite imagery. (iii) The georeferencing procedure involves identifying images, enabling a computer to pinpoint the precise whereabouts of different land cover characteristics. In contrast, the geometry correction transfers a pixel's location coordinates.

Table 1. Acquisition dates for satellite imagery from Landsat 7 (+ETM) and Landsat 8 (OLI) for specific paths and rows.

Path	Row	Landsat 7 (+ETM)			Landsat 8 (OLI)		
168	37	9 Jul 2004	20 Jul 2008	15 Jul 2012	18 Jul 2016	13 Jul 2020	22 Jul 2023
168	38	9 Jul 2004	20 Jul 2008	15 Jul 2012	18 Jul 2016	13 Jul 2020	22 Jul 2023
169	37				25 Jul 2016	20 Jul 2020	29 Jul 2023

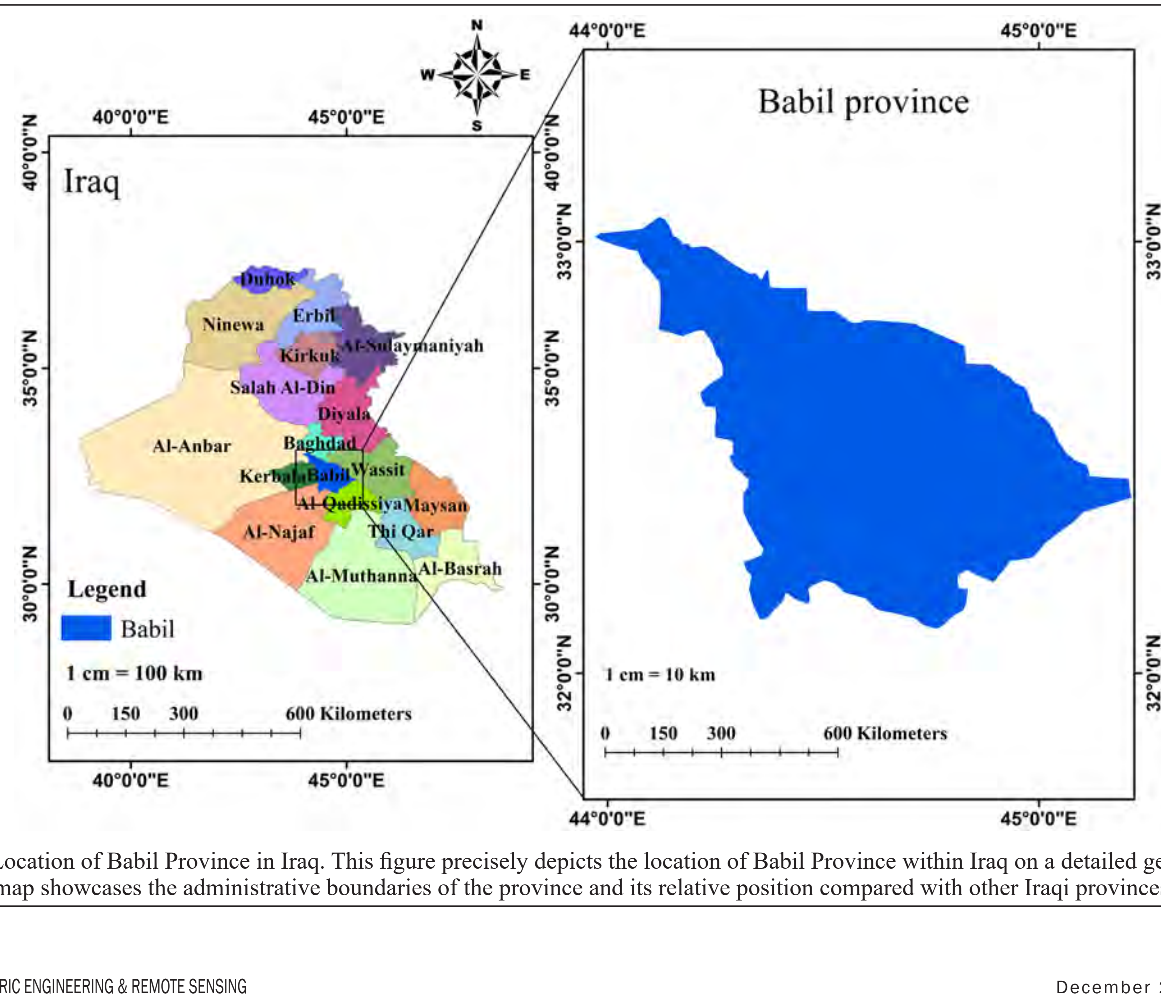

Figure 2. Location of Babil Province in Iraq. This figure precisely depicts the location of Babil Province within Iraq on a detailed geographical map. The map showcases the administrative boundaries of the province and its relative position compared with other Iraqi provinces.

After that, the geometric correction is executed using ArcMap 10.8 and the WGS 1984 UTM 38 N projection, wherein the pixel units are positioned at the appropriate coordinates on the map (x, y). (iv) Radiometric correction is a fundamental step in land cover classification. It processes digital images to minimize inaccuracies and discrepancies in the brightness values of images (Kuemmerle *et al.* 2013). Product accuracy is improved through geometric correction and radiometric correction, which are highly beneficial in removing the effects caused by different correction procedures. Calibration and atmospheric correction are performed to recalculate the pixel radiance to prevent radiometric distortions. Geometric corrections involve registration to remove geometric distortions and correct the local incidence angle using a topographic sheet. The correction depends on determining the latitude and longitude coordinates of the relevant ground locations (Verburg *et al.* 2011; Kuemmerle *et al.* 2013; Shi *et al.* 2020; Alshari and Gawali , 2021b). (v) Gap filling: On May 31, 2003, the scan line corrector of the ETM+ sensor on the Landsat 7 satellite failed. As a result, wedge-shaped gaps appeared in the images, ranging in width from one pixel near the center of the image to about 12 pixels towards the edges of the scene. These gaps constitute approximately 22% of the image pixels (Arvidson *et al.* 2006). The Nearest Similar Pixel Interpolator algorithm was adopted to address these gaps. This algorithm assumes that neighboring pixels of the same class, such as land cover, have similar spectral characteristics. Therefore, the values of neighboring pixels can be used to estimate the value of the missing pixel (Chen *et al.* 2011). The study's objective was achieved using ENVI 5.6 software, relying on the "single fill gap fill (triangulation)" tool after performing radiometric correction (radiometric calibration and atmospheric correction). (vi) Layer stacking images: Layer stacking technology merges diverse data layers into satellite images, like near-infrared (NIR), visible, and shortwave infrared. These images unlock hidden details like reflectance and vegetation indices, enabling us to pinpoint and map various land use and cover features precisely. (vii) Layout maps use reflectance patterns observed in satellite imagery to demarcate the boundaries of land cover categories. An illustration of this concept would be categorizing regions exhibiting high NIR reflectance, such as agricultural land and annually laden forests, as regions displaying little visible and NIR reflectance.

Results and Discussion

A study on the changes in land uses and land cover in Babil Province, Iraq, during the period from 2004 to 2023 was presented in this research. Satellite images were classified using the maximum likelihood classifier based on specific image characteristics. The discriminant function for each pixel in the image is defined by Equation 1 (Darem *et al.* 2023). This function calculates the probability that each pixel belongs to a particular class based on its statistical properties. The classified images were used to analyze trends over time. Five land cover types were identified: urban lands, bare soil land, water bodies, vegetation lands, and other lands. The details of the classes are illustrated in Figures 3 and 4 and Tables 2 and 3.

$$\boldsymbol{g}_i(\boldsymbol{x}) = \ln \boldsymbol{p}(\boldsymbol{w}_i) - \frac{1}{2}\ln\left|\sum_i\right| - \frac{1}{2}(\boldsymbol{x}-\boldsymbol{m}_i)^T \sum_i^{-1}(\boldsymbol{x}-\boldsymbol{m}_i) \tag{1}$$

where $\boldsymbol{x}$ represents the number of band-dimensional data and i refers to class. For all classes, $p(\boldsymbol{w}_i)$ denotes the probability that class $\boldsymbol{w}_i$ appears in the image and is presumed to be the same. $\left|\sum_i\right|$ represents the determinant of the covariance matrix of the data in class $\boldsymbol{w}_i$. $\boldsymbol{m}_i$ represents the mean vector, and $\sum_i^{-1}$ refers to the inverse matrix.

There were changes in all land categories in Babil Province, as shown in Table 4. Urban lands experienced remarkable growth during the specified period, increasing in area from 1196.168 544 km² in 2004 to 1839.946 969 km² in 2023. This growth reflects the increasing urban sprawl in the governorate, driven by social and economic factors. Meanwhile, the bare soil lands category experienced a decrease in area from 2127.713 508 km² in 2004 to 1927.647 689 km² in 2023. The decrease is attributed to the conversion of some bare soil lands to other uses, such as infrastructure projects, industrial or commercial facilities, or residential areas. The area of water bodies fluctuated over the years but generally decreased from 126.736 297 km² in 2004 to 61.105 112 km² in 2023. The water decrease is attributed to a combination of factors, including reduced water flows from neighboring countries, local government adjustments to water management policies, and increased evaporation rates due to climate change. The area of vegetation also fluctuated over the years but generally decreased from 1884.820 132 km² in 2004 to 1506.688 961 km² in 2023. This decrease is due to several factors, including converting vegetation land to urban areas and water bodies. In addition, a decrease in rainfall and an increase in temperatures due to climate change have led to the loss of vegetation cover and the desertification of some areas. Additionally, a marketing plan for agricultural crop cultivation was identified by the relevant government agencies. Other lands, which include land that cannot be classified into any of the other four categories, remained relatively stable, representing around 0.00% of the total area throughout the study period.

This method has valuable applications in various fields, as land use and land cover maps provide vital information about the nature of land use and its surface. These maps are essential for multiple applications, including urban planning, agricultural land management, and biodiversity conservation.

Accuracy assessment is a crucial component of any image classification project. It involves comparing the classified image with a reference data source, considered ground truth data collected in the field using GPS. However, gathering ground truth data can be a significant time and financial burden, as it can be costly and time-consuming. Moreover, ground truth data may only sometimes be available or may be limited in geographic scope, hindering practical accuracy assessment.

The most common method used for accuracy assessment in image classification involves generating random points from ground truth data and comparing them with the classified data in a confusion matrix. This process quantitatively assesses the classification's performance across different land cover or object classes. Although this is a two-step process, these steps may necessitate comparing results of classification methods or training sites, or ground truth data may not be available, requiring reliance on the exact images that were used to create the classification. This process uses three geo-processing tools to accommodate other workflows: create accuracy assessment points, update accuracy assessment points, and compute confusion matrix. Random point samples were verified against Google Earth Pro. This involved converting the random points to the KML format used by the program, ensuring that the coordinates and the time stamp of the image used for classification were consistent and that the difference between them was insignificant. Coordinates were assigned to the points to facilitate fieldwork.

Confusion matrices are a standard tool for evaluating land use and land cover classification methods (Tan *et al.* 2021; Alshari *et al.* 2022; Rizvon and Jayakumar 2022). They provide a detailed picture of classification performance by revealing the number of correctly and incorrectly classified pixels for each land cover class. Tables 5 to 10 present the results of these confusion matrices. The kappa coefficient, calculated using Equation 2 (Darem *et al.* 2023), measures the agreement between the classified data and the ground truth data, considering the possibility of random agreement.

$$K = \frac{N\sum_{i=1}^{n} m_{i,i} - \sum_{i=1}^{n}(G_i C_i)}{N^2 - \sum_{i=1}^{n}(G_i C_i)} \tag{2}$$

where N is the total number of classified values relative to truth values. i refers to the class number. The value of $m_{i,i}$ represents the count of

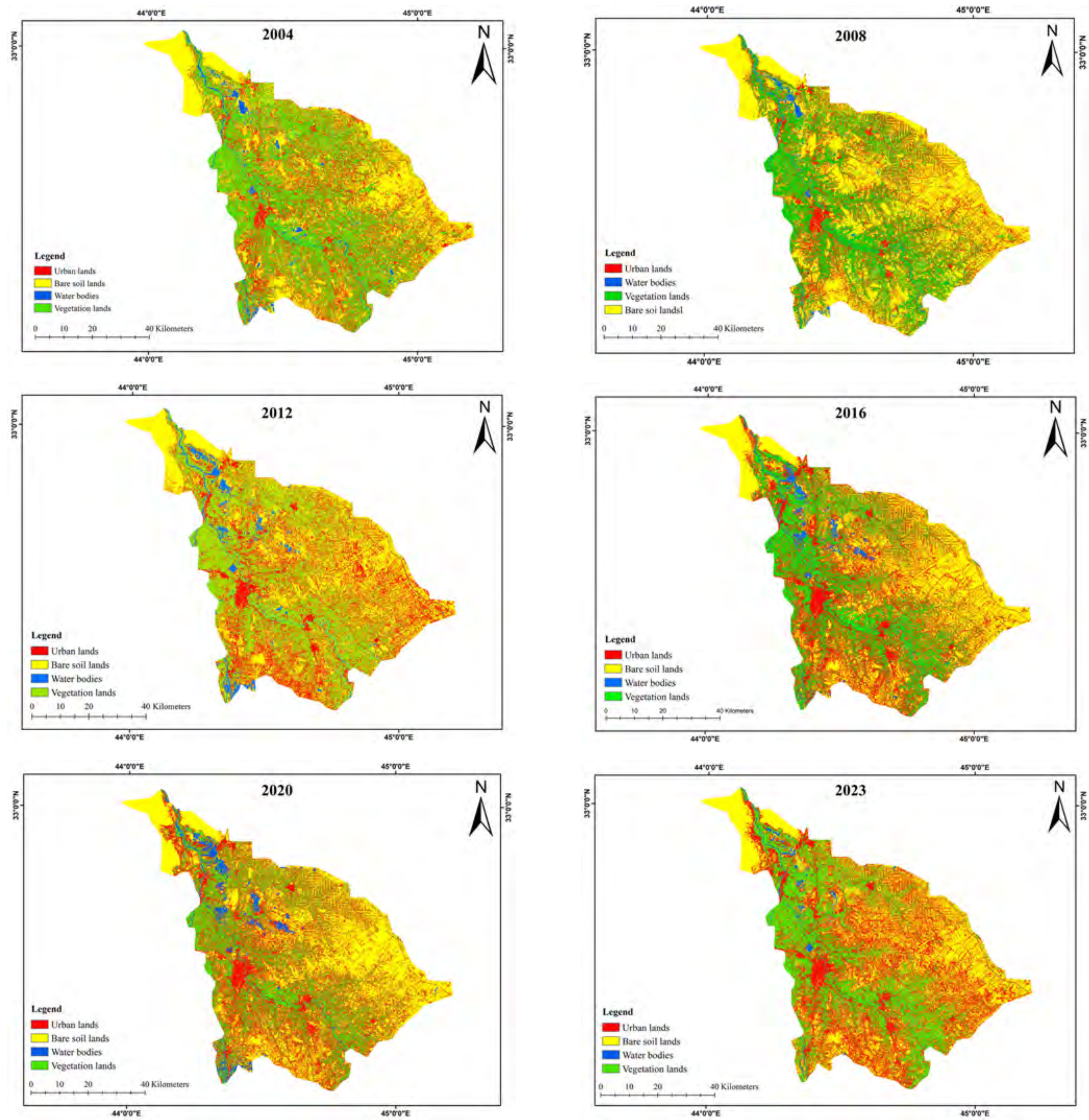

Figure 3. LULC classification maps for Babil Province (2004–2023). This figure displays the classification results for Babil Province from 2004 to 2023 using the maximum likelihood classification algorithm. Land cover and land use classes identified include urban lands, bare soil lands, water bodies, and vegetation lands. The classification was based on the spectral signatures of Landsat satellite imagery with a spatial resolution of 30 m. LULC = Land use and Land cover.

actual class i values that have been categorized as class i. G_i represents the sum of all truth values associated with class i. C_i represents the sum of all predicted values associated with class i.

The kappa coefficient ranges from 0 to 1, where a value of 0 indicates perfect agreement and a value of 1 indicates complete random agreement. Table 11 summarizes the overall accuracy and kappa coefficient values. The results showed high classification accuracy, with kappa coefficient values ranging from 85% to 95% and an overall accuracy of 93.55%.

This study provides a detailed and comprehensive analysis of land use and land cover changes in Babil Province between 2004 and 2023. The results indicate significant trends in urban expansion,

Table 2. Detailed descriptions of the LULC classes used in the study.

No.	Class	Description
1	Urban lands	Land that is covered with buildings
2	Bare soil lands	Territory devoid of vegetation, land use, and agricultural activities
3	Water bodies	Lakes, rivers, and irrigation canals
4	Vegetation lands	Agricultural produce, public parks, and orchards
5	Other	

LULC = Land use and Land cover

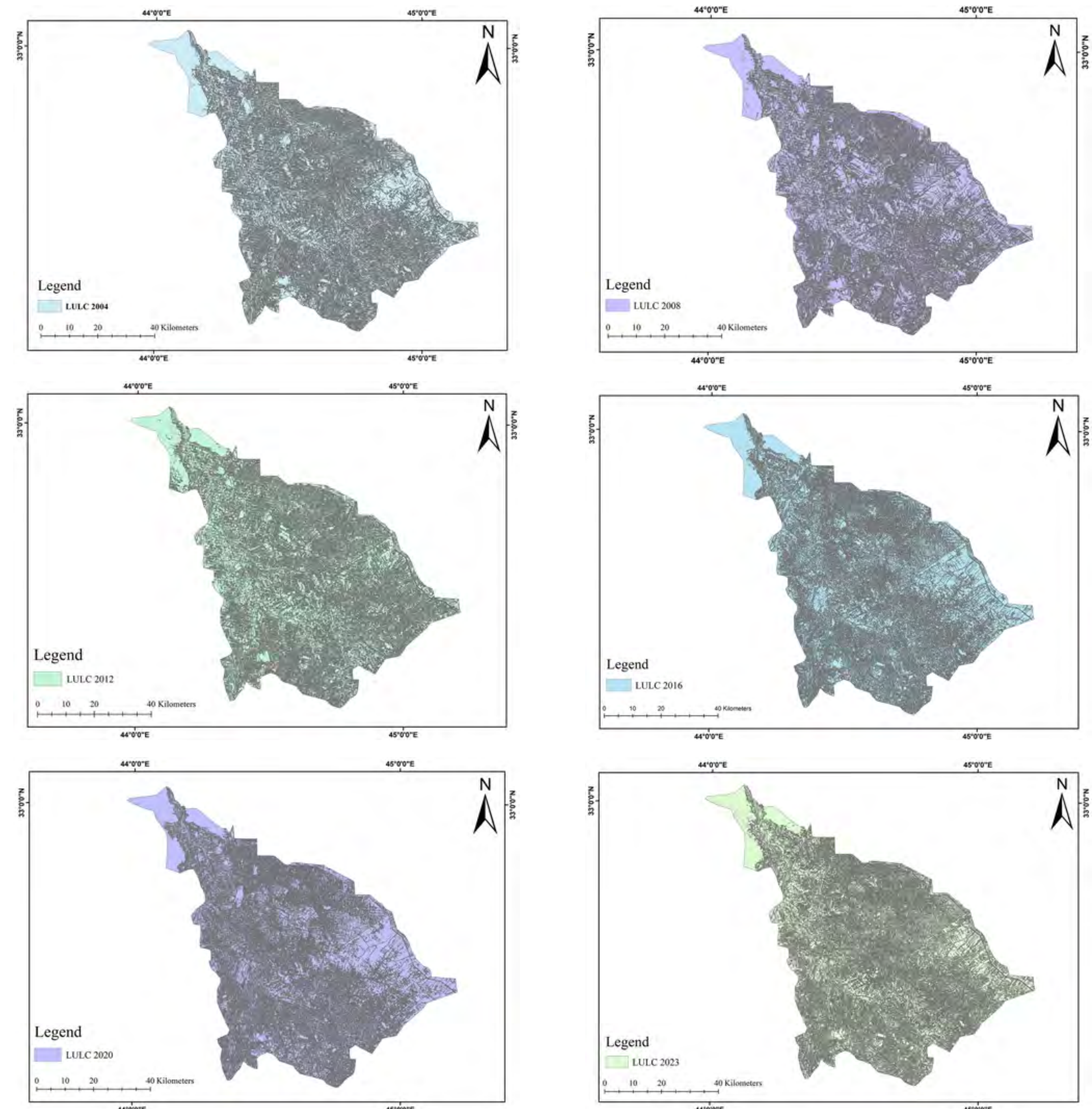

Figure 4. Spatial changes in bare soil land area (2004–2023). This figure depicts the bare soil area alterations across the study period (2004–2023). It presents the geographical distribution of bare soil lands, emphasizing areas that have undergone increases and decreases in extent.

Table 3. Land use and land cover changes in Babil Province (2004–2023). The table presents each land use category's area (in km²) for every four years from 2004 to 2023 in Babil Province.

Class	Area (km²) 2004	2008	2012	2016	2020	2023
Urban lands	1196.168 544	1123.547 653	1412.691 223	1817.892 158	1632.471 293	1839.946 969
Bare soil lands	2127.713 508	2626.267 766	2027.001 082	2065.132 050	2322.594 018	1927.647 689
Water bodies	126.736 297	79.376 639	163.097 428	102.137 675	161.497 599	61.105 112
Vegetation lands	1884.820 132	1506.239 834	1732.606 458	1350.242 099	1218.855 146	1506.688 961
Other	0.200 598	0.207 187	0.242 888	0.235 097	0.221 023	0.250 348
Total	5335.639 079	5335.639 079	5335.639 079	5335.639 079	5335.639 079	5335.639 079

Table 4. Land use and land cover change analysis in Babil Province (2004–2023). The table analyzes changes in land use and land cover in Babil Province between 2004 and 2023. It presents percentage changes in each land use category area, highlighting a significant increase in urban lands, a decrease in vegetation lands and water bodies, and minor changes in bare soil lands and the "other" category.

	2004		2023		
Classes	**Area (km²)**	**%**	**Area (km²)**	**%**	**LULC Change 2004–2023 (%)**
Urban lands	1196.168 544	22.418 468	1839.946 969	34.484 097	+12.065 629
Bare soil lands	2127.713 508	39.877 388	1927.647 689	36.127 775	−3.749 613
Water bodies	126.736 297	2.375 279	61.105 112	1.145 226	−1.230 053
Vegetation lands	1884.820 132	35.325 105	1506.688 961	28.238 210	−7.086 895
Other	0.200 598	0.003 760	0.250 348	0.004 692	+0.000 932
Total	5335.639 079	100	5335.639 079	100	0.000 000

LULC = Land use and Land cover.

Table 5. Confusion matrix for 2004 land cover classification model. The table presents a confusion matrix to assess the agreement between the 2004 land cover classification model and ground truth data.

ID	Class	Urban Lands	Bare Soil Lands	Water Bodies	Vegetation Lands	Row	User_ Accuracy	Kappa
1	Urban lands	69	6	0	4	79	0.873 418	0
2	Bare soil lands	0	60	0	1	61	0.983 607	0
3	Water bodies	0	0	9	1	10	0.9	0
4	Vegetation lands	0	7	1	97	105	0.923 81	0
5	Column	69	73	10	103	255	0	0
6	Producer_ Accuracy	1	0.821 918	0.9	0.941 748	0	0.921 569	0
7	Kappa	0	0	0	0	0	0	0.884 631

Table 6. Confusion matrix for 2008 land cover classification model. The table presents a confusion matrix to assess the agreement between the 2008 land cover classification model and ground truth data.

ID	Class	Urban Lands	Bare Soil Lands	Water Bodies	Vegetation Lands	Row	User_ Accuracy	Kappa
1	Urban lands	65	10	0	2	77	0.844 156	0
2	Bare soil lands	0	79	0	4	83	0.951 807	0
3	Water bodies	0	0	9	1	10	0.9	0
4	Vegetation lands	0	7	0	79	86	0.918 605	0
5	Column	65	96	9	86	256	0	0
6	Producer_ Accuracy	1	0.822 917	1	0.918 605	0	0.906 25	0
7	Kappa	0	0	0	0	0	0	0.8637

Table 7. Confusion matrix for 2012 land cover classification model. The table presents a confusion matrix to assess the agreement between the 2012 land cover classification model and ground truth data.

ID	Class	Urban Lands	Bare Soil Lands	Water Bodies	Vegetation Lands	Row	User_ Accuracy	Kappa
1	Urban lands	58	9	0	1	68	0.852 941	0
2	Bare soil lands	0	106	0	3	109	0.972 477	0
3	Water bodies	0	0	9	1	10	0.9	0
4	Vegetation lands	0	7	0	64	71	0.901 408	0
5	Column	58	122	9	69	258	0	0
6	Producer_ Accuracy	1	0.868 852	1	0.927 536	0	0.918 605	0
7	Kappa	0	0	0	0	0	0	0.877 789

Table 8. Confusion matrix for 2016 land cover classification model. The table presents a confusion matrix to assess the agreement between the 2016 land cover classification model and ground truth data.

ID	Class	Urban Lands	Bare Soil Lands	Water Bodies	Vegetation Lands	Row	User_ Accuracy	Kappa
1	Urban lands	32	2	0	1	35	0.914 286	0
2	Bare soil lands	0	89	0	2	91	0.978 022	0
3	Water bodies	0	0	10	0	10	1	0
4	Vegetation lands	0	4	0	114	118	0.966 102	0
5	Column	32	95	10	117	254	0	0
6	Producer_ Accuracy	1	0.936 842	1	0.974 359	0	0.964 567	0
7	Kappa	0	0	0	0	0	0	0.944 032

Table 9. Confusion matrix for 2020 land cover classification model. The table presents a confusion matrix to assess the agreement between the 2020 land cover classification model and ground truth data.

ID	Class	Urban Lands	Bare Soil Lands	Water Bodies	Vegetation Lands	Row	User_ Accuracy	Kappa
1	Urban lands	31	3	0	0	34	0.911 765	0
2	Bare soil lands	0	95	0	3	98	0.969 388	0
3	Water bodies	0	0	9	1	10	0.9	0
4	Vegetation lands	0	3	0	108	111	0.972 973	0
5	Column	31	101	9	112	253	0	0
6	Producer_ Accuracy	1	0.940 594	1	0.964 286	0	0.960 474	0
7	Kappa	0	0	0	0	0	0	0.937 585

Table 10. Confusion matrix for 2023 land cover classification model. The table presents a confusion matrix to assess the agreement between the 2023 land cover classification model and ground truth data.

ID	Class	Urban Lands	Bare Soil Lands	Water Bodies	Vegetation Lands	Row	User_ Accuracy	Kappa
1	Urban lands	38	4	0	0	42	0.904 762	0
2	Bare soil lands	1	99	0	4	104	0.951 923	0
3	Water bodies	0	0	9	1	10	0.9	0
4	Vegetation lands	0	5	0	96	101	0.950 495	0
5	Column	39	108	9	101	257	0	0
6	Producer_ Accuracy	0.974 359	0.916 667	1	0.950495	0	0.941 634	0
7	Kappa	0	0	0	0	0	0	0.910 115

Table 11. Classification accuracy and kappa coefficient (2004–2023). This table presents the changes in overall classification accuracy and kappa coefficient for land cover classification between 2004 and 2023. These metrics are essential for assessing classification quality by comparing results **with** ground truth data.

Year	Accuracy (%)	Kappa Coefficient (%)
2004	92.1569	88.4631
2008	90.625	86.37
2012	91.8605	87.7789
2016	96.4567	94.4032
2020	96.0474	93.7585
2023	94.1634	91.0115
Total accuracy	93.5517	90.2975

desertification control, and natural resource use. The information derived from this study is crucial for decision-makers, land managers, and researchers to develop sustainable land use practices and protect natural resources in Babil Province.

Difficulties and constraints

While progress has been made in classifying land use and land cover using remote sensing and GIS, obstacles persist. The veracity of data is a significant concern due to its dependence on many factors, including the conditions and sensors employed during the data collection process. This is particularly critical due to the difficulty in detecting minute land-use changes and classification complexity. Possible solutions might consist of the following. First, implementing more sophisticated remote sensing platforms and algorithms. Second, more intelligent algorithms: integrating machine learning and deep learning techniques to enhance precision. Third, multi-modal data: incorporating information from multiple sources for a more complete picture. Fourth, particle-based techniques are more adept at capturing nuanced variations in land cover and use. Cost is an additional obstacle. Specific organizations and researchers may encounter challenges in obtaining the necessary resources to acquire and process data. Lastly, imagery with a higher resolution may be required to identify tiny land use and land cover features precisely. Precision, expense, and resolution concerns must be resolved to improve classification of land use and land cover.

Conclusions

Over the last 20 years, this study evaluated changes in land cover and land use in Babil Province, Iraq. The study used remote sensing data from Landsat images taken between 2004 and 2023 to understand the patterns and factors affecting land use and land cover. By conducting temporal analysis, the study identified changes in land use and land cover over time, categorizing the Landsat images into four main types: urban areas, arid regions, bodies of water, and green spaces. The study found three main trends in land use and land cover changes in Babil Province between 2004 and 2023: substantial urban expansion, decreased arid land area, and changes in green space. These changes were caused by human factors such as economic development and population growth and environmental factors such as water discharge policies and precipitation. The study showed that remote sensing and GIS practices are helpful for mapping and monitoring land use and land cover changes over time. Still, more advanced methods, such as artificial intelligence and machine learning, are needed to predict future changes accurately. To improve the accuracy of land use and land cover prediction and classification, future research should incorporate artificial intelligence and machine learning methods, including deep learning. Incorporating diverse data sources, including social, economic, and environmental variables, fosters a comprehensive exploration of the forces shaping land use and land cover dynamics. The findings of this study can help inform sustainable development planning and land management strategies and enhance our understanding of land use and land cover dynamics in Babil Province and similar regions.

Acknowledgments

We would like to express our sincere gratitude to all those who contributed to the success of this research, especially the Hindiya Dam Irrigation Project Directorate in Babil and the Babil Municipality Directorate, for providing us with valuable information and data that contributed to the completion of this work.

References

Abdallah, S., M. Abd elmohemen, S. Hemdan and K. Ibrahem. 2019. Assessment of land use/land cover changes induced by Jizan Dam, Saudi Arabia, and their effect on soil organic carbon. *Arabian Journal of Geosciences* 12(11):350.

Alawamy, J. S., S. K. Balasundram, A. H. M. Hanif and C. T. Boon Sung. 2020. Detecting and analyzing land use and land cover changes in the region of Al-Jabal Al-Akhdar, Libya using time-series Landsat data from 1985 to 2017. *Sustainability* 12(11):4490.

Alqurashi, A. F. and L. Kumar. 2014. Land use and land cover change detection in the Saudi Arabian desert cities of Makkah and Al-Taif using satellite data. *Advances in Remote Sensing* 3(3):106.

Alshari, E. A. and B. W. Gawali. 2021b. Development of classification system for LULC using remote sensing and GIS. *Global Transitions Proceedings* 2(1):8–17.

Alshari, E. A., B. W. Gawali and Y. Li. 2022. Analysis of machine learning techniques for Sentinel-2A satellite images. *Journal of Electrical and Computer Engineering* 2022:9092299.

Aslami, F., A. Ghorbani, B. Sobhani and M. Panahandeh. 2015. Comparing artificial neural network, support vector machine and object-based methods in preparation land use/cover mapsusing landSat-8 images. *Journal of RS and GIS for Natural Resources* 6(3):1–14.

Arvidson, T., S. Goward, J. Gasch and D. Williams. 2006. Landsat-7 long-term acquisition plan: Development and validation. *Photogrammetric Engineering and Remote Sensing* 72(10):1137−1146.

Balarabe, A. T. and I. Jordanov. 2021. LULC image classification with convolutional neural network, *IGARSS 2021—2021 IEEE International Geoscience and Remote Sensing Symposium,* 12–16 July, 2021, Virtual Symposium, Brussels, Belgium (IEEE), pp. 5985–5988.

Bhattacharya, R. K., N. Das Chatterjee and K. Das. 2021. Land use and land cover change and its resultant erosion susceptible level: An appraisal using RUSLE and Logistic Regression in a tropical plateau basin of West Bengal, India. *Environment, Development and Sustainability* 23(2):1411–1446.

Chen, J., X. Zhu, J. E. Vogelmann, F. Gao and S. Jin. 2011. A simple and effective method for filling gaps in Landsat ETM+ SLC-off images. *Remote Sensing of Environment* 115(4):1053–1064.

Dibs, H., H. A. Hasab, J. K. Al-Rifaie and N. Al-Ansari. 2020. An optimal approach for land-use/land-cover mapping by integration and fusion of multispectral landsat OLI images: case study in Baghdad, Iraq. *Water, Air, and Soil Pollution* 231(9):488.

Darem, A. A., A. A. Alhashmi, A. M. Almadani, A. K. Alanazi and G. A. Sutantra. 2023. Development of a map for land use and land cover classification of the Northern Border Region using remote sensing and GIS. *Egyptian Journal of Remote Sensing and Space Science* 26(2):341–350.

Ghayour, L., A. Neshat, S. Paryani, H. Shahabi, A. Shirzadi, W. Chen, N. Al-Ansari, M. Geertsema, M. Pourmehdi Amiri, M. Gholamnia, J. Dou and A. Ahmad. 2021. Performance evaluation of Sentinel-2 and Landsat 8 OLI data for land cover/use classification using a comparison between machine learning algorithms. *Remote Sensing* 13(7):1349.

Hamad, R. 2020. An assessment of artificial neural networks, support vector machines and decision trees for land cover classification using sentinel-2A data. *Sciences* 8(6):459–464.

Hashim, A. H., O. Z. Jasim and M. M. Salih. 2022. The establishing of geospatial database for agricultural lands of Islamic WAQF in Iraq: Case study Babil Province. *IOP Conference Series: Earth and Environmental Science* 961(1):012025.

Kadavi, P. R. and C. W. Lee. 2018. Land cover classification analysis of volcanic island in Aleutian Arc using an artificial neural network (ANN) and a support vector machine (SVM) from Landsat imagery. *Geosciences Journal* 22(4):653–665.

Kaya, İ. A. and E. K. Görgün. 2020. Land use and land cover change monitoring in Bandırma (Turkey) using remote sensing and geographic information systems. *Environmental Monitoring and Assessment* 192(7):430.

Khwarahm, N. R. 2021. Spatial modeling of land use and land cover change in Sulaimani, Iraq, using multitemporal satellite data. *Environmental Monitoring and Assessment* 193(3):148.

Khwarahm, N. R., S. Qader, K. Ararat and A. M. Fadhil Al-Quraishi. 2021. Predicting and mapping land cover/land use changes in Erbil/Iraq using CA-Markov synergy model. *Earth Science Informatics* 14(1):393–406.

Kuemmerle, T., K. Erb, P. Meyfroidt, D. Müller, P. H. Verburg, S. Estel, H. Haberl, P. Hostert, M. R. Jepsen, T. Kastner, C. Levers, M. Lindner, C. Plutzar, P. J. Verkerk, E. H. van der Zanden and A. Reenberg. 2013. Challenges and opportunities in mapping land use intensity globally. *Current Opinion in Environmental Sustainability* 5(5):484–493.

Lv, Q., Y. Dou, X. Niu, J. Xu, J. Xu and F. Xia. 2015. Urban land use and land cover classification using remotely sensed SAR Data through Deep Belief Networks. *Journal of Sensors* 2015(1):538063.

Mahmoud, S. H. and A. A. Alazba. 2016. A coupled remote sensing and the Surface Energy Balance based algorithms to estimate actual evapotranspiration over the western and southern regions of Saudi Arabia. *Journal of Asian Earth Sciences* 124:269–283.

Naik, N., K. Chandrasekaran, V. Meenakshi Sundaram and P. Panneer. 2024. Assessment of land use and land cover change detection and prediction using deep learning techniques for the southwestern coastal region, Goa, India. *Environmental Monitoring and Assessment* 196(6):1–34.

Rahman, M. T. 2016. Detection of land use/land cover changes and urban sprawl in Al-Khobar, Saudi Arabia: An analysis of multi-temporal remote sensing data. *ISPRS International Journal of Geo-Information* 5(2):15.

Ramdani, F., B. Setiawan, A. Rusydi and M. Furqon. 2021. An artificial neural network approach to predict the future land use land cover of great Malang Region, Indonesia.

Rezaei Moghaddam, M., K. Valizadeh Kamran, S. Andaryani and F. Almaspoor. 2015. Comparison of ANN and SVM methods in extraction land use/land cover maps from Landsat 8 satellite image (case study: Sufi Chay Basin). *Geography and Planning* 19(52):163–183.

Rizvon, S. S. and K. Jayakumar. 2022. Strength prediction models for recycled aggregate concrete using Random Forests, ANN and LASSO. *Journal of Building Pathology and Rehabilitation* 7(1):5.

Saddique, N., T. Mahmood and C. Bernhofer. 2020. Quantifying the impacts of land use/land cover change on the water balance in the afforested River Basin, Pakistan. *Environmental Earth Sciences* 79(19):1–13.

Salih, A. 2018. Classification and mapping of land cover types and attributes in Al-Ahsaa Oasis, Eastern Region, Saudi Arabia using Landsat-7 data. *Journal of Remote Sensing and GIS* 7(1):228–234.

Sang, X., Q. Guo, X. Wu, T. Xie, C. He, J. Zang, Y. Qiao, H. Wu and Y. Li. 2021. The effect of DEM on the land use/cover classification accuracy of Landsat OLI images. *Journal of the Indian Society of Remote Sensing* 49 (7):1507–1518.

Shi, W., M. Zhang, R. Zhang, S. Chen and Z. Zhan. 2020. Change detection based on artificial intelligence: State-of-the-art and challenges. *Remote Sensing* 12(10):1688.

Singh, R. K., V. S. P. Sinha, P. K. Joshi and M. Kumar. 2021. A multinomial logistic model-based land use and land cover classification for the South Asian Association for Regional Cooperation nations using Moderate Resolution Imaging Spectroradiometer product. *Environment, Development and Sustainability* 23(4):6106–6127.

Tan, J., J. Zuo, X. Xie, M. Ding, Z. Xu and F. Zhou. 2021. MLAs land cover mapping performance across varying geomorphology with Landsat OLI-8 and minimum human intervention. *Ecological Informatics* 61:101227.

Verburg, P. H., K. Neumann and L. Nol. 2011. Challenges in using land use and land cover data for global change studies. *Global Change Biology* 17(2):974–989.

Vignesh, T. and K. K. Thyagharajan. 2019. Land use and land cover classification using deep belief network for LISS-III multispectral satellite images. *International Journal of Innovative Technology and Exploring Engineering (IJITEE)* 9:94–98.

Wijitkosum, S. 2016. The impact of land use and spatial changes on desertification risk in degraded areas in Thailand. *Sustainable Environment Research* 26(2):84–92.

WHO'S WHO IN ASPRS

Founded in 1934, the American Society for Photogrammetry and Remote Sensing (ASPRS) is a scientific association serving thousands of professional members around the world. Our mission is to advance knowledge and improve understanding of mapping sciences to promote the responsible applications of photogrammetry, remote sensing, geographic information systems (GIS) and supporting technologies.

BOARD OF DIRECTORS

BOARD OFFICERS

President
Bandana Kar
U. S. Department of Energy (DOE)

President-Elect
Amr Abd-Elrahman
University of Florida

Vice President
Alvan Karlin, PhD, CMS-L, GISP
Dewberry

Past President
Lorraine B. Amenda, PLS, CP
Towill, Inc

Treasurer
John McCombs
NOAA

Secretary
Harold Rempel
ESP Associates, Inc.

COUNCIL OFFICERS

ASPRS has six councils. To learn more, visit https://www.asprs.org/Councils.html.

Sustaining Members Council
Chair: Paul Badr
Deputy Chair: Melissa Martin

Technical Division Directors Council
Chair: Hope Morgan
Deputy Chair: Tao Liu

Early-Career Professionals Council
Chair: Greg Stamnes

Region Officers Council
Chair: Demetrio Zourarakis
Deputy Chair: Cody Condron

Committee Chairs Council
Chair: David Day

Student Advisory Council
Chair: Oscar Duran
Deputy Chair: Ali Alruzuq

TECHNICAL DIVISION OFFICERS

ASPRS has seven professional divisions. To learn more, visit https://www.asprs.org/Divisions.html.

Geographic Information Systems Division
Director: Jin Lee
Assistant Director: Michael Baranowski

Lidar Division
Director: Matt Bethel
Assistant Director: Nora May

Photogrammetric Applications Division
Director: Hank Theiss
Assistant Director: Jae Sung Kim

Primary Data Acquisition Division
Director: Srini Dharmapuri
Assistant Director: Ravi Soneja

Professional Practice Division
Director: Hope Morgan
Assistant Director: Christian Stallings

Remote Sensing Applications Division
Director: Tao Liu
Assistant Director: Indu Jeyachandran

Unmanned Autonomous Systems (UAS)
Director: Bahram Salehi
Assistant Director: Rebecca Capps

REGION PRESIDENTS

ASPRS has 13 regions to serve the United States. To learn more, visit https://www.asprs.org/regions.html.

Alaska Region
Dave Parret

Cascadia Region
Jimmy Schulz

Eastern Great Lakes Region
Greg Lemke

Florida Region
Matt LaLuzerne

Gulf South
Cody Condron

Heartland Region
Whit Lynn

Mid-South Region
David Hughes

North Atlantic Region
Kurt Lutz

Northeast Region
Trevis Gigliotti

Pacific Southwest Region
Omar Mora

Potomac Region
Jason Brown

Rocky Mountain Region
Trent Casi

Western Great Lakes Region
Adam Smith

Image Fusion in Remote Sensing: An Overview and Meta-Analysis

Hessah Albanwan, Rongjun Qin, and Yang Tang

Abstract

Remote sensing image fusion is consistently used to turn raw images of different resolutions, sources, and modalities into accurate, complete, and spatiotemporally coherent images. It facilitates downstream applications such as pan sharpening, change detection, and classification. However, image fusion solutions are highly disparate to various remote sensing problems and are often narrowly defined in existing reviews as topical applications (e.g., pan sharpening). Theoretically, image fusion can be applied to any gridded data through pixel-level operations; thus, we expand its scope by comprehensively surveying relevant works. We develop a simple taxonomy for many-to-one and many-to-many image fusion, defining it as a mapping problem turning one or multiple images into another set based on desired coherence. Furthermore, we provide a meta-analysis to cover 10,420 peer-reviewed papers from the 1980s to 2023 studying various types of image fusion and their applications. Finally, we discuss image fusion's benefits and emerging challenges to provide open research directions.

Introduction

Image fusion can be broadly defined as the process of combining information from multiple images into more accurate, complete, and spatiotemporally and semantically coherent output. It has received significant attention in remote sensing (RS) over the years due to the ever-growing development of sensors and platforms, which provide a nearly unlimited archive of earth observation data. Complementary images from different sensors/platforms enable augmented observations of RS data to enrich and expand the knowledge around them (Ghamisi *et al.* 2019; Ghassemian 2016; Pandit and Bhiwani 2015; Pohl and Van Genderen 1998). Existing image fusion methods that fundamentally achieve augmented observations were shown to be of great interest in many RS applications (Alparone *et al.* 2016; Ehlers *et al.* 2010; Ghamisi *et al.* 2019; Ghassemian 2016; Meng *et al.* 2019; Pandit and Bhiwani 2015; Pohl and Van Genderen 1998; Restaino *et al.* 2017). These methods aim to enhance spatial, temporal, and spectral resolutions at the image level while improving the learnable features from various sources to achieve better image interpretation performances (Ghassemian 2016; Pandit and Bhiwani 2015; Pohl and Van Genderen 1998). For instance, by combining low-spatial high-temporal resolution images from MODIS with high-spatial low-temporal resolution images from Landsat, we can generate high-spatial and high-temporal images for more accurate land cover and biomass monitoring applications (Alparone *et al.* 2016; Ehlers *et al.* 2010; Gao *et al.* 2006; Restaino *et al.* 2017). Similarly, high-spectral low-spatial resolution data (e.g., multi-spectral/hyperspectral images) can be used to enhance the spectral resolution of panchromatic images, i.e., pan sharpening (Ehlers *et al.* 2010; Meng *et al.* 2019; Witharana *et al.* 2013; Zhang, Zhang, Wan *et al.* 2023). Beyond single-modal data (i.e., optical images), researchers have also explored using multi-modality data for image-based feature learning (Gómez-Chova *et al.* 2015; Ji *et al.* 2020). These multi-modality data include but are not limited to optical images, lidar (light detection and ranging), and synthetic aperture radar (SAR) data, which have shown that such a feature-level fusion can significantly enhance the performance of machine learning tasks for remote sensing (Ding *et al.* 2022; Huang *et al.* 2022; Kong *et al.* 2021; Rajah *et al.* 2018; Suh and Ouimet 2023; Tan *et al.* 2022; Zhang 2010).

Past literature has provided syntheses of the existing image fusion efforts, focusing on individual topical applications and their specific fusion algorithms. Most review articles focus on the fusion stage, meaning pixel-level, feature-level, or decision-level fusion (Belgiu and Stein 2019; Pandit and Bhiwani 2015; Schmitt and Zhu 2016; Shen *et al.* 2016). Although this provides a technically deep taxonomy for specific fusion tasks (like pan sharpening or multi-modal classification), it largely ignores that these image fusion concepts can also be applicable to other RS tasks and problems. For instance, with some adaptation, fusion techniques used in pan sharpening can be applied to super-resolution or spatiotemporal inference problems (Cai and Huang 2021). In RS, the majority of data is still operating through a raster format defined under a geo-referenced coordinate frame (i.e., projection space) (Chi *et al.* 2016; Liu 2015). On the one hand, this made it relatively easy to register data with respect to each other, and on the other hand, this made it highly effective to implement algorithms to two-dimensional grids where multiple data layers can be fused. Hence, fusion applications on two-dimensional image grids can be easily extended through various RS applications and data products, such as optical images, classification maps, thematic maps, feature maps, digital surface models (DSMs), lidar, and radar images (Alparone *et al.* 2016; Ehlers *et al.* 2010; Ghamisi *et al.* 2019; Ghassemian 2016; Meng *et al.* 2019; Pandit and Bhiwani 2015; Pohl and Van Genderen 1998; Restaino *et al.* 2017; Wang *et al.* 2022). These products, although presented as two-dimensional rasters, possess completely different content associated with different uncertainties and numerical values and are used in completely different applications. Therefore, a comprehensive survey of current image fusion practices is necessary to gain a broader understanding of the concept and explore ways to adapt their methods to various RS tasks and image types.

This systematic review focuses on providing a comprehensive review and a meta-analysis on the topic of image fusion in the RS field. Despite the significant difference in the type of image fusion and its applications, we consider that their fusion methods can share similar concepts. Therefore, the framework used in one method can be used to augment other types of images and applications. For example, fusion techniques used for super-resolution can also be applied for pan

Hessah Albanwan is with the Civil Engineering Department, Kuwait University and the Geospatial Data Analytics Lab, The Ohio State University (hessah.albanwan@ku.edu.kw).

Rongjun Qin is with the Geospatial Data Analytics Lab, the Department of Civil, Environmental and Geodetic Engineering, the Department of Electrical and Computer Engineering, and the Translational Data Analytics Institute, The Ohio State University (qin.324@osu.edu).

Yang Tang is with the Geospatial Data Analytics Lab and the Department of Civil, Environmental and Geodetic Engineering, The Ohio State University.

Corresponding author: Rongjun Qin (qin.324@osu.edu)

Received October 11, 2024, accepted November 11, 2024.

Photogrammetric Engineering & Remote Sensing
Vol. 90, No. 12, December 2024, pp. 755–775.
0099-1112/22/755–775

doi: 10.14358/PERS.24-00110R1

sharpening (Cai and Huang 2021; Chen, Qi *et al.* 2022; Su *et al.* 2022), while methods used to process and fuse time-series analysis, such as filtering, can be used for image preprocessing (Bisquert *et al.* 2015; Chen *et al.* 2004; Reiche *et al.* 2015). In this paper, we expand the scope of image fusion, as practiced in the RS community, by providing a simple yet comprehensive taxonomy that defines fusion as a mapping function operating on different numbers of images to output single or multiple images. We also show that despite the significant "input–output" difference, the fusion problem can be explained by a framework that is conceptually easy yet comprehensive enough to encapsulate the existing technical taxonomy of fusion on its fusion stages. In addition, publications informed by the meta-analysis are used as measuring entities to evaluate current scientific activities and future projections, such as fusion algorithms and applications. We conducted a search in Scopus for all original peer-reviewed publications on the subject of image fusion in RS published between 1980 and 2023. We reviewed 10,420 articles related to image fusion and its applications in RS, covering specific fusion algorithms and downstream applications in studying urban and environmental issues. The meta-analysis plays a significant role in providing insights into the most recent fusion techniques and current applications, specifically the learning-based and deep-learning methods, which have become very popular and require a literature update.

The rest of the paper is divided into four main sections. The section after this one provides an overview of the image fusion problem in RS; it introduces the background information on the main challenges of fusion in the RS field, the proposed taxonomy, and the most recent fusion approaches. The ensuing section describes the structure and guidelines followed in this meta-analysis to review image fusion and its evolution in RS over the years; this includes the paper selection criteria and assessment methods. The section after that presents the results of this meta-analysis, including the quantitative statistical analysis of the number of publications, applications, approaches, etc. The final section concludes the key findings of this review with an open discussion on the main challenges and potential future works of RS image fusion.

Overview of Remote Sensing Image Fusion

Despite current RS technologies and sensor advances, image fusion still faces many challenges. Factors of concern such as the image quality (e.g., noise level, blurriness, and radiometric imbalances), the complexity of the scene (e.g., convoluted dense urban and greenspace, homogeneous vegetated regions with high seasonal differences), and the processing algorithms (e.g., modeling errors and propagated errors) play important roles in the fusion solutions. Therefore, understanding these contributing factors is essential to comprehend the fusion problem and the capabilities of its algorithms. In this section, we discuss the main factors affecting image fusion quality, the proposed taxonomy that categorizes fusion into two groups based on current practices, and finally, the fusion methods currently in use for various RS applications.

Factors Affecting the Quality of Remote Sensing Image Fusion

As mentioned in the previous section, a typical RS image is two-dimensional raster data representing physical information about a surface area on Earth. The raster "data" can be of any type, such as optical images, elevation maps (e.g., digital elevation model [DEM], digital surface model [DSM], and digital terrain model [DTM]), classification maps, thematic maps, radar images, feature maps, etc. The pixel information of these images can be directly obtained from sensors (e.g., radiometry) or derived from specific algorithms (e.g., elevation maps from photogrammetry methods). In both cases, inconsistency invariably exists due to the varying imaging conditions (e.g., acquisition angle, weather, and season) or errors propagating through the processing algorithms (e.g., DSM errors), leading to low-quality input and fusion output. This section summarizes three crucial factors: radiometric inconsistency, spatiotemporal consistency, and derived/propagated errors from image products such as elevation maps. Details are in the following sections.

Radiometric Inconsistency

Radiometric inconsistency refers to heterogeneous spectral information of objects when observed by different images under varying acquisition conditions (Barsi *et al.* 2019). For instance, Figure 1a shows the same objects in images under different sun angles and sensor viewing directions, where corresponding pixels show different brightness and chromaticity. Sensors themselves, due to different calibration and spectral responses, may also produce spectral heterogeneities (Chen *et al.* 2018; Syariz *et al.* 2019; Yuan and Elvidge 1996). As another example, Figure 1b shows two images for an area in Haiti taken by GeoEye (original ground sampling distance [GSD]: 0.5 m) and IKONOS (original GSD: 1 m), resampled to the same GSD (1 m), which still show very different contrasts and saturations. Phenological changes, such as those affected by atmospheric conditions and seasons, may also produce spectrally variant images (Albanwan and Qin 2018; Lin *et al.* 2013). Figure 1c shows an example of five Planet satellite images capturing the same scene within 1 year, with significant appearance differences among different collections, as shown by the varying histogram of intensity in the same spectral band across different images. Varying imaging conditions can lead to temporally inconsistent information between input images. For instance, shadow in images can block partial information on critical features (e.g., building corners), land cover types, or vegetation health (Zhu *et al.* 2018; Messina *et al.* 2020; Asokan and Anitha 2019) . Because most fusion algorithms expect spectrally homogenous images, these problems may lead to incorrect use of pixel information data, leading to low-quality fusion results. In some applications, radiometric differences and temporal consistency are more important to consider, while these factors are less important to other applications. For instance, satellite images used to monitor vegetation health often have significant radiometric differences because of their long revisiting times (e.g., days, weeks, or months). In contrast, UAV/drone images can capture images within 1 to 3 days, which can lower the radiometric differences significantly for a better study of vegetation health (Messina *et al.* 2020).

Spatiotemporal Inconsistency

The spatiotemporal inconsistency of RS data refers to images covering the same geographical area but presenting different scene content due to land cover changes over time (Asokan and Anitha 2019). This type of inconsistency can sometimes be convoluted by the radiometric inconsistency caused by sensors (explained under "Radiometric Inconsistency") because images capturing a scene of a different time may come from a different sensor in one or multiple satellite constellations. Typically, spatiotemporal inconsistencies are due to natural causes such as seasons, phenological cycles, disasters, etc., or anthropogenic activities such as urban development, wars, demolitions, etc. An example of the phenological growth of crops is shown in Figure 2a, in which we can see the vegetated area in the suburban terrain in September turned into barren land in December, leading to significant appearance changes. Figure 2b shows another example of the spatiotemporal inconsistency, presenting land cover and land use differences caused by the 2010 earthquake in Haiti and the status of the same areas in 2015. The images show newly constructed buildings (highlighted in the top and middle circle pairs between 2010 and 2015 in Figure 2b) and a barren land previously occupied by shelters due to the earthquake (see the bottom circle pair between 2010 and 2015 in Figure 2b). On the one hand, these inconsistencies tell the surface dynamics; on the other hand, when these images are directly used for super-resolution, they will undoubtedly produce haunted effects (Zhu, Tang *et al.* 2018). Therefore, strategies for dealing with or avoiding these inconsistencies are necessary for successful fusion applications.

Propagated Error

Processed RS data, such as classification maps or stereo-based DSM, may contain errors during data processing (Hamid *et al.* 2020; Zhou *et al.* 2020). For example, a typical DSM generation pipeline includes steps such as epipolar rectification, stereo matching, and triangulation from point clouds, which may accumulate errors due to numerical and modeling approximation (Bosch *et al.* 2016; Qin 2019) in these steps. An example DSM generated using a semiglobal matching (SGM) algorithm (Hirschmuller 2005) is shown in Figure 3a, where visible noises can be observed on both flat surfaces and building boundaries. Such errors are typical and can be algorithm-dependent; for example, certain stereo-matching algorithms produce sharper boundaries but produce

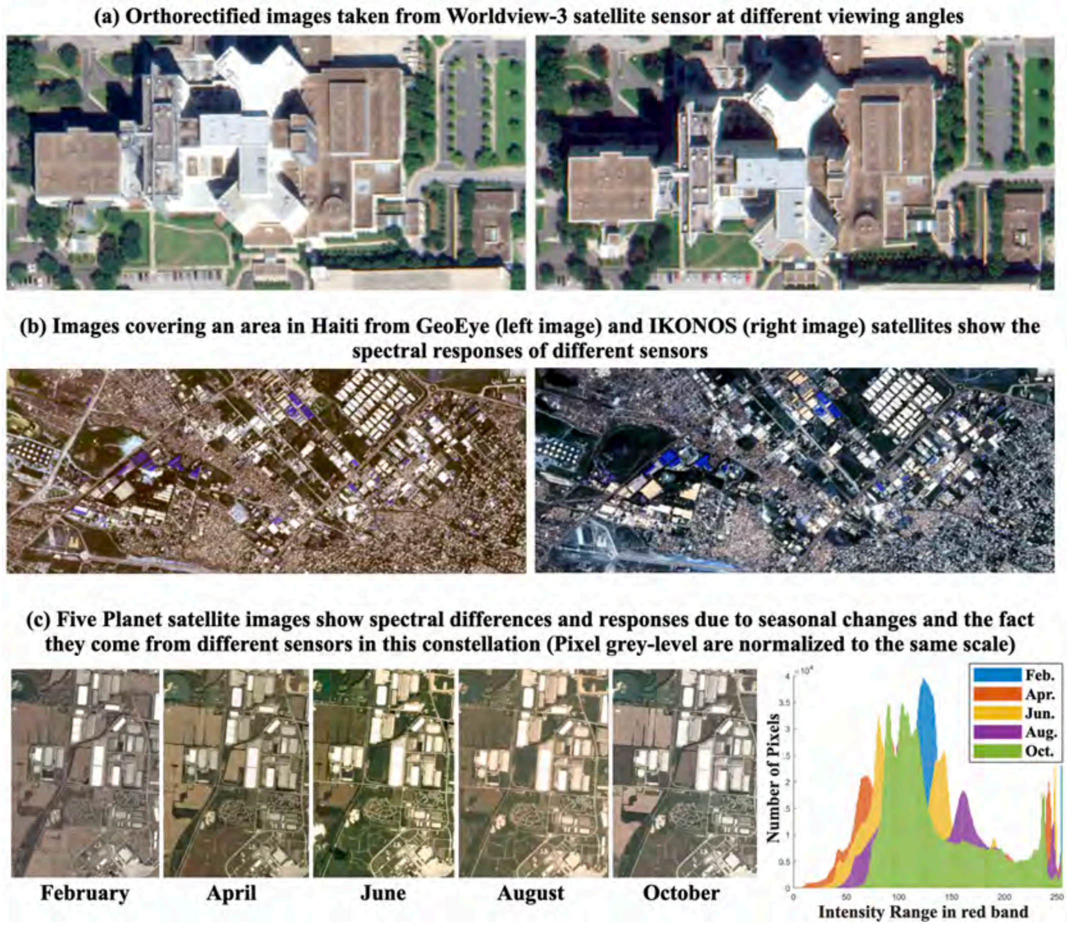

Figure 1. Examples of radiometric inconsistencies between RS images due to differences in (a) viewing direction (different shading), (b) sensors (oblivious visual differences), and (c) season (evidenced by the varying histograms of different images of the same scene).

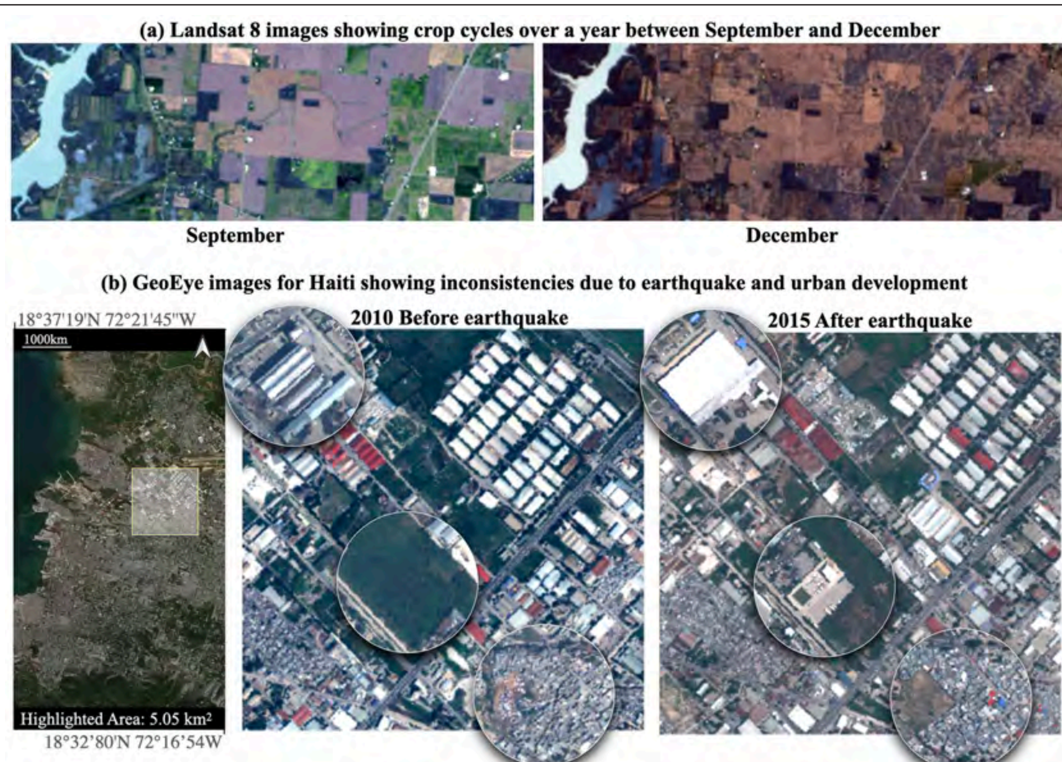

Figure 2. Examples of spatiotemporal inconsistencies are shown in RS images due to (a) natural causes, such as crop cycles, and (b) natural and human causes, like earthquakes and new constructions.

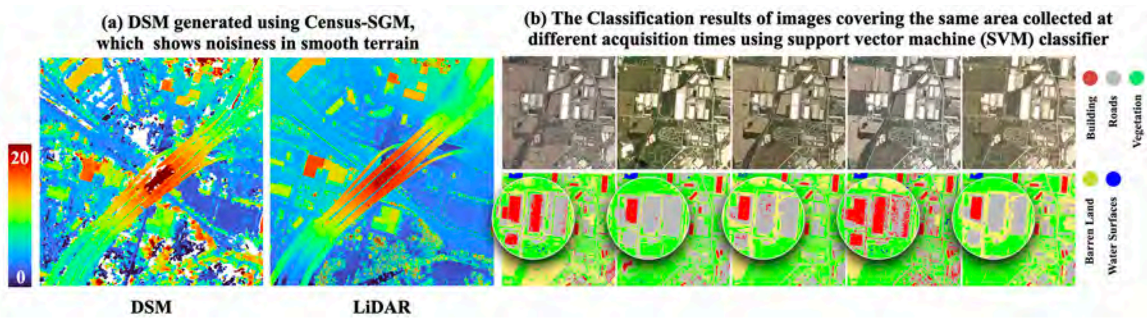

Figure 3. Examples of algorithmic errors producing noisy data at their respective modalities. (a) Digital surface model (DSM) generated by stereo matching algorithm showing salt-and-pepper noise on smooth objects (e.g., roads and building roofs). (b) Classification maps with wrong and inconsistent labels, affected by the image illustration variance. For example, the three buildings in the circled region are misclassified (in different ways) as roads and other classes. LiDAR = light detection and ranging.

salt-and-pepper noises (such as using normalized cross-correlation algorithms [Wan *et al.* 2019]), whereas algorithms that enforce smoothness (e.g., global matching algorithms, such as SGM and deep-learning methods such as PSMNet [Chang and Chen 2018]) will produce less salt-and-pepper noise but may omit important elements and sharpen structures , such as small and tall buildings. Therefore, understanding such characteristics as priors for fusion is beneficial.

Following a similar consideration, when classification maps are used for fusion, errors from classification maps may yield inconsistent fusion results. For example, Figure 3b shows classification maps predicted from images captured at different times with only days of difference, where the illumination differences result in different noise levels, sometimes being quite substantial (i.e., a large portion of the barren land is mixed with the vegetation class over the short time) due to the variable factors in both the modeling training and the bias of the data sets (Al-Najjar *et al.* 2019). The errors introduced by these learning models may create large outliers in semantic inconsistency and typically no longer follow a simple Gaussian distribution, which may directly lead to the failure of fusion algorithms that simply consider linear, weighted, and concatenation fusion.

Generic Taxonomy of Remote Sensing Image Fusion

Image fusion is a highly disparate topic that can be applied to various RS tasks. In the current literature, these different fusion tasks are often narrowly defined within their own methodological domain. For example, pan sharpening is often considered an independent task other than super-resolution. However, many of these fusion tasks are of a similar nature, and their methodologies share common strategies. The generic fusion problem can be described mathematically: given a set of observations $X = \{x_1, x_2, x_3, \ldots, x_n | x_i \in \mathbb{R}^{w,h,c_x}\}$, where w, h and c_x refer to the width, length, and number of channels for raster data. Thus, X can be represented as a tensor belonging to $\mathbb{R}^{w \times h \times c_x \times n}$. A simple linear fusion algorithm aims to convolute the tensor X, through each individual observation via a mapping function $f(X)$ and output another tensor $Y = \{y_1, y_2, y_3, \ldots, y_m | y_i \in \mathbb{R}^{w,h,c_x}\}$, where c_y refers to the number of channels for each one of the m outputs; thus, Y can be represented as a tensor belonging to $\mathbb{R}^{w \times h \times c_y \times n}$ as follows:

$$Y = f(X) \tag{1}$$

This is easily extendable when $f(\bullet)$ is a nonlinear function involving more complex and multi-step mappings (Belgiu and Stein 2019; Pohl and Van Genderen 1998; Shen *et al.* 2016). Here, depending on $m \geq 1$, we categorize these strategies into two parts, with the simplest "input–output" fashion, being either 1) "many-to-one (M2O)," meaning that multiple input images are fused into a single-image output representing enhanced results, where these several inputs often refer to multiple homogenous observations and the fusion of which refers to output with enhanced spatial/spectral resolution or accuracy, or 2) "many-to-many (M2M)," meaning that several input images are fused into several outputs (often an equivalent number) with enhanced spatiotemporal resolution. Figure 4 illustrates how the taxonomy integrates pixel-, feature-, and decision-level fusion paradigms within both many-to-one and many-to-many frameworks. This provides a broader contextual framework for understanding how data fusion can be applied across different stages of analysis. The relationship between these fusion levels is separative and adjustable, meaning that each level can be applied independently and multiple times. For example, decision-level fusion can occur before/after either or both of the other levels, depending on the specific analysis requirements. The following subsections will further explain the details of M2O and M2M.

Many-to-One Image Fusion

M2O image fusion refers to the process of combining several images into a single image. M2O problem serves many applications, such as examples illustrated in Figure 4, including pan sharpening, super-resolution, DSM fusion, multi-modal feature learning for classification, background image generation for tracking, etc. (Du *et al.* 2019; Gao and Lim 2019; Geng *et al.* 2022; Ji *et al.* 2020; Kang *et al.* 2014; Ma *et al.* 2019; Meng *et al.* 2017; Nguyen *et al.* 2020; Palsson *et al.* 2014; Papathanassiou and Petrou 2005; Qin *et al.* 2022; Restaino *et al.* 2017; Vivekananda *et al.* 2021; Zerrouki *et al.* 2022). These fusion problems have been intensively investigated over the years (Ghassemian 2016; Pandit and Bhiwani 2015; Pohl and Van Genderen 1998). The general premise is that the information of different inputs residing in the same pixel location should refer to the same static object with the same or complementary modality. Therefore, the goal of the fusion can be generally categorized into three aspects: 1) estimate a more accurate observation of the same pixel using the redundant pixel information from these multiple inputs (e.g., super-resolution, pan sharpen, and DSM fusion) (Belov and Denisova 2020; Kawulok *et al.* 2020; Liu *et al.* 2021; Meng *et al.* 2019; Papathanassiou and Petrou 2005; Qin *et al.* 2022; Stucker and Schindler 2020; Vivone 2019; Zhu, Tang *et al.* 2018); 2) generate a background image to represent the static scene in preparation for object tracking (Carvalho *et al.* 2011; Chen, Ferreira *et al.* 2022; Lu *et al.* 2006; Prakash and Gupta 1998; Wu *et al.* 2016; Zhang *et al.* 2022); and 3) extract and fuse features from different modalities (different spectral bands, height, microwave reflectance) to achieve enhanced classification results to generate accurate thematic maps (Albanwan *et al.* 2020; Bruzzone and Carlin 2006; Cui *et al.* 2018; Du *et al.* 2012; Gao and Lim 2019; Lo *et al.* 2022; Lucas *et al.* 2007; Nguyen *et al.* 2020; Vivekananda *et al.* 2021; Zhou *et al.* 2008).

Many-to-Many Image Fusion

M2M image fusion combines the knowledge/information from multiple images by simultaneously or sequentially processing them to yield a group of refined images, often matching the number of inputs. This type of fusion is mostly used for applications that require a bundle of enhanced images, such as multi-image filtering, change detection over time, multi-view three-dimensional reconstruction, spectral coherence between a group of images, and constant monitoring of the earth's surface (Albanwan and Qin 2018; Albanwan *et al.* 2020; Bovolo and Bruzzone 2007; Camps-Valls *et al.* 2008; Erkkilä and Kalliola 2004; Gulácsi and Kovács 2015; Vivekananda *et al.* 2021; Yanovsky and Qin 2021). The general premise of this type of image fusion is that the information of different inputs residing in the same pixel location represents a certain state of the objects in that pixel, which are complementary to each other, such that these inputs can be used to augment others and produce refined outputs that have more accurate pixel information per output. For example, shown in Figure 4, spatiotemporal filtering approaches aim to denoise individual images using inputs in a temporal direction, such that pixels polluted by atmospheric conditions can be recovered using other images acquired under better atmospheric conditions. Thus, similar to the M2O category, it exploits spatial and temporal correlations between images, which are the key ingredients to providing accurate and reliable fused images. Examples of applications in this category may include spatiotemporal fusion to achieve an augmented spatial and temporal resolution of an image sequence, satellite video data augmentation, object tracking, and time-series analysis (Chen, Ferreira *et al.* 2022; Gan *et al.* 2021; Viana *et al.* 2019; Wu, Ge *et al.* 2018; Wu, Sun *et al.* 2018; Xie *et al.* 2017; Zeng *et al.* 2013; Zhang *et al.* 2022).

General Fusion Approaches in Remote Sensing

Image fusion approaches have been developing rapidly over the years to tackle the fundamental challenges mentioned under "Factors Affecting the Quality of Remote Sensing Image Fusion" and fuel various RS applications. Methods supporting both M2O and M2M fusion can range from simple arithmetic operations to complex learning-based approaches (i.e., machine learning [ML] and deep learning [DL] methods). The choice of fusion approach mainly depends on the type of integrated images and applications. For example, combining multi-modal or multi-source images (e.g., RGB image and DSM) to synthesize mixed modality data requires adaptation of differences in image structures, viewing perspectives, resolutions, platforms, etc. Feature-level fusion integrates these diverse modality data into a common feature space prior to fusion. In contrast, unimodal image fusion, due to the modality information, can be directly fused (through linear operations) and often starts from pixel-based operations (e.g., averaging). The RS applications themselves define the necessary level of accuracy for the fusion algorithm. For example, averaging multi-temporal images can be sufficient to achieve moderate accuracy for scene-level information extraction (e.g., crop yields prediction), while performing per-pixel image interpretation (e.g., semantic and panoptic segmentation) for urban scenes with buildings and trees of different scales, weighted averaging, or learned fusion at various levels can be more effective (Albanwan and Qin 2020; Albanwan *et al.* 2020; Dadrass Javan *et al.* 2021; Pandit and Bhiwani 2015). Understanding these factors is essential to developing an efficient fusion algorithm that can adapt to different images, scenes, and applications.

In general, fusion methods can be categorized into two groups: classic arithmetic methods (called "classic methods" hereafter) and machine- and deep-learning methods (called "learning-based methods" hereafter). Classic fusion methods perform basic operations to combine images based on statistical, numerical, and domain transform methods (Albanwan and Qin 2018; Amrani *et al.* 2017; Gan *et al.* 2021; Helmer and Ruefenacht 2005; Lacewell *et al.* 2010; Nagamani *et al.* 2021; Xie *et al.* 2017; Yu *et al.* 2011). These methods (mostly based on linear operations) are primarily pixel-based and are operated locally (e.g., color transformation from RGB to intensity–hue–saturation [IHS]). Classic fusion methods are not data driven and do not require complex structures to formulate the fusion problem; thus, they are considered simple to implement and efficient to run. However, these methods assume fixed and known data and noise distribution (e.g., normally distributed) and thus may not adapt well to different data types, scene contents, and distributions. On the other hand, the learning-based methods have recently shown remarkable performances in many image fusion tasks (Maxwell *et al.* 2018; Wang *et al.* 2023). Examples of these methods include classic statistical ML and DL methods (Arefin *et al.* 2020; Camps-Valls *et al.* 2008; Erkkilä and Kalliola 2004; Gao and Lim 2019; Kawulok *et al.* 2020; Lucas *et al.* 2007; Ma *et al.* 2019; Salvetti *et al.* 2020), which outperform many classic fusion methods due to their ability to extract complex features and patterns from images. Nevertheless, adaptivity and generalization of these methods are considered a challenge unless high-quality input training data are available, which can be very expensive considering the geographically diverse domain of RS images. This section will review the classic and learning-based image fusion methods and highlight their unique advantages and limitations. A summary of image fusion methods is shown in Table 1.

Classic Image Fusion Methods

Classic image fusion methods are mostly nonlearning approaches based on statistical, numerical, and domain transformation methods.

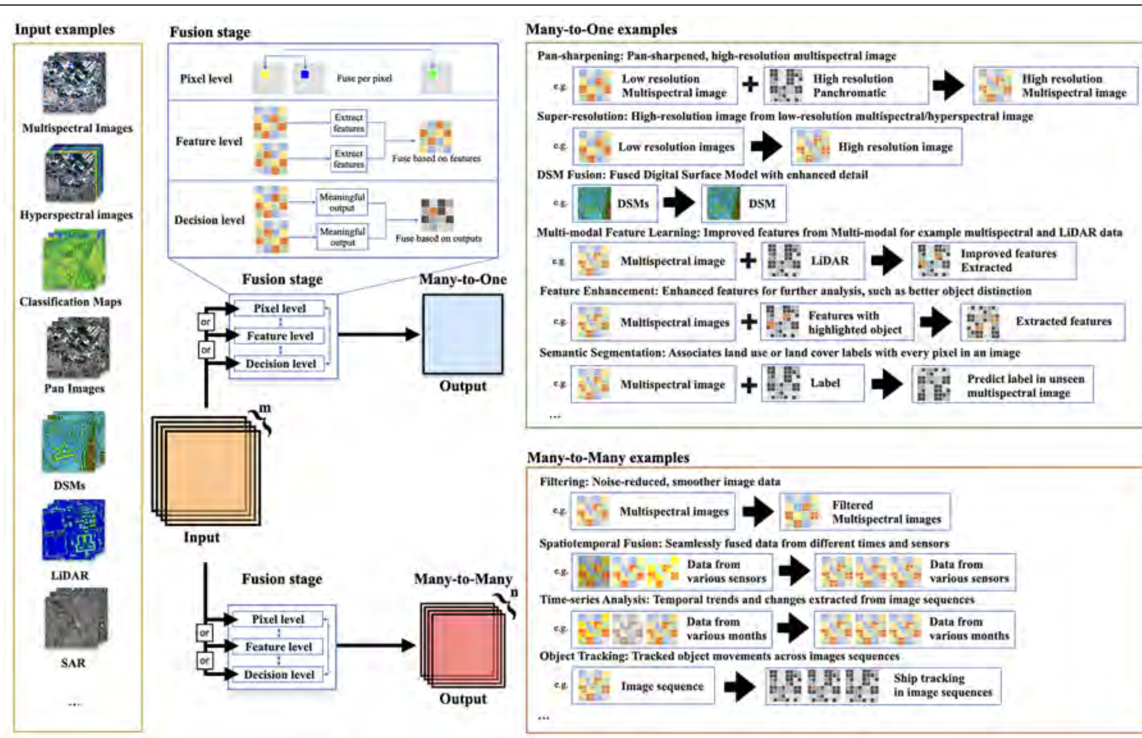

Figure 4. Overview of the types of image fusion in remote sensing. Note: the letters m and n in the figure denote the numbers of input and output images, respectively. DSM = digital surface model; SAR = synthetic aperture radar; LiDAR = light detection and ranging.

Table 1. Image fusion methods in remote sensing field.

Type of Method			Method		Examples	M2O	M2M
Image Fusion Methods in Remote Sensing	Classic Image Fusion Methods	*Statistical/probability-based methods*	Statistical filtering	Basic statistical methods	Average	Kang *et al.* 2014; Wu *et al.* 2005	Li *et al.* 2023
					Median	Qin 2017	NA
					Standard deviation	Yıldırım and Güngör 2012	Ezimand *et al.* 2021
					Histogram	Nagamani *et al.* 2021	Helmer and Ruefenacht 2005
				Spatiotemporal filtering	Bilateral filter	Kotwal and Chaudhuri 2010	Albanwan and Qin 2018
					Spatiotemporal filter	Gao *et al.* 2006	Albanwan *et al.* 2020; Gan *et al.* 2021
					Statistical weighting	Qin *et al.* 2022	Lu *et al.* 2014
					Image-guided filter	Albanwan and Qin 2022, 2020	Guo *et al.* 2021; Huang *et al.* 2020
			Probabilistic modeling		Maximum a posteriori	Shen and Zhang 2009	He *et al.* 2020
					Bayesian fusion	Xue *et al.* 2017; Zhang *et al.* 2009	He *et al.* 2017
					Dempster–Shafer theory	Lu *et al.* 2006	Cayuela *et al.* 2006
		Transformation-based fusion	Interpolation/ extrapolation		Spline	Anger *et al.* 2020	Pan *et al.* 2017
					Bicubic	Jing *et al.* 2023	NA
					Kriging	Li *et al.* 2020	Hu *et al.* 2017
			Regression		Linear regression	Vivone *et al.* 2018	Wu, Sun *et al.* 2018; Zeng *et al.* 2013; Zhang *et al.* 2015
					Least squares method	Huang *et al.* 2017	Nielsen 2002; Zeng *et al.* 2013
			Partial differential equations			Bavirisetti *et al.* 2017; Liu *et al.* 2012	Nazari *et al.* 2015
			Optimization		Iterative methods	Canty and Nielsen 2008; Vivone *et al.* 2018	Albanwan *et al.* 2020
		Transformation-based fusion	Spatial domain transformation	Color transformation	Intensity–hue–saturation	Chavez *et al.* 1991	Leung *et al.* 2014
					Brovey transformation	Gharbia *et al.* 2014	Nichol and Wong 2005; Yang *et al.* 2012
				Projection and substitution	Principal component substitution	Chen *et al.* 2020	Achour *et al.* 2022
					Gram–Schmidt	Restaino *et al.* 2017	Dalla Mura *et al.* 2015
			Frequency domain transformation		Fourier transform	Chen *et al.* 2023; Zeng *et al.* 2020	Denipote and Paiva 2008; Lillo-Saavedra *et al.* 2005
					Discrete Fourier transform	Akoguz *et al.* 2014; Zhou *et al.* 2022	Cui *et al.* 2010
					Discrete cosine transform	Alhatami *et al.* 2022; Yu *et al.* 2008	Yang *et al.* 2022
			Wavelet transformation		Continuous wavelets transform	Amolins *et al.* 2007; Cheng *et al.* 2015; Wu *et al.* 2005	Muhammad *et al.* 2002; Zhang *et al.* 2020
					Discrete wavelets transform	Jinju *et al.* 2019; Lacewell *et al.* 2010; Zhuang *et al.* 2017	Cui and Datcu 2012
			MRA		Curvelet transform	Choi *et al.* 2005	Nencini *et al.* 2007; Rao *et al.* 2014
					Laplacian pyramids transform	Alparone *et al.* 2016; Su *et al.* 2021	NA
	Learning-based Image Fusion Methods	*ML methods*			Support vector machine	Du *et al.* 2012; Zheng *et al.* 2008	Wang *et al.* 2019
					Random forest	Nie *et al.* 2021; Seo *et al.* 2018	Farhadi and Najafzadeh 2021
					K-means clustering	Lv *et al.* 2019	Fuss *et al.* 2016
		DL methods	DL for spatial–spectral image fusion		CNNs	Scarpa *et al.* 2018; Shao and Cai 2018; Zhong *et al.* 2016	Kavran *et al.* 2023; Yin *et al.* 2021
					ResNet	Kawulok *et al.* 2020; Wei *et al.* 2017	Dang and Li 2021
					U-Net	Qin *et al.* 2019; Yao *et al.* 2018	Fang *et al.* 2023
			DL for spatiotemporal image fusion		RNNs	Yang *et al.* 2021	Wang *et al.* 2023
					LSTM	Chang and Luo 2019; Theran *et al.* 2019	Mou *et al.* 2019
					Gated recurrent unit	Arefin *et al.* 2020; Zhou *et al.* 2023	Zeng *et al.* 2022
					Attention mechanism	Liu and Wang 2022; Salvetti *et al.* 2020	Gong *et al.* 2022
					Transformers	Roy *et al.* 2023; Scheibenreif *et al.* 2022	Aleissaee *et al.* 2023; Li, Chen *et al.* 2022

CNN = Convolutional neural network; DL = deep learning; LSTM = long short-term memory; M2M = many-to-many; M2O = many-to-one; MRA = multi-resolution analysis; NA = not applicable; ResNet = residual network; RNN = recurrent neural network.

These methods have a simple structure and do not require complex modeling of the fusion problem or learning from large data sets; thus, they are relatively easy to implement and considered computationally fast, and for a long time, they served as the mainstream methods for practical uses. Most of these methods perform local operations to inform from neighboring pixels in space or time and eventually apply them for noise removal and purifying the fused results. Figure 5 shows an overview of the classic image fusion, in which several DSMs are fused using median filtering and per-pixel operations to update every pixel using information from their neighbors. Depending on how the local pixel information is used, the classic fusion methods are further divided into three categories: 1) statistical/probability-based methods, which mostly assume linear operations on local pixel values to yield fused results; 2) prediction-based methods, which use designated functions to explicitly model the mapping between the input pixel values and the fused values; and 3) transformation-based fusion, which fuses information under a transformed space. Nevertheless, classic methods are less effective in using long-range dependencies to handle complex nonlinear input inconsistencies. Therefore, they may only address fusion problems of which the inconsistencies are due to assumed/relatively simple noise distributions (e.g., Gaussian distribution), while they may fall short when processing input images that come with inconsistency due to complex/unknown noise distributions.

Statistical/Probability-based Methods

Statistical methods explore the statistical properties of pixel values within a local window (spatially and/or temporally) and can be used effectively for both types of image fusion (i.e., M2O and M2M). Examples of these methods include using mean, median, standard deviation, and histograms as means to compute the updated pixel values. For a long time, statistical filter-based methods have dominated the fusion approaches (Albanwan and Qin 2018, 2020; Cheng *et al.* 2017; Rothermel *et al.* 2016) due to their simplicity and the ability to easily scale to large-format remote sensing images. Given the input of a stack of images, statistical filters produce smoothed images and suppress unwanted noise during the fusion process, in which the statistical quantities play roles (i.e., mean, median, etc.). The window size was considered a hyperparameter, which may affect the fusion results depending on the noise level of the input. A tangible strategy is to create "soft" weighting for pixels within a window to reflect the contribution of each pixel in the fusion process. To adaptively determine the weight of each pixel, statistical quantities, such as entropy, can be used as the uncertainty/confidence of the pixels, meaning that the higher the entropy value, the more informative it can be, which should receive a higher weight. Of course, there are also other means of defining the weights, such as the use of an adaptive filtering kernel (Qin 2017) or through guided filtering (Guo *et al.* 2021; Huang *et al.* 2020), as well as filters based on derived statistical hypotheses from the images themselves, such as maximum likelihood, maximum posterior, Dempster–Shafer theory, and Bayesian fusion (Ghassemian 2016; Lu *et al.* 2006; Shen and Zhang 2009; Xue *et al.* 2017). Many studies have suggested using image segments to guide the fusion (Albanwan and Qin 2022; Ma *et al.* 2019; Qin *et al.* 2019), which would change the window size adaptively based on semantic segmentation.

Prediction-based Methods

Pixel-level prediction considers image fusion as a pixel-level prediction problem, meaning that given a set of input images, the image fusion problem aims to predict pixel values for a new grid as the fused results. Different from the statistical filter method, the pixel-level prediction method allows the prediction of pixel values of a grid with a size different from the original grid, which extrapolates pixel values at cells in which the original information is unavailable or at a coarser granularity. Examples of pixel-level prediction methods include super-resolution (Xie *et al.* 2017) and spatiotemporal prediction for time-series analysis (Hu *et al.* 2017; Pan *et al.* 2017; Wu, Ge *et al.* 2018). For instance, for super-resolution, images are up-sampled to larger sizes, creating a new mesh or gridded format of an image with old values and empty cells, which are to be filled by interpolated values calculated from neighboring pixels using methods such as spline, bicubic, Kriging , etc. (Belov and Denisova 2020; Lanaras *et al.* 2017; Nasrollahi and Moeslund 2014; Xie *et al.* 2017; Yanovsky and Qin 2021). Typical interpolation methods operate in local domains, which are fast yet can be easily polluted by data impurities and noise of neighboring pixels. Methods like regression-based approaches aim to use a wider data receptive field, which can provide better inference by modeling the relationship between the raw pixel values and the predicted values (Helmer and Ruefenacht 2005; Luppino *et al.* 2019; Zhang *et al.* 2015; Haack and Rafter 2010; Vivone *et al.* 2018; Zeng *et al.* 2013). Kernel regression serves as one of the key approaches, in which the model parameters (e.g., weights and biases) of the regression kernel can be estimated with robust estimation approaches such as robust least squares (Huang *et al.* 2017) with sometimes outlier removal algorithms such as random sample consensus (Fischler and Bolles 1981). Postprocessing methods, such as Bayesian regularization (He *et al.* 2017) and Markov–Random Field (Touati *et al.* 2020), can be used to create fusion results under certain priors.

Transformation-based Fusion

Domain-transformation methods decompose images into different domains or representations and perform the data fusion under the transformed domain, such as different color space, frequency, or wavelet domains (Guo *et al.* 2017; Lacewell *et al.* 2010; Sirguey *et al.* 2008). These approaches can improve the robustness of image fusion for some tasks. For example, they can be used for spatial resolution enhancement due to their ability to preserve spatial information and fine details in images (e.g., in the frequency domain); at the same time, they are not affected by spectral distortions. Domain transformation methods can be operated in the spatial, frequency, or other transformed domains, such as wavelet transformation (Amolins *et al.* 2007; Amro *et al.* 2011; Cheng *et al.* 2015; Dadrass Javan *et al.* 2021; Jinju *et al.* 2019; Pohl and Van Genderen 1998; Wu *et al.* 2005). The spatial domain includes techniques such as color transformation (e.g., IHS and Brovey transformation) or projection and substitution (e.g., principal component substitution, Gram–Schmidt [GS]) (Amro *et al.* 2011; Dadrass Javan *et al.* 2021; Pohl and Van Genderen 1998). The frequency domain uses techniques related to the Fourier transform and its variants (e.g., discrete Fourier transform or cosine transform) (Alhatami *et al.* 2022; Denipote and Paiva 2008). In contrast, wavelet transform includes

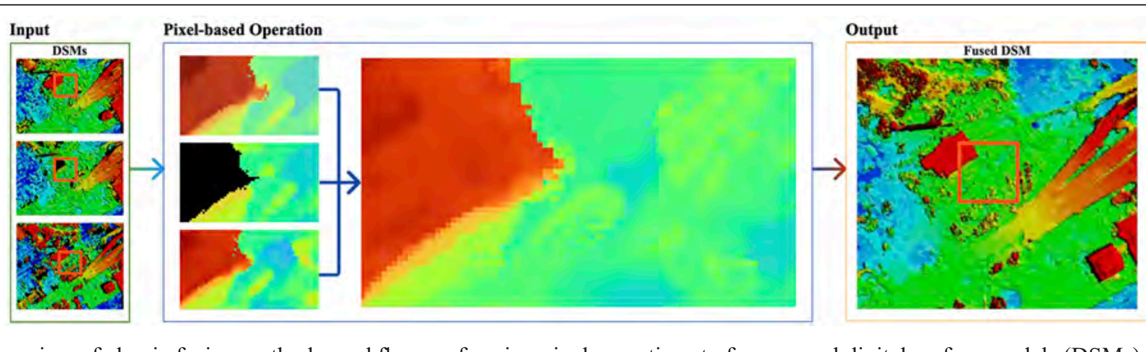

Figure 5. Overview of classic fusion methods workflow performing pixel operations to fuse several digital surface models (DSMs) into a single DSM (as a case of many-to-other image fusion), where the value of the central pixel in the orange box is updated using their neighboring pixels in space and time.

methods like continuous wavelet transform and discrete wavelet transform, as well as their variants (Amolins *et al.* 2007; Cheng *et al.* 2015; Jinju *et al.* 2019; Ouma *et al.* 2008; Wu *et al.* 2005). Multi-resolution analysis (MRA) is another domain transform approach; it is a part of compressive sensing and includes methods such as curvelet transform and Laplacian pyramid transform (Amro *et al.* 2011; Dadrass Javan *et al.* 2021; Pohl and Van Genderen 1998). These methods follow a similar processing pipeline, including image transformation, coefficient selection, coefficient fusion, and inverse transformation to the image's original domain. For example, pan sharpening requires converting the panchromatic and multi-spectral images to their frequency components using Fourier, wavelet, curvelet, or any multi-scale transform-based approach. These coefficients will then be selected and fused prior to an inverse transformation. Finally, the image will be reconstructed to its original form and domain by inversing the transformation. Domain transformation-based fusion has several advantages: 1) it identifies surface characteristics such as roughness and repeated patterns or structures (Amolins *et al.* 2007; Ouma *et al.* 2008; Pohl and Van Genderen 1998); 2) MRA can apply fusion at multiple scales and resolutions and thus can effectively extract spatial details, spectral, and textural information; and 3) operating in the frequency domain allows more computationally efficient analysis. Nevertheless, these methods can also introduce new artifacts because they are sensitive to noise in the input images, i.e., augmented noises in the frequency domain (Amolins *et al.* 2007). They also require domain expert knowledge to determine the suitable approach for a specific RS task, which may not be adaptive to all scene variations and applications.

Learning-based Fusion Methods

Learning how to produce fused results through examples via means of ML and DL has become increasingly attractive for many image fusion tasks. The learning-based approach encompasses both conventional machine learning and deep-learning methods, which differ in architecture, extracted features, data dependence (i.e., with or without labels), and computational complexity. The conventional ML fusion methods use algorithms through simple models such as support vector machine, random forest, decision trees, K-nearest neighbor, K-mean clustering, etc. (Albanwan *et al.* 2020; Deng *et al.* 2023; Gao and Lim 2019; Mezouar *et al.* 2023; Sheykhmousa *et al.* 2020). The ML models can either learn parameters for statistical filtering or perform pixel-level prediction by examples in applications such as super-resolution and time-series analysis. In comparison, DL methods apply fusion through more complex models such as convolutional neural networks (CNNs), recurrent neural networks (RNNs), generative adversarial networks (GAN), attention mechanisms, and Transformers (Arefin *et al.* 2020; Chen, Luan *et al.* 2021; Liu and Wang 2022; Liu *et al.* 2018; Salvetti *et al.* 2020; Scarpa *et al.* 2018; Wei *et al.* 2017). Both learning-based methods have the advantage of working with or without labeled data through supervised and unsupervised methods and, in some cases, semi-supervised methods with a smaller set of labeled data. Learning-based methods are generally considered data driven, meaning they can extract features and learn patterns directly and automatically from images, enabling image fusion to be performed mostly on the feature and decision levels. The feature-level fusion is where learned features (i.e., feature vectors or feature maps) are extracted separately from images and combined in the following steps using methods such as feature concatenation (e.g., CNNs), feature reduction (e.g., Principal Components Analysis), averaging, feature selection (e.g., attention mechanism), etc. An example of feature-level image fusion is shown in Figure 6. On the other hand, the decision-level fusion combines the predicted images directly using their pixel value as a postprocessing step. As is a common problem in ML/DL, learning-based approaches have limited transferability and generalization to new scenes or data sets due to large domain gaps between training and testing images (Li *et al.* 2017; Pan *et al.* 2011, 2008; Shi *et al.* 2010; Tasar *et al.* 2021). Often, there is also limited RS-based training data, which can affect the performance of such models. Fine-tuning is often proposed to overcome transferability and generalization issues, because it adapts pretrained foundation models to specific tasks (Chaudhuri *et al.* 2022; He *et al.* 2024; Li, Kong *et al.* 2021; Song *et al.* 2024; Wu *et al.* 2020).

Conventional Machine Learning Methods for Image Fusion

Conventional ML methods are very popular for image fusion tasks; they can be divided into feature-level and decision-level fusion (Nie *et al.* 2021; Pastorino *et al.* 2021; Seo *et al.* 2018; Shingare *et al.* 2014). The feature-level fusion performs linear or statistical fusion at the feature space (i.e., hand-crafted feature) in the prediction pipeline (Camps-Valls *et al.* 2008; Kang *et al.* 2014; Kong *et al.* 2021; Rajah *et al.* 2018; Zhang 2010, Zhu, Cai, *et al.* 2018), the key to which is to learn feature descriptions of multi-modal data into a space where these features can be easily fused without creating a conflict of evidence (Ghamisi *et al.* 2019; Pastorino *et al.* 2021; Pohl and Van Genderen 1998; Seo *et al.* 2018). Feature-level fusion is mostly used in multi-source and multi-modal data-based fusion, which serves as a means to effectively use complementary information for typical tasks such as semantic segmentation, instance segmentation, etc. The decision-level fusion, as the name suggests, performs fusion on the predicted results, such as from classification/semantic segmentation maps. Compared

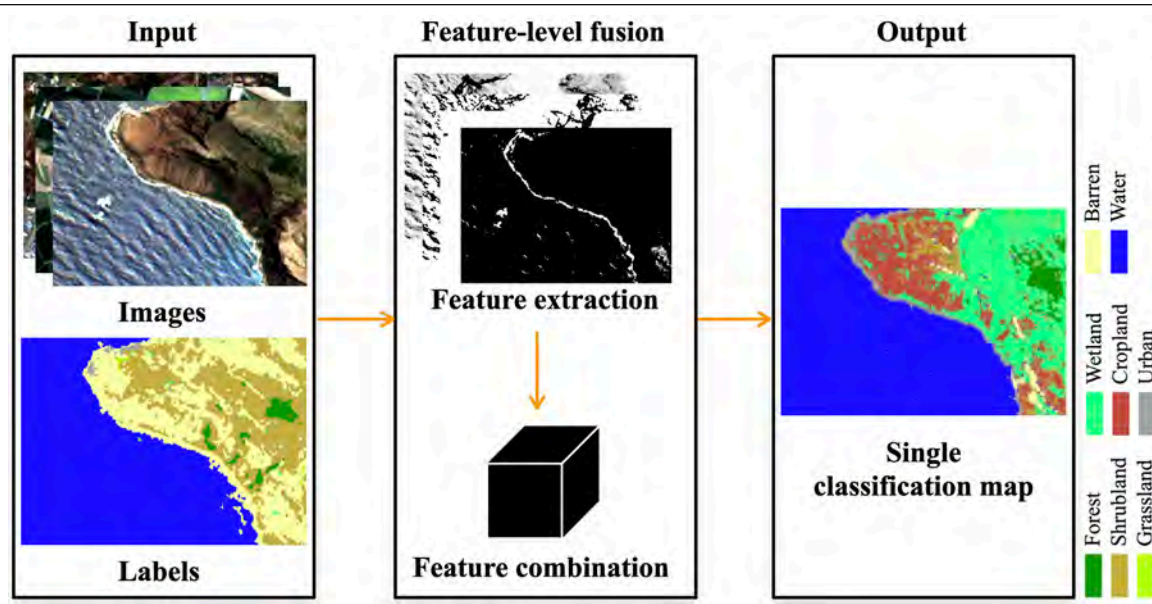

Figure 6. Example of many-to-other image fusion used for classification applying learning-based fusion at the feature level.

to feature-level fusion, decision-level fusion is made simpler because the predicted results are already in the same modality with simple fusing strategies such as weight fusion or majority voting, averaging, median, etc. (Albanwan *et al.* 2020; Cui *et al.* 2018; Lucas *et al.* 2007; Vivekananda *et al.* 2021; Yuan *et al.* 2005). Of course, the downside of the decision-level fusion is the lack of flexibility to infer earlier processes in feature selection. In sum, both approaches dominated classic fusion literature when handling multi-modal data.

Deep-learning Methods for Image Fusion

DL models possess significant advances in learning complex features and pixel-level prediction, as shown in recent literature (Wang *et al.* 2023). While technically it introduces methodological complexity, it mostly differs from conventional ML by using models that are highly parameterized, whereas the concept of fusion strategies remains, such as the data-level, feature-level, or decision-level fusion. Unlike ML methods, DL methods can automatically extract low to high-level features without manual interference; however, they may require significant training data and time to process and learn from images. From an application perspective, DL methods are used in two ways: spatial–spectral image fusion focusing on M2O and spatiotemporal fusion providing predictions through time (M2M). The following subsections entail relevant works related to these two types.

Deep learning for spatial–spectral image fusion: A prime RS task for the M2O and M2M image fusion is creating a spatially and spectrally enhanced image from a set of spatially/spectrally low-resolution images (e.g., pan sharpening or super-resolution). Earlier success in DL fusion apply methods such as CNNs, ResNet, and GANs and sometimes specific models such as U-Net and AlexNet. (Kawulok *et al.* 2020; Li, Meng *et al.* 2022; Sarker 2021; Scarpa *et al.* 2018; Shao and Cai 2018; Wei *et al.* 2017). These methods are tailored to process spatial data rather than temporal data, where they can efficiently extract spatial details and valuable contextual information. For image fusion, these methods extract basic spatial features, such as edges, corners, lines, and blobs, and match them to their corresponding features in other images. For example, using CNN for pan sharpening combines the spatial details from the PAN image with the spectral information in the MS image. The typical steps would be: 1) extracting spatial features from both images individually using convolutional layers, 2) adding a pooling layer to down-sample features and maintain only important features, 3) fully connecting the layers for linear transformation of the feature vector, 4) combining the features using either concatenation or weighted average, and finally, 5) up-sampling to match the size of the PAN image. CNN with specific models, such as U-Net and AlexNet, follow the same strategy, except their methods are modified to accommodate better functionality to process large-scale images with higher resolutions, and this may include deeper networks, residual blocks, encoder-decoder structure, etc.

Classic image fusion methods extract and augment high-frequency details to reserve in the final image while blending spectral information in the low-frequency domain; this process will consequently augment noises from the original images. Meanwhile, DL models can segregate noise from spatial details by learning from examples, such that when fusing the MS and PAN images into the pan-sharpened image, unwanted noises are suppressed to the minimum. Due to the higher model capacity, DL models can also directly learn, again from examples, predicting pixel-level results directly from MS and PAN images, which learns complex feature representations that best fit the prediction results towards the ground truth. For instance, as a classic case of M2O image fusion, Zhong *et al.* (2016) performed super-resolution CNN on MS images and then combined the new high-resolution MS with the PAN image using the GS method (a classic fusion method) to get more accurate spatial and spectral representation. A similar line of work can be found in the application of super-resolution (Arun *et al.* 2020; Kavran *et al.* 2023; Liebel and Körner 2016) and multi-modality fusion-based learning (Zeng *et al.* 2021; Zhang *et al.* 2021).

Deep learning for spatiotemporal image fusion: DL for spatiotemporal image fusion provides powerful connections for modeling long-range dependencies in the spatial and temporal directions, advancing applications that include time-series analysis, change detection, and crop and vegetation dynamics prediction (Kavran *et al.* 2023; Wang *et al.* 2019, Yang *et al.* 2021) . Well-parameterized DL architectures such as RNNs, attention mechanisms, and Transformers have been widely used in such applications. These networks have a built-in structure to store and reuse information with an increasing range of dependencies (from RNN to Transformers) (Arefin *et al.* 2020; Bergado *et al.* 2018; Chen, Luan *et al.* 2021; Li, Cao *et al.* 2021; Maggiori *et al.* 2017; Zhu *et al.* 2022). Thus, they can perform spatiotemporal (and general M2M) image fusion by considering well-modeled trends to improve the accuracy of the fusion. For example, typical spatiotemporal filters only consider local neighborhood tensors and are parameterized by simple one-pass linear weights and biases, which lack the capability to model complex phenological patterns. In contrast, DL models with millions of parameters can easily perform (Wang *et al.* 2023). The typical DL models accounting for temporal dependencies, i.e., RNNs and Transformers, differ in their structure, mechanism, and memory length due to their design. Thus, fusion can be applied at different stages depending on the network. For instance, RNNs operate in a loop structure in which important information is stored from the first input image (in what is called a hidden state) and fused with the following image to be processed in an RNN cell and so forth until the network is set to terminate at a given condition or when all images are consumed. This gives fusion tasks the opportunity to retain pixel information that is static throughout the time. Long short-term memory (LSTM) and gated recurrent unit are specific models to RNNs, where they have similar procedures. However, they have a longer memory to store temporal dependencies and contextual information, where they use gates to control input, output, and information flow (Sarker 2021). One challenge of these methods is the range of dependencies in the sequential data (e.g., multi-temporal images) is still limited. Recently, researchers explored alternatives that can leverage performance and resources, especially for geographical data, which can be in the form of self-supervision. This led to the adoption of attention mechanisms through Transformers, a seminal work that outperforms traditional DL networks in incorporating global dependencies, and thus, it can be naturally used in image fusion tasks (Aleissaee *et al.* 2023; Bazi *et al.* 2021; Chen, Zou *et al.* 2021; Gong *et al.* 2022; Li, Chen *et al.* 2022; Li, Cao *et al.* 2021; Liu and Wang 2022; Roy *et al.* 2023; Salvetti *et al.* 2020; Scheibenreif *et al.* 2022; Shajahan *et al.* 2022). Transformer, an adaptation of the attention mechanism through even longer-range dependencies, can exploit global information, outperforming RNN/LSTM-based structures. Transformers can also extract features in both the spatial and temporal directions. For example, Vision Transformer divides images into multiple smaller patches to allow the attention mechanism (cross-attention) in the Transformer to explore global information within the image (Aleissaee *et al.* 2023; Gong *et al.* 2022; Li, Chen *et al.* 2022; Li, Cao *et al.* 2021; Roy *et al.* 2023; Scheibenreif *et al.* 2022). Similarly, cross-attention can be applied to divided patches among images captured at different times, enabling temporal information encoding (Roy *et al.* 2023). Attention mechanisms and transformers are developing rapidly, and their progress is expected to be promising with further advancements in RS image fusion.

Meta-analysis of Existing Works Using Remote Sensing Fusion as a Core Technique

We aim to review the topic of remote sensing image fusion in a broad sense. Thus, we have included a meta-analysis on papers that involve image fusion as a core technique, aiming to analyze the effect of image fusion on the field of RS. The meta-analysis is designed to help inform existing and most recent practices of image fusion methods in the RS field. On the one hand, this enabled us to develop our new taxonomy that divides image fusion based on the strategy and the "input–output" formation; on the other hand, it helped us understand the most recent fusion methods that have not yet been investigated in previous review literature. For our meta-analysis, we will first present our search method, which includes keywords, publication sources, etc. In the following section, we will present the statistical analysis results showing the development of fusion methods and applications over the years.

Data Selection and Extraction

For this review, we searched for articles on the topic of remote sensing image fusion using the Scopus database (as of 2023). We generated several search criteria through queries to search for peer-reviewed articles based on title, abstract, and keywords. The search query includes several statements such as "Remote sensing" AND "Image fusion"; "Remote sensing" AND "Fusion"; "Fusion" AND "Digital Surface Models" AND "Fusion"; "Digital Elevation Models" AND "Fusion"; "RADAR Image" AND "Fusion"; "SAR Image" AND "Fusion"; and "Lidar" AND "Fusion" (Table 2). We then refined the search by selecting only peer-reviewed journal and conference articles and voiding

Table 2. Queries of this review.

Queries
"Image fusion" AND "Remote sensing"
"Remote sensing" AND "Fusion"
"Digital surface models (DSM)" AND "Fusion"
"Digital elevation models (DEM)" AND "Fusion"
"RADAR" AND "Fusion"
"SAR" AND "Image fusion"
"Lidar" AND "Fusion"

Table 3. Titles of the conferences and journals selected for the review with the number of published articles concerning fusion in remote sensing (as of 2023).

Conference or Journal Name	Number of publications (N = 10,420)
Conferences	4,382
International Geoscience and Remote Sensing Symposium IGARSS	1,225
Proceedings of SPIE The International Society for Optical Engineering	935
IEEE ISPRS Joint Workshop on Remote Sensing and Data Fusion Over Urban Areas DFUA 2001	68
2nd GRSS ISPRS Joint Workshop on Remote Sensing and Data Fusion Over Urban Areas Urban 2003	64
ISPRS Annals of The Photogrammetry Remote Sensing and Spatial Information Sciences	57
Proceedings International Conference on Image Processing ICIP	27
2011 International Conference on Remote Sensing Environment and Transportation Engineering RSETE 2011 Proceedings	18
Proceedings Applied Imagery Pattern Recognition Workshop	12
IEEE Aerospace Conference Proceedings	12
International Conference on Signal Processing Proceedings ICSP	11
IEEE Computer Society Conference on Computer Vision and Pattern Recognition Workshops	9
Digest International Geoscience and Remote Sensing Symposium IGARSS	8
Conference Record IEEE Instrumentation and Measurement Technology Conference	7
IEEE Conference on Intelligent Transportation Systems Proceedings ITSC	7
Journals	6,038
Remote Sensing	837
IEEE Transactions in Geoscience and Remote Sensing	619
IEEE Journal of Selected Topics in Applied Earth Observations and Remote Sensing	419
IEEE Geoscience and Remote Sensing Letters	320
International Journal of Remote Sensing	288
Remote Sensing of Environment	166
ISPRS Journal of Photogrammetry and Remote Sensing	142
Journal of Applied Remote Sensing	121
International Journal of Applied Earth Observation and Geoinformation	99
Photogrammetric Engineering and Remote Sensing	62
ISPRS International Journal of Geo-Information	54
Information Fusion	46
Applied Sciences Switzerland	45
International Journal of Image and Data Fusion	34
Journal of Geo-Information Science	31
Remote Sensing Letters	31
Canadian Journal of Remote Sensing	26
IEEE Transactions on Image Processing	22
European Journal of Remote Sensing	18
IEEE Transactions on Instrumentation and Measurement	17
IEEE Transactions on Neural Networks and Learning Systems	17
Computers and Geosciences	13
IEEE Sensors Journal	11
Journal of Environmental Management	10
Photogrammetric Record	9
Pattern Recognition Letters	9

IEEE = Institute of Electrical and Electronics Engineers; IGARSS = Geoscience and Remote Sensing Society; ISPRS = International Society for Photogrammetry and Remote Sensing; SPIE = Society of Photo-Optical Instrumentation Engineers.

everything else. The initial results led to a total number of 10,420 articles, which we sorted into journal or conference articles that total 6,038 and 4,382 articles, respectively.

Data Information Sources

Our results only include journal and conference articles that have been peer-reviewed and are well recognized in the remote sensing society. We summarize the sources in the list shown in Table 3. Our list comes from several sources, such as the Institute of Electrical and Electronics Engineers Geoscience and Remote Sensing Society, the International Society for Photogrammetry and Remote Sensing, the Society of Photo-Optical Instrumentation Engineers, etc. Table 3 indicates that the total number of published conference articles is about 4,382, whereas the list of peer-reviewed articles from well-established journals is about 6,038.

Meta-analysis Results

In this section, we present and discuss the meta-analysis results for the selected data from the previous query, as described under "Meta-analysis of Existing Works Using Remote Sensing Fusion as a Core Technique." First, we present a word cloud that shows the keywords from our search and their frequency of use, which can help inform current practices and know the most researched topics and subtopics in image fusion. Second, we present the statistics of the annual number of conferences and journal publications, which can reveal the pattern of publications and indicate the most targeted hosting environment for such advancements. Lastly, we compare the statistics of different image fusion approaches (i.e., classic and learning-based methods) and the percentages of the publications covering specific RS applications. The last statistical analysis is critical to informing image fusion's current practices, field gaps, and projected directions in the future.

Statistical Analysis of the Keywords in This Review

Figure 7 shows the main keywords as they appear in the selected articles. Words with large fonts indicate their appearance in high frequency, whereas words with smaller fonts appear infrequently . Our results in Figure 7 indicate that the words "data fusion," "image fusion," "sensor data fusion," "optical radar," "synthetic aperture radar," "feature extraction," "deep learning," "neural networks," and "convolutional neural networks" are the most frequent words to appear. These terms in large font signify the following points: 1) the image fusion concept is very general, and it has been used to process various types of RS images and applications; 2) the term "sensor data fusion" in large font suggests that multi-modal modal images are intensively combined in RS, especially for applications using radar and lidar images; 3) deep learning, neural networks, and convolutional neural networks also stand out prominently, indicating that they are currently the most used approaches for image fusion tasks over other classical machine learning methods such as Kalman filters, decision trees, and support vector machines (Ghorbanzadeh *et al.* 2019; Han *et al.* 2023; Youssef *et al.* 2020), and CNNs appear to be used more often than other DL methods; 4) the terms "feature extraction" (in a large font) and "features fusion" (with a relatively smaller font) indicate that many of the fusion approaches occur at feature level, which is mostly preferred for multi-modal data fusion. Terms such as "image enhancement," "object detection," and "semantics" are relatively large and noticeable, indicating that the RS applications mostly benefit from image fusion. Image enhancement usually refers to radiometric or spatial enhancement of images, which also appears in the figure with a smaller font, like "pan sharpening" or "radiometric calibration." On the other hand, in addition to the word semantics, we have also noticed the associated applications frequently appearing in Figure 7, such as classification, segmentation, and land use land cover (LULC). Other less frequent applications include environmental tasks (related to geology and vegetation) and three-dimensional image reconstruction (e.g., stereoscopy and image reconstruction). The types of images have also been mentioned in the word cloud with fonts ranging from large, such as radar and lidar, to small, such as hyperspectral and multi-spectral.

Statistical Analysis of the Annual Publications

In Figure 8, we can see the pattern of the number of articles published over the years. We compare the total number of articles from journals, conferences, and both, as demonstrated by the blue, yellow, and red, respectively. The figure shows that image fusion has been in the field for decades, starting in the 1980s. The red line shows a gradual increase in the total number of publications per year, ranging from a few dozen to a thousand, with a noticeable jump after 2017. This jump is led by the significant advancements and development of deep-learning methods. These methods have made a substantial breakthrough in the

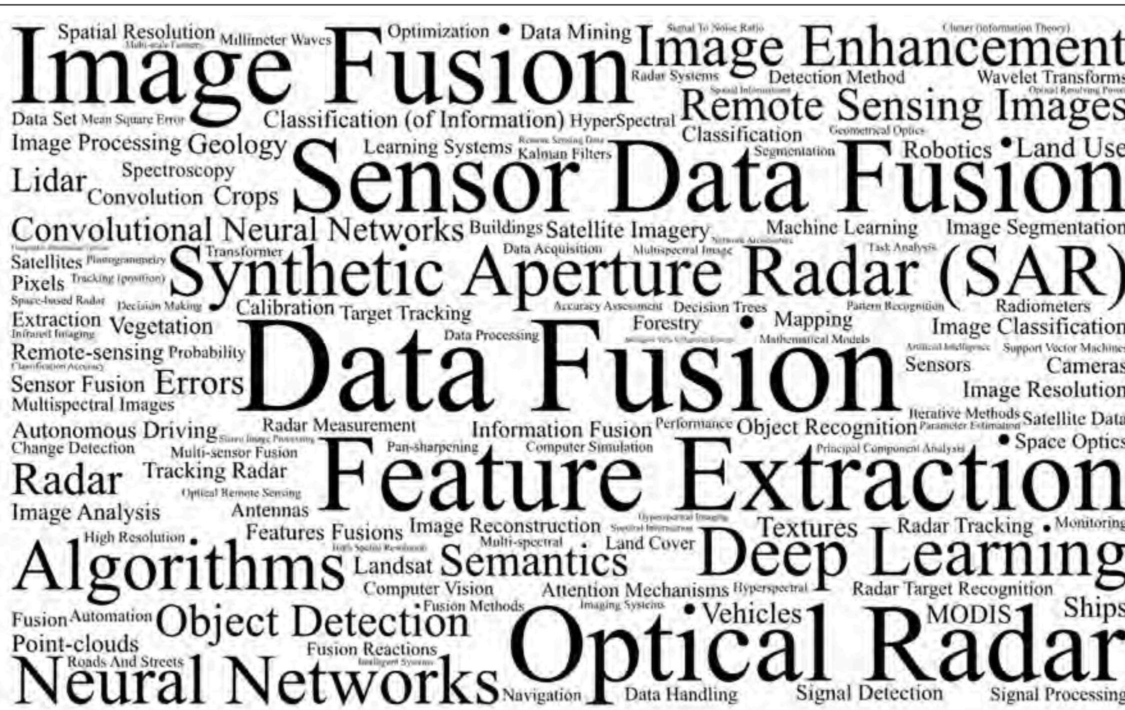

Figure 7. Word cloud for the keywords of this review.

computer vision field in general and in RS specifically, leading the number of publications to grow exponentially over the years. Until almost 2019, the number of conference articles was higher than journal articles, but both have had a steady progression and increase over the years, with dozens of publications annually. However, with the development of attention mechanisms and transformers in 2019, there was a significant shift in the trajectory of the type and number of publications. Journal publications have experienced a great surge, outgrowing conference publications, increasing to several hundred publications annually, reaching their maximum of ~1,000 in 2023. The general growth in the number of publications indicates that image fusion is still a hot topic under investigation, with a lot of room for development.

Statistical Analysis of the Image Fusion Approaches

Image fusion methods, as explored under "General Fusion Approaches in Remote Sensing," are categorized into classic and learning-based methods. The classic methods cover statistical-based, prediction-based, and domain transform-based methods (Helmer and Ruefenacht 2005; Lacewell *et al.* 2010; Nagamani *et al.* 2021), whereas learning-based methods incorporate classic learning (i.e., ML) and DL methods (Arefin *et al.* 2020; Gao and Lim 2019; Kawulok *et al.* 2020; Lucas *et al.* 2007; Salvetti *et al.* 2020). The number of publications concerning the development of the classic (yellow line) and learning-based (blue line) image fusion methods over the past 30+ years is shown in Figure 9, which highlights a significant difference. The publications on learning-based image fusion methods have grown exponentially over the years, mainly driven by the rapid development of DL methods. In particular, after 2017, we can see a sharp notable increase in the number of publications (indicated by the blue and green lines), reaching approximately 1,000 annually. The current trend of DL methods (shown by the green line) indicates a significant interest in their usage for image fusion, and they are expected to continue progressing in the upcoming years. On the other hand, classic learning-based methods (pink line) have had less interest with smaller progress, not exceeding 100 publications per year, due to their limited performance compared to DL methods. The classic methods, such as statistical-based approaches, consistently produce around 200 publications annually (see the yellow line in Figure 9). Classic methods' progress has been consistent due to their simple per-pixel operations and minimal requirements, making them a common starting point for new researchers.

Statistical Analysis of the Applications of Image Fusion

M2O and M2M image fusion have been used with various RS applications. These applications can be classified into six main categories:

1. **Classification refinement:** refining the accuracy and precision of the classification maps, such as supervised classification, LULC, segmentation, etc. (Albanwan *et al.* 2020; Camps-Valls *et al.* 2008; Cui *et al.* 2018; Gao and Lim 2019; Ji *et al.* 2020; Lucas *et al.* 2007; Nguyen *et al.* 2020; Papasaika *et al.* 2011; Viana *et al.* 2019; Yuan *et al.* 2005; Zhou *et al.* 2008).
2. **Detection and recognition:** identifying temporal changes and objects, such as change detection or building detection (Achour *et al.* 2022; Atasever *et al.* 2014; Bovolo and Bruzzone 2007; Lin, Liu *et al.* 2023; Liu *et al.* 2023; Luppino *et al.* 2019; Wu *et al.* 2016; Zerrouki *et al.* 2022; Zhang *et al.* 2017).
3. **Spectral image enhancement:** correcting or normalizing the spectral values within images, for example, spectral coherence, denoising, filtering, and restoration (Albanwan and Qin 2018; Canty *et al.* 2004; Canty and Nielsen 2008; Chen *et al.* 2018; Du *et al.* 2002; Gan *et al.* 2021; Nielsen 2007; Syariz *et al.* 2019; Wu, Ge *et al.* 2018).
4. **Spatial resolution enhancement:** enhancing the level of detail and spatial resolution of images through pan sharpening or super-resolution (Arefin *et al.* 2020; Diao *et al.* 2022; Ehlers *et al.* 2010; Kawulok *et al.* 2020; Shen *et al.* 2008; Yang *et al.* 2023; Yanovsky and Qin 2021; Zhang, Yang *et al.* 2023; Zhang, Zhang *et al.* 2023; Zhu *et al.* 2016).
5. **Three-dimensional modeling and reconstruction:** processing and accuracy enhancement of three-dimensional data, for example, DSM fusion, DEM fusion, and stereo-matching (Akumu and Dennis 2023; Albanwan and Qin 2020; Fidan *et al.* 2023; Fuss *et al.* 2016; Lin, He *et al.* 2023; Papasaika *et al.* 2011; Qin *et al.* 2022; Rumpler *et al.* 2013; Stucker and Schindler 2020).
6. **Environmental studies:** monitoring and managing natural events or resources, for example, landslide identification or post-disaster management (Erkkilä and Kalliola 2004; Liu and Wang 2022; Ma, Shen *et al.* 2022; Ma, Yao *et al.* 2022; Theron *et al.* 2022; Voutilainen *et al.* 2007).

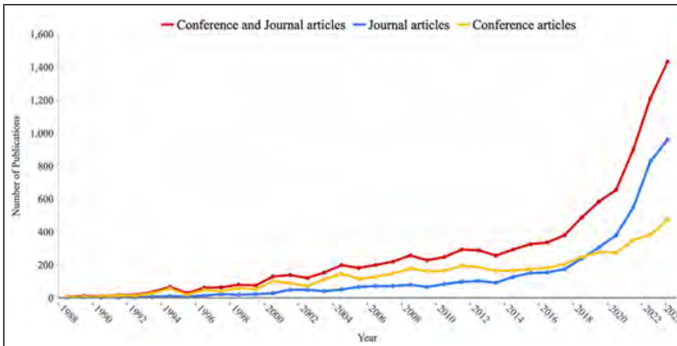

Figure 8. Statistical analysis of the annual conference and journal publications.

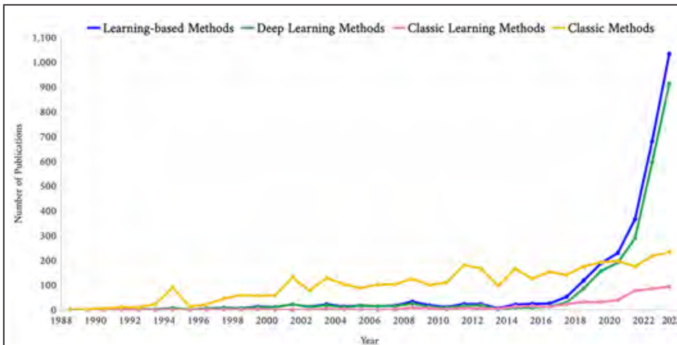

Figure 9. Overview of image fusion approaches in remote sensing showing the publication numbers over the years.

For this analysis, we examined a total of 10,420 peer-reviewed articles, sorted them based on their corresponding application category, and then computed their percentage in each category. A summary of the results is shown in Figure 10. We can notice from the chart in Figure 9 that two categories dominate the application percentage distribution: classification refinement and environmental studies, with percentages of nearly 30% and 26.2% of the total publications, respectively. The two categories combined account for almost 60% of the total publications, while other categories maintain relatively smaller percentages, with each less than 15%. For example, spatial resolution enhancement, three-dimensional reconstruction, and spectral image enhancement have comparable publication shares ranging from 11% to 14.5%, while detection and recognition hold about 7% of total publications. Unlike traditional image fusion review articles, which claim that image fusion is mostly used for spatial resolution enhancement, we here prove that image fusion is widely used for various RS applications.

Summary and Future Directions

Summary and Conclusion

In this article, we reviewed the topic of image fusion for most areas in the RS field, including images of different types, fusion techniques, and applications. We focused on providing a comprehensive perspective on the fusion problem. In doing so, we introduced a new taxonomy highlighting the two predominant categories of image fusion commonly used in RS, i.e., many-to-one (M2O) and many-to-many

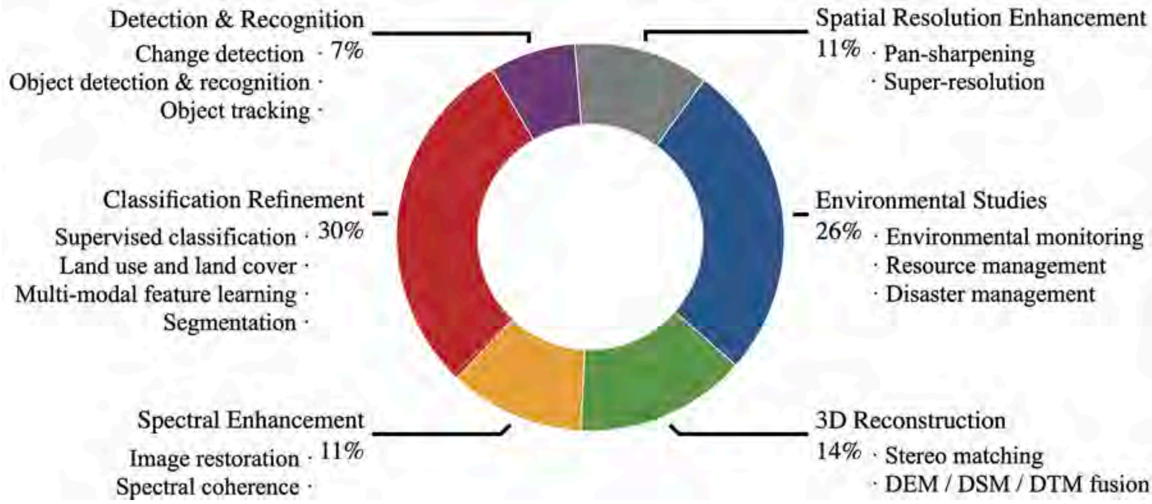

Figure 10. Publication percentage of image fusion applications covered in remote sensing over the years. The total number of articles surveyed is 10,420. DEM = digital elevation model; DSM = digital surface model; DTM = digital terrain model.

(M2M) image fusion. Although this taxonomy is simple in notion, it is fundamental because it presents fusion as a mapping function that can process different numbers of inputs and outputs irrespective of their types as long as they have a similar raster format. The fusion strategies can therefore be augmented to a broader range of RS applications and not be limited to specific types of images (i.e., spectral) or applications (i.e., pan sharpening) as presented in previous literature. To provide coherent guidance on using image fusion across different image types and tasks, we present a meta-analysis covering 10,420 peer-reviewed articles. The meta-analysis provides a statistical analysis of the progression of image fusion methods and applications over the years. The meta-analysis indicates that 1) there is a significant growth in the publications of image fusion in RS, mainly due to the introduction of DL methods, leading publications to increase from several hundred to thousands a year; this growth indicates that image fusion is still a hot topic under study, with plenty of room for further development; 2) multi-modal image fusion is intensively used in RS, especially to combine images from different sensors or types (e.g., spectral images and lidar), which is often processed through feature-level image fusion; 3) although DL image fusion methods have superior performance and have been heavily used in the last few years, classic fusion methods have continued their progress steadily over the years, where due to their simplicity and per-pixel operations, still being used by new learning researchers; and 4) classification and environmental studies are the top two applications benefiting from image fusion, accounting for almost ~60% of all publications, while spectral and spatial resolution enhancement account for almost ~11% of all publications. This conclusion leads to rethinking the past literature reviewing RS image fusion, which almost described the fusion problem as an approach for spatial resolution enhancement, specifically for pan sharpening.

Discussion and Future Directions

Image fusion has been a long-investigated topic, yet it has grown to become increasingly complex due to the ever-developing sensory data and diversified inputs (sources, derived products, different modalities). Therefore, existing syntheses focused on their subtopics due to the divergent applications associated with image fusion, such as image super-resolution, spatiotemporal filtering, and pan sharpening. In our investigation, we resynergize these works back to the fundamentals of fusion by categorizing the image fusion through two simple strategies, i.e., M2O and M2M image fusion. With an overview, we describe typical strategies and used models related to these general tasks to provide a starting point overview for researchers interested in image fusion approaches and applications, thus fueling future research. Obviously, due to the highly disparate image-fusion tasks, specific considerations should be accounted for when addressing specific image-fusion challenges. At the same time, with the technological developments (both in sensors and algorithms), there is a converging trend of using deeper models for image-fusion tasks. Specific conclusions and recommendations are as follows:

Understanding the Origin of Inconsistency

When preparing images for fusion, i.e., M2O or M2M applications, it is essential to understand the tasks and causes of inconsistency for devising the fusion algorithms. The section “Factors Affecting the Quality of Remote Sensing Image Fusion” explains various examples of the causes of inconsistency; thus, specific algorithms addressing such challenges in fusion applications should be considered. Moreover, M2O algorithms emphasize information homogeneity among different inputs, while M2M algorithms focus on information compensation and signal-noise separation due to their task of using multiple images to augment each other. These constitute the core challenges to address, which are being tackled by both classic and various deep learning models (“Generic Taxonomy of Remote Sensing Image Fusion” and “General Fusion Approaches in Remote Sensing”)

Multi-modality Learning

The recent advance of learning models suggests a trend towards using multi-modality remote sensing data for fusion, specifically the use of radar, optical, and cross-modal input such as geographical information system data. It is seen that the fundamentals of these tasks are the fusion algorithms in yielding informative remote sensing assets for better interpretation, such as for information retrieval via augmented spatial–temporal resolution, as well as unique two-dimensional/three-dimensional signatures (such as thermal, cloud-penetrating radar, as well as lidar) for improved classification, detection, and quantification of ground objects. Many of these tasks serve critical environmental and civilian applications.

Trends and Future Directions

Our meta-analysis over 10,420 articles (“Meta-analysis of Existing Works Using Remote Sensing Fusion as a Core Technique” and “Meta-analysis Results”) yields several conclusions. First, the use of image fusion appears to be highest in publications related to the subdomain of “remote sensing and geosciences,” for which the fusion of images for image interpretation is critical. Second, image fusion is mostly used in applications for image classification and environmental studies, more than 50% of the published works. The rest are shared (roughly equal) among three-dimensional fusion, spatial/spectral enhancement, and detection. Third, there is a converging trend of using deep models for image fusion, whereas classic methods, although taking a significantly smaller fraction of published works, remain a fair number as compared to previous years, noting that there is still a good use of older methods, because they require much fewer labels. Although with a relatively smaller number, we note that there is increasing work on building foundational models that could interact with various remote sensing tasks, including image fusion and the fusion of cross-modality data, such as the use of images, texts, and audio via using large language models (Cheng *et al.* 2021; Guo *et al.* 2019; Mao *et al.* 2018).

In summary, our review suggests that image fusion, or the fusion of gridded data, still plays a vital role in this era, when both sensors and models are developed at a rapid pace. In addition to improving classic image fusion algorithms to accommodate newer sensory data and derived data (e.g., DSMs), there has been a paradigm shift from canonical methods to using complex learning and generative models to yield more accurate and comprehensively fused results. Although there has been less focus on already-used algorithms such as pan sharpening, there is a lot of room for development when involving multi-modality, nonraster data.

Acknowledgment

Rongjun Qin is partially funded by Office of Naval Research Grants N000142012141 and N000142312670.

References

Achour, S., M. Chikr Elmezouar, N. Taleb, K. Kpalma and J. Ronsin. 2022. A PCA-PD fusion method for change detection in remote sensing multi temporal images. *Geocarto International* 37:196–213. https://doi.org/10.1080/10106049.2020.1713228.

Akoguz, A., B. Kurt and S. K. Pinar. 2014. Pansharpening of multispectral images using filtering in fourier domain. *Proceedings of SPIE 9244, Image and Signal Processing for Remote Sensing*, 23 October 2014, Amsterdam, Netherlands, p. 92441X. https://doi.org/10.1117/12.2067255.

Akumu, C. E. and S. Dennis. 2023. Exploring the addition of airborne lidar-DEM and derived TPI for urban land cover and land use classification and mapping. *Photogrammetric Engineering and Remote Sensing* 89:19–26. https://doi.org/10.14358/PERS.21-00029R2.

Albanwan, H. and R. Qin. 2018. A novel spectrum enhancement technique for multi-temporal, multi-spectral data using spatial-temporal filtering. *ISPRS Journal of Photogrammetry and Remote Sensing* 142:51–63. https://doi.org/10.1016/j.isprsjprs.2018.05.020.

Albanwan, H. and R. Qin. 2020. Enhancement of depth map by fusion using adaptive and semantic-guided spatiotemporal filtering. *ISPRS Annals of the Photogrammetry, Remote Sensing and Spatial Information Sciences* III-3:227–232. https://doi.org/10.5194/isprs-annals-V-3-2020-227-2020.

Albanwan, H. and R. Qin. 2022. An adaptive and image-guided fusion for stereo satellite image derived digital surface models. *Journal of Geodesy and Geoinformation Science* 5:1–9. https://doi.org/10.11947/j.JGGS.2022.0401.

Albanwan, H., R. Qin, X. Lu, M. Li, D. Liu and J.-M. Guldmann. 2020. 3D iterative spatiotemporal filtering for classification of multitemporal satellite data sets. *Photogrammetric Engineering and Remote Sensing* 86:23–31. https://doi.org/10.14358/PERS.86.1.23.

Aleissaee, A. A., A. Kumar, R. M. Anwer, S. Khan, H. Cholakkal, G.-S. Xia and F. S. Khan. 2023. Transformers in remote sensing: A survey. *Remote Sensing* 15:1860. https://doi.org/10.3390/rs15071860.

Alhatami, E., U. A. Bhatti, M. Huang and S. L. Feng. 2022. Image fusion based on discrete cosine transform with high compression. *7th International Conference on Signal and Image Processing*, 20–22 July 2022, Suzhou, China, pp. 606–610. https://doi.org/10.1109/ICSIP55141.2022.9887300.

Al-Najjar, H.A.H., B. Kalantar, B. Pradhan, V. Saeidi, A. A. Halin, N. Ueda and S. Mansor. 2019. Land cover classification from fused DSM and UAV images using convolutional neural networks. *Remote Sensing* 11:1461. https://doi.org/10.3390/rs11121461.

Alparone, L., S. Baronti, B. Aiazzi and A. Garzelli. 2016. Spatial methods for multispectral pansharpening: Multiresolution analysis demystified. *IEEE Transactions on Geoscience and Remote Sensing* 54:2563–2576. https://doi.org/10.1109/TGRS.2015.2503045.

Amolins, K., Y. Zhang and P. Dare. 2007. Wavelet based image fusion techniques—An introduction, review and comparison. *ISPRS Journal of Photogrammetry and Remote Sensing* 62:249–263. https://doi.org/10.1016/j.isprsjprs.2007.05.009.

Amrani, N., J. Serra-Sagristà, P. Peter and J. Weickert. 2017. Diffusion-based inpainting for coding remote-sensing data. *IEEE Geoscience and Remote Sensing Letters* 14:1203–1207. https://doi.org/10.1109/LGRS.2017.2702106.

Amro, I., J. Mateos, M. Vega, R. Molina and A. K. Katsaggelos. 2011. A survey of classical methods and new trends in pansharpening of multispectral images. *EURASIP Journal on Advances in Signal Processing* 2011:79. https://doi.org/10.1186/1687-6180-2011-79.

Anger, J., T. Ehret, C. de Franchis and G. Facciolo. 2020. Fast and accurate multi-frame super-resolution of satellite images. *ISPRS Annals of the Photogrammetry, Remote Sensing and Spatial Information Sciences* V-1-2020:57–64. https://doi.org/10.5194/isprs-annals-V-1-2020-57-2020.

Arefin, M. R., V. Michalski, P.-L. St-Charles, A. Kalaitzis, S. Kim, S. E. Kahou and Y. Bengio. 2020. Multi-image super-resolution for remote sensing using deep recurrent networks. *Proceedings of the IEEE/CVF Conference on Computer Vision and Pattern Recognition Workshops*, 13–19 June 2020, Seattle, Washington, pp. 206–207.

Arun, P. V., K. M. Buddhiraju, A. Porwal and J. Chanussot. 2020. CNN based spectral super-resolution of remote sensing images. *Signal Processing* 169:107394. https://doi.org/10.1016/j.sigpro.2019.107394.

Asokan, A. and J. Anitha. 2019. Change detection techniques for remote sensing applications: A survey. *Earth Science Informatics* 12:143–160. https://doi.org/10.1007/s12145-019-00380-5.

Atasever, U. H., P. Civicioglu, E. Besdok and C. Ozkan. 2014. A new unsupervised change detection approach based on DWT image fusion and backtracking search optimization algorithm for optical remote sensing data. *International Archives of the Photogrammetry, Remote Sensing and Spatial Information Sciences* XL–7:15–18. https://doi.org/10.5194/isprsarchives-XL-7-15-2014.

Barsi, Á., Z. Kugler, A. Juhász, G. Szabó, C. Batini, H. Abdulmuttalib, G. Huang and H. Shen. 2019. Remote sensing data quality model: From data sources to lifecycle phases. *International Journal of Image and Data Fusion* 10:280–299. https://doi.org/10.1080/19479832.2019.1625977.

Bavirisetti, D. P., G. Xiao and G. Liu. 2017. Multi-sensor image fusion based on fourth order partial differential equations. *20th International Conference on Information Fusion*, 10–13 July 2017, Xi'an, China, pp. 1–9. https://doi.org/10.23919/ICIF.2017.8009719.

Bazi, Y., L. Bashmal, M.M.A. Rahhal, R. A. Dayil and N. A. Ajlan. 2021. Vision transformers for remote sensing image classification. *Remote Sensing* 13:516. https://doi.org/10.3390/rs13030516.

Belgiu, M. and A. Stein. 2019. Spatiotemporal image fusion in remote sensing. *Remote Sensing* 11:818. https://doi.org/10.3390/rs11070818.

Belov, A. and A. Y. Denisova. 2020. Remote sensing data fusion algorithm for super-resolution: Multi-temporal case. *Eighth International Conference on Remote Sensing and Geoinformation of the Environment*, 16–18 March 2020, Paphos, Cyprus, p. 4. https://doi.org/10.1117/12.2569653.

Bergado, J. R., C. Persello and A. Stein. 2018. Recurrent multiresolution convolutional networks for VHR image classification. *IEEE Transactions on Geoscience and Remote Sensing* 99:1–14.https://doi.org/10.1109/TGRS.2018.2837357

Bisquert, M., G. Bordogna, A. Bégué, G. Candiani, M. Teisseire and P. Poncelet. 2015. A simple fusion method for image time series based on the estimation of image temporal validity. *Remote Sensing* 7:704–724. https://doi.org/10.3390/rs70100704.

Bosch, M., Z. Kurtz, S. Hagstrom and M. Brown. 2016. A multiple view stereo benchmark for satellite imagery. *IEEE Applied Imagery Pattern Recognition Workshop*, 18–20 October 2016, Washington, DC, pp. 1–9. https://doi.org/10.1109/AIPR.2016.8010543.

Bovolo, F. and L. Bruzzone. 2007. A theoretical framework for unsupervised change detection based on change vector analysis in the polar domain. *IEEE Transactions on Geoscience and Remote Sensing* 45:218–236. https://doi.org/10.1109/TGRS.2006.885408.

Bruzzone, L. and L. Carlin. 2006. A multilevel context-based system for classification of very high spatial resolution images. *IEEE Transactions on Geoscience and Remote Sensing* 44:2587–2600. https://doi.org/10.1109/TGRS.2006.875360.

Cai, J. and B. Huang. 2021. Super-resolution-guided progressive pansharpening based on a deep convolutional neural network. *IEEE Transactions on Geoscience and Remote Sensing* 59:5206–5220. https://doi.org/10.1109/TGRS.2020.3015878.

Camps-Valls, G., L. Gomez-Chova, J. Munoz-Mari, J. L. Rojo-Alvarez and M. Martinez-Ramon. 2008. Kernel-based framework for multitemporal and multisource remote sensing data classification and change detection. *IEEE Transactions on Geoscience and Remote Sensing* 46:1822–1835. https://doi.org/10.1109/TGRS.2008.916201.

Canty, M. J. and A. A. Nielsen. 2008. Automatic radiometric normalization of multitemporal satellite imagery with the iteratively re-weighted mad transformation. *Remote Sensing of Environment* 112:1025–1036. https://doi.org/10.1016/j.rse.2007.07.013.

Canty, M. J., A. A. Nielsen and M. Schmidt. 2004. Automatic radiometric normalization of multitemporal satellite imagery. *Remote Sensing of Environment* 91:441–451. https://doi.org/10.1016/j.rse.2003.10.024.

Carvalho Jr, O. A., R. F. Guimarães, A. R. Gillespie, N. C. Silva and R. A. T. Gomes. 2011. A new approach to change vector analysis using distance and similarity measures. *Remote Sensing* 3:2473–2493. https://doi.org/10.3390/rs3112473.

Cayuela, L., J. D. Golicher, J. S. Rey and J.M.R. Benayas. 2006. Classification of a complex landscape using Dempster–Shafer theory of evidence. *International Journal of Remote Sensing* 27:1951–1971. https://doi.org/10.1080/01431160500181788.

Chang, J.-R. and Y.-S. Chen. 2018. Pyramid stereo matching network. *Proceedings of the IEEE Conference on Computer Vision and Pattern Recognition*, 19–23 June 2018, Salt Lake City, Utah, pp. 5410–5418.

Chang, Y. and B. Luo. 2019. Bidirectional convolutional LSTM neural network for remote sensing image super-resolution. *Remote Sensing* 11:2333. https://doi.org/10.3390/rs11202333.

Chaudhuri, U., R. Bose, B. Banerjee, A. Bhattacharya and M. Datcu. 2022. Zero-shot cross-modal retrieval for remote sensing images with minimal supervision. *IEEE Transactions on Geoscience and Remote Sensing* 60:1–15. https://doi.org/10.1109/TGRS.2022.3196307.

Chavez, J., S. C. Sides and J. A. Anderson. 1991. Comparison of three different methods to merge multiresolution and multispectral data: Landsat TM and SPOT panchromatic. *Photogrammetric Engineering and Remote Sensing* 57:295–303.

Chen, C., X. He, B. Guo, X. Zhao and Y. Chu. 2020. A pixel-level fusion method for multi-source optical remote sensing image combining the principal component analysis and curvelet transform. *Earth Science Informatics* 13:1005–1013. https://doi.org/10.1007/s12145-020-00472-7.

Chen, C., D. Luan, S. Zhao, Z. Liao, Y. Zhou, J. Jiang and Q. Pei. 2021. Flood discharge prediction based on remote-sensed spatiotemporal features fusion and graph attention. *Remote Sensing* 13:5023. https://doi.org/10.3390/rs13245023.

Chen, J., P. Jönsson, M. Tamura, Z. Gu, B. Matsushita and L. Eklundh. 2004. A simple method for reconstructing a high-quality NDVI time-series data set based on the Savitzky–Golay filter. *Remote Sensing of Environment* 91:332–344. https://doi.org/10.1016/j.rse.2004.03.014.

Chen, K., Z. Zou and Z. Shi. 2021. Building extraction from remote sensing images with sparse token transformers. *Remote Sensing* 13:4441. https://doi.org/10.3390/rs13214441.

Chen, R., V. G. Ferreira and X. Li. 2022. Detecting moving vehicles from satellite-based videos by tracklet feature classification. *Remote Sens*ing 15:34. https://doi.org/10.3390/rs15010034.

Chen, S., H. Qi and K. Nan. 2022. Pansharpening via super-resolution iterative residual network with a cross-scale learning strategy. *IEEE Transactions on Geoscience and Remote Sensing* 60:1–16. https://doi.org/10.1109/TGRS.2021.3138096.

Chen, Y., K. Sun, D. Li, T. Bai and W. Li. 2018. Improved relative radiometric normalization method of remote sensing images for change detection. *Journal of Applied Remote Sensing* 12:045018. https://doi.org/10.1117/1.JRS.12.045018.

Chen, Z., P. Zhang, Y. Zhang, X. Xu, L. Ji and H. Tang. 2023. Thick cloud removal in multi-temporal remote sensing images via frequency spectrum-modulated tensor completion. *Remote Sensing* 15:1230. https://doi.org/10.3390/rs15051230.

Cheng, J., H. Liu, T. Liu, F. Wang and H. Li. 2015. Remote sensing image fusion via wavelet transform and sparse representation. *ISPRS Journal of Photogrammetry and Remote Sensing* 104:158–173. https://doi.org/10.1016/j.isprsjprs.2015.02.015.

Cheng, Q., H. Liu, H. Shen, P. Wu and L. Zhang. 2017. A spatial and temporal nonlocal filter-based data fusion method. *IEEE Transactions on Geoscience and Remote Sensing* 55:4476–4488. https://doi.org/10.1109/TGRS.2017.2692802.

Cheng, Q., Y. Zhou, P. Fu, Y. Xu and L. Zhang. 2021. A deep semantic alignment network for the cross-modal image-text retrieval in remote sensing. *IEEE Journal of Selected Topics in Applied Earth Observations and Remote Sensing* 14:4284–4297. https://doi.org/10.1109/JSTARS.2021.3070872.

Chi, M., A. Plaza, J. A. Benediktsson, Z. Sun, J. Shen and Y. Zhu. 2016. Big data for remote sensing: Challenges and opportunities. *Proceedings of the IEEE* 104:2207–2219. https://doi.org/10.1109/JPROC.2016.2598228.

Choi, M., R. Y. Kim, M.-R. Nam and H. O. Kim. 2005. Fusion of multispectral and panchromatic satellite images using the curvelet transform. *IEEE Geoscience and Remote Sensing Letters* 2:136–140. https://doi.org/10.1109/LGRS.2005.845313.

Cui, G., Z. Lv, G. Li, J. Atli Benediktsson and Y. Lu. 2018. Refining land cover classification maps based on dual-adaptive majority voting strategy for very high resolution remote sensing images. *Remote Sensing* 10:1238. https://doi.org/10.3390/rs10081238.

Cui, M., S. Xue and Y. Huang. 2010. Land cover classification base on Fourier analysis. *Fourth International Conference on Genetic and Evolutionary Computing*, 13–15 December 2010, Shenzhen, China, pp. 390–393. https://doi.org/10.1109/ICGEC.2010.103.

Cui, S. and M. Datcu. 2012. Statistical wavelet subband modeling for multi-temporal SAR change detection. *IEEE Journal of Selected Topics in Applied Earth Observations and Remote Sensing* 5:1095–1109. https://doi.org/10.1109/JSTARS.2012.2200655.

Dadrass Javan, F., F. Samadzadegan, S. Mehravar, A. Toosi, R. Khatami and A. Stein. 2021. A review of image fusion techniques for pan-sharpening of high-resolution satellite imagery. *ISPRS Journal of Photogrammetry and Remote Sensing* 171:101–117. https://doi.org/10.1016/j.isprsjprs.2020.11.001.

Dalla Mura, M., G. Vivone, R. Restaino, P. Addesso and J. Chanussot. 2015. Global and local Gram–Schmidt methods for hyperspectral pansharpening. IEEE International Geoscience and Remote Sensing Symposium, 26–31 July 2015, Milan, Italy, pp. 37–40. https://doi.org/10.1109/IGARSS.2015.7325691.

Dang, B. and Y. Li. 2021. MSResNet: Multiscale residual network via self-supervised learning for water-body detection in remote sensing imagery. *Remote Sensing* 13:3122. https://doi.org/10.3390/rs13163122.

Deng, Z., X. Fan and J. Chen. 2023. A machine learning method for building height estimation based on Sentinel-2 bi-temporal images. *Photogrammetric Engineering and Remote Sensing* 89:27–36. https://doi.org/10.14358/PERS.22-00054R2.

Denipote, J. G. and M.S.V. Paiva. 2008. A Fourier transform-based approach to fusion high spatial resolution remote sensing images. *Sixth Indian Conference on Computer Vision, Graphics and Image Processing*, 16–19 December 2008, Bhubaneswar, India, pp. 179–186. https://doi.org/10.1109/ICVGIP.2008.108.

Diao, W., F. Zhang, H. Wang, J. Sun and K. Zhang. 2022. Pansharpening via triplet attention network with information interaction. *IEEE Journal of Selected Topics in Applied Earth Observations and Remote Sensing* 15:3576–3588. https://doi.org/10.1109/JSTARS.2022.3171423.

Ding, Q., Z. Shao, X. Huang, O. Altan and Y. Fan. 2022. Improving urban land cover mapping with the fusion of optical and SAR data based on feature selection strategy. *Photogrammetric Engineering and Remote Sensing* 88:17–28. https://doi.org/10.14358/PERS.21-00030R2.

Du, P., J. Xia, J. Chanussot and X. He. 2012. Hyperspectral remote sensing image classification based on the integration of support vector machine and random forest. IEEE International Geoscience and Remote Sensing Symposium, 22–27 July 2012, Munich, Germany, pp. 174–177. https://doi.org/10.1109/IGARSS.2012.6351609.

Du, W., Z. Qin, J. Fan, M. Gao, F. Wang and B. Abbasi. 2019. An efficient approach to remove thick cloud in VNIR bands of multi-temporal remote sensing images. *Remote Sens*ing 11:1284. https://doi.org/10.3390/rs11111284.

Du, Y., P. M. Teillet and J. Cihlar. 2002. Radiometric normalization of multitemporal high-resolution satellite images with quality control for land cover change detection. *Remote Sensing of Environment* 82:123–134. https://doi.org/10.1016/S0034-4257(02)00029-9.

Ehlers, M., S. Klonus, P. Johan Åstrand and P. Rosso. 2010. Multi-sensor image fusion for pansharpening in remote sensing. *International Journal of Image and Data Fusion* 1:25–45. https://doi.org/10.1080/19479830903561985.

Erkkilä, A. and R. Kalliola. 2004. Patterns and dynamics of coastal waters in multi-temporal satellite images: Support to water quality monitoring in the Archipelago Sea, Finland. *Estuarine, Coastal and Shelf Science* 60:165–177. https://doi.org/10.1016/j.ecss.2003.11.024.

Ezimand, K., M. Chahardoli, M. Azadbakht and A. A. Matkan. 2021. Spatiotemporal analysis of land surface temperature using multi-temporal and multi-sensor image fusion techniques. *Sustainable Cities and Society* 64:102508. https://doi.org/10.1016/j.scs.2020.102508.

Fang, J., J. Yang, A. Khader and L. Xiao. 2023. A multiresolution details enhanced attentive dual-UNet for hyperspectral and multispectral image fusion. *IEEE Journal of Selected Topics in Applied Earth Observations and Remote Sensing* 16:638–655. https://doi.org/10.1109/JSTARS.2022.3228941.

Farhadi, H. and M. Najafzadeh. 2021. Flood risk mapping by remote sensing data and random forest technique. *Water* 13:3115. https://doi.org/10.3390/w13213115.

Fidan, Ş., A. Ulvi, A. Y. Yiğit, S.N.G. Hamal and M. Yakar. 2023. Combination of terrestrial laser scanning and unmanned aerial vehicle photogrammetry for heritage building information modeling: A case study of Tarsus St. Paul Church. *Photogrammetric Engineering and Remote Sensing* 89:753–760. https://doi.org/10.14358/PERS.23-00031R2.

Fischler, M. A. and R. C. Bolles. 1981. Random sample consensus: A paradigm for model fitting with applications to image analysis and automated cartography. *Communnunications of the Association of Computing Machinery* 24:381–395. https://doi.org/10.1145/358669.358692.

Fuss, C. E., A. A. Berg and J. B. Lindsay. 2016. DEM fusion using a modified K-means clustering algorithm. *International Journal of Digital Earth* 9:1242–1255. https://doi.org/10.1080/17538947.2016.1208685.

Gan, W., H. Albanwan and R. Qin. 2021. Radiometric normalization of multitemporal Landsat and Sentinel-2 images using a reference MODIS product through spatiotemporal filtering. *IEEE Journal of Selected Topics in Applied Earth Observations and Remote Sensing* 14:4000–4013. https://doi.org/10.1109/JSTARS.2021.3069855.

Gao, F., J. Masek, M. Schwaller and F. Hall. 2006. On the blending of the Landsat and MODIS surface reflectance: Predicting daily Landsat surface reflectance. *IEEE Transactions on Geoscience and Remote Sensing* 44:2207–2218. https://doi.org/10.1109/TGRS.2006.872081.

Gao, Q. and S. Lim. 2019. A probabilistic fusion of a support vector machine and a joint sparsity model for hyperspectral imagery classification. *GIScience and Remote Sensing* 56:1129–1147. https://doi.org/10.1080/15481603.2019.1623003.

Geng, W., W. Zhou and S. Jin. 2022. Multi-view urban scene classification with a complementary-information learning model. *Photogrammetric Engineering and Remote Sensing* 88:65–72. https://doi.org/10.14358/PERS.21-00062R2.

Ghamisi, P., R. Gloaguen and P. M. Atkinson, J. A. Benediktsson, B. Rasti, N. Yokoya, Q. Wang, B. Hofle, L. Bruzzone, F. Bovolo, M. Chi and K. Anders. 2019. Multisource and multitemporal data fusion in remote sensing: A comprehensive review of the state of the art. *IEEE Geoscience and Remote Sensing Magazine* 7:6–39. https://doi.org/10.1109/MGRS.2018.2890023.

Gharbia, R., A. H. El Baz, A. E. Hassanien and M. F. Tolba. 2014. Remote sensing image fusion approach based on Brovey and wavelets transforms. *Proceedings of the Fifth International Conference on Innovations in Bio-Inspired Computing and Applications*, 23–25 June 2014, Ostrava, Czech Republic, pp. 311–321. https://doi.org/10.1007/978-3-319-08156-4_31.

Ghassemian, H. 2016. A review of remote sensing image fusion methods. *Information Fusion* 32:75–89. https://doi.org/10.1016/j.inffus.2016.03.003.

Ghorbanzadeh, O., T. Blaschke, K. Gholamnia, S. R. Meena, D. Tiede and J. Aryal. 2019. Evaluation of different machine learning methods and deep-learning convolutional neural networks for landslide detection. *Remote Sensing* 11:196. https://doi.org/10.3390/rs11020196.

Gómez-Chova, L., D. Tuia, G. Moser and G. Camps-Valls. 2015. Multimodal classification of remote sensing images: A review and future directions. *Proceedings of the IEEE* 103:1560–1584. https://doi.org/10.1109/JPROC.2015.2449668.

Gong, H., T. Mu, Q. Li, H. Dai, C. Li, Z. He, W. Wang, F. Han, A. Tuniyazi, H. Li, X. Lang, Z. Li and B. Wang. 2022. Swin-transformer-enabled YOLOv5 with attention mechanism for small object detection on satellite images. *Remote Sensing* 14:2861. https://doi.org/10.3390/rs14122861.

Gulácsi, A. and F. Kovács. 2015. Drought monitoring with spectral indices calculated from MODIS satellite images in Hungary. *Journal of Environmental Geography* 8:11–20. https://doi.org/10.1515/jengeo-2015-0008.

Guo, M., C. Zhou and J. Liu. 2019. Jointly learning of visual and auditory: A new approach for RS image and audio cross-modal retrieval. *IEEE Journal of Selected Topics in Applied Earth Observations and Remote Sensing* 12:4644–4654. https://doi.org/10.1109/JSTARS.2019.2949220.

Guo, Q., J. Zhang and Y. Zhang. 2021. Multitemporal hyperspectral images change detection based on joint unmixing and information coguidance strategy. *IEEE Transactions on Geoscience and Remote Sensing* 59:9633–9645. https://doi.org/10.1109/TGRS.2020.3045799.

Guo, T., H. S. Mousavi, T. H. Vu and V. Monga. 2017. Deep wavelet prediction for image super-resolution. *IEEE Conference on Computer Vision and Pattern Recognition Workshops*, 21–26 July 2017, Honolulu, Hawaii, pp. 1100–1109. https://doi.org/10.1109/CVPRW.2017.148.

Haack, B. and A. Rafter. 2010. Regression estimation techniques with remote sensing: A review and case study. *Geocarto International* 25:71–82. https://doi.org/10.1080/10106040802711679.

Hamid, M. S., N. A. Manap, R. A. Hamzah and A. F. Kadmin. 2020. Stereo matching algorithm based on deep learning: A survey. *Journal of King Saud University – Computer and Information Sciences* https://doi.org/10.1016/j.jksuci.2020.08.011.

Han, W., X. Zhang, Y. Wang, L. Wang, X. Huang, J. Li, S. Wang, W. Chen, X. Li, R. Feng, R. Fan, X. Zhang and Y. Wang. 2023. A survey of machine learning and deep learning in remote sensing of geological environment: Challenges, advances and opportunities. *ISPRS Journal of Photogrammetry and Remote Sensing* 202:87–113. https://doi.org/10.1016/j.isprsjprs.2023.05.032.

He, C., Z. Zhang, D. Xiong, J. Du and M. Liao. 2017. Spatio-temporal series remote sensing image prediction based on multi-dictionary Bayesian fusion. *ISPRS International Journal of Geo-Information* 6:374. https://doi.org/10.3390/ijgi6110374.

He, D., Y. Zhong and L. Zhang. 2020. Spectral–spatial–temporal MAP-based sub-pixel mapping for land-cover change detection. *IEEE Transactions on Geoscience and Remote Sensing* 58:1696–1717. https://doi.org/10.1109/TGRS.2019.2947708.

He, X., Y. Chen, L. Huang, D. Hong and Q. Du. 2024. Foundation model-based multimodal remote sensing data classification. *IEEE Transactions on Geoscience and Remote Sensing* 62:1–17. https://doi.org/10.1109/TGRS.2023.3344698.

Helmer, E. H. and B. Ruefenacht. 2005. Cloud-free satellite image mosaics with regression trees and histogram matching. *Photogrammetric Engineering and Remote Sensing* 71:1079–1089.

Hirschmuller, H. 2005. Accurate and efficient stereo processing by semi-global matching and mutual information. *IEEE Computer Society Conference on Computer Vision and Pattern Recognition*, 20–25 June 2005, San Diego, California, pp. 807–814. https://doi.org/10.1109/CVPR.2005.56.

Hu, D., H. Shu, H. Hu and J. Xu. 2017. Spatiotemporal regression Kriging to predict precipitation using time-series MODIS data. *Cluster Computing* 20:347–357. https://doi.org/10.1007/s10586-016-0708-0.

Huang, D., P. Yang, J. Li and C. Ma. 2017. Remote sensing image fusion using bidimensional empirical mode decomposition and the least squares theory. *Journal of Computer and Communications* 5:35–48. https://doi.org/10.4236/jcc.2017.512004.

Huang, H., Q. Cheng, Y. Pan, N. N. Lyimo, H. Peng and G. Cheng. 2022. Cloud detection in ZY-3 multi-angle remote sensing images. *Photogrammetric Engineering and Remote Sensing* 88:129–138. https://doi.org/10.14358/PERS.21-00086R2.

Huang, Z., L. Fang and S. Li. 2020. Subpixel-pixel-superpixel guided fusion for hyperspectral anomaly detection. *IEEE Transactions on Geoscience and Remote Sensing* 58:5998–6007. https://doi.org/10.1109/TGRS.2019.2961703.

Ji, S., Z. Zhang, C. Zhang, S. Wei, M. Lu and Y. Duan. 2020. Learning discriminative spatiotemporal features for precise crop classification from multi-temporal satellite images. *International Journal of Remote Sensing* 41:3162–3174. https://doi.org/10.1080/01431161.2019.1699973.

Jing, W., T. Lou, Z. Wang, W. Zou, Z. Xu, L. Mohaisen, C. Li and J. Wang. 2023. A rigorously-incremental spatiotemporal data fusion method for fusing remote sensing images. *IEEE Journal of Selected Topics in Applied Earth Observations and Remote Sensing* 16:6723–6738. https://doi.org/10.1109/JSTARS.2023.3296468.

Jinju, J., N. Santhi, K. Ramar and B. Sathya Bama. 2019. Spatial frequency discrete wavelet transform image fusion technique for remote sensing applications. *Engineering Science and Technology* 22:715–726. https://doi.org/10.1016/j.jestch.2019.01.004.

Kang, X., S. Li and J. A. Benediktsson. 2014. Feature extraction of hyperspectral images with image fusion and recursive filtering. *IEEE Transactions on Geoscience and Remote Sensing* 52:3742–3752. https://doi.org/10.1109/TGRS.2013.2275613.

Kavran, D., D. Mongus, B. Žalik and N. Lukač. 2023. Graph neural network-based method of spatiotemporal land cover mapping using satellite imagery. *Sensors* 23:6648. https://doi.org/10.3390/s23146648.

Kawulok, M., P. Benecki, S. Piechaczek, K. Hrynczenko, D. Kostrzewa and J. Nalepa. 2020. Deep learning for multiple-image super-resolution. *IEEE Geoscience and Remote Sensing Letters* 17:1062–1066. https://doi.org/10.1109/LGRS.2019.2940483.

Kong, Y., B. Yan, Y. Liu, H. Leung and X. Peng. 2021. Feature-level fusion of polarized SAR and optical images based on random forest and conditional random fields. *Remote Sensing* 13:1323. https://doi.org/10.3390/rs13071323.

Kotwal, K. and S. Chaudhuri. 2010. Visualization of hyperspectral images using bilateral filtering. *IEEE Transactions on Geoscience and Remote Sensing* 48:2308–2316. https://doi.org/10.1109/TGRS.2009.2037950.

Lacewell, C. W., M. Gebril, R. Buaba and A. Homaifar. 2010. Optimization of image fusion using genetic algorithms and discrete wavelet transform. *Proceedings of the IEEE National Aerospace Electronics Conference*, 14–16 July 2010, Dayton, Ohio, pp. 116–121. https://doi.org/10.1109/NAECON.2010.5712933.

Lanaras, C., J. Bioucas-Dias, E. Baltsavias and K. Schindler. 2017. Super-resolution of multispectral multiresolution images from a single sensor. *IEEE Conference on Computer Vision and Pattern Recognition Workshops*, 21–26 July 2017, Honolulu, Hawaii, pp. 1505–1513. https://doi.org/10.1109/CVPRW.2017.194.

Leung, Y., J. Liu and J. Zhang. 2014. An improved adaptive intensity–hue–saturation method for the fusion of remote sensing images. *IEEE Geoscience and Remote Sensing Letters* 11:985–989. https://doi.org/10.1109/LGRS.2013.2284282.

Li, H., X. Cui, M. Li, J. Deng and S. Chen. 2023. Adaptive speckle filter for multi-temporal PolSAR image with multi-dimensional information fusion. *Remote Sensing* 15:3679. https://doi.org/10.3390/rs15143679.

Li, Q., Y. Chen and Y. Zeng. 2022. Transformer with transfer CNN for remote-sensing-image object detection. *Remote Sensing* 14:984. https://doi.org/10.3390/rs14040984.

Li, W., D. Cao, Y. Peng and C. Yang. 2021. MSNet: A multi-stream fusion network for remote sensing spatiotemporal fusion based on transformer and convolution. *Remote Sensing* 13:3724. https://doi.org/10.3390/rs13183724.

Li, W., F. Meng, L. Bai, Y. Yu, I. Ullah, J. Duan and X. Zhang. 2022. The use of indices and modified U-Net network in improving the classification of planting structures. *Photogrammetric Engineering and Remote Sensing* 88:699–706. https://doi.org/10.14358/PERS.22-00032R2.

Li, X., L. Zhang, B. Du, L. Zhang and Q. Shi. 2017. Iterative reweighting heterogeneous transfer learning framework for supervised remote sensing image classification. *IEEE Journal of Selected Topics in Applied Earth Observations and Remote Sensing* 10:2022–2035. https://doi.org/10.1109/JSTARS.2016.2646138.

Li, Y., D. Kong, Y. Zhang, Y. Tan and L. Chen. 2021. Robust deep alignment network with remote sensing knowledge graph for zero-shot and generalized zero-shot remote sensing image scene classification. *ISPRS Journal of Photogrammetry and Remote Sensing* 179:145–158. https://doi.org/10.1016/j.isprsjprs.2021.08.001.

Li, Y., M. Li, Z. Liu and C. Li. 2020. Combining Kriging interpolation to improve the accuracy of forest aboveground biomass estimation using remote sensing data. *IEEE Access* 8:128124–128139. https://doi.org/10.1109/ACCESS.2020.3008686.

Liebel, L. and M. Körner. 2016. Single-Image Super Resolution for Multispectral Remote Sensing Data Using Convolutional Neural Networks. *International Archives of the Photogrammetry, Remote Sensing and Spatial Information Sciences* XLI-B3:883–890. https://doi.org/10.5194/isprs-archives-XLI-B3-883-2016.

Lillo-Saavedra, M., C. Gonzalo, A. Arquero and E. Martinez. 2005. Fusion of multispectral and panchromatic satellite sensor imagery based on tailored filtering in the Fourier domain. *International Journal of Remote Sensing* 26:1263–1268. https://doi.org/10.1080/01431160412331330239.

Lin, C.-H., P.-H. Tsai, K.-H. Lai and J.-Y. Chen. 2013. Cloud removal from multitemporal satellite images using information cloning. *IEEE Transactions on Geoscience and Remote Sensing* 51:232–241. https://doi.org/10.1109/TGRS.2012.2197682.

Lin, Y., J. He, G. Liu, B. Mou, B. Wang and R. Fu. 2023. UAS-based multi-temporal rice plant height change prediction. *Photogrammetric Engineering and Remote Sensing* 89:301–310. https://doi.org/10.14358/PERS.22-00107R2.

Lin, Z., W. Liu, Y. Wang, Y. Xu and C. Niu. 2023. Change detection in SAR images through clustering fusion algorithm and deep neural networks. *Photogrammetric Engineering and Remote Sensing* 89:373–384. https://doi.org/10.14358/PERS.22-00108R2.

Liu, J., H. Chen and S. Yang. 2021. Research on building DSM fusion method based on adaptive spline and target characteristic guidance. *Information* 12:467. https://doi.org/10.3390/info12110467.

Liu, J. and Y. Wang. 2022. Water body extraction in remote sensing imagery using domain adaptation-based network embedding selective self-attention and multi-scale feature fusion. *Remote Sensing* 14:3538. https://doi.org/10.3390/rs14153538.

Liu, P. 2015. A survey of remote-sensing big data. *Frontiers in Environmental Science* 3:45.

Liu, P., F. Huang, G. Li and Z. Liu. 2012. Remote-sensing image denoising using partial differential equations and auxiliary images as priors. *IEEE Geoscience and Remote Sensing Letters* 9:358–362. https://doi.org/10.1109/LGRS.2011.2168598.

Liu, T., S. Duan, J. Chen, L. Zhang, D. Li and X. Li. 2023. Rice identification under complex surface conditions with CNN and integrated remote sensing spectral-temporal-spatial features. *Photogrammetric Engineering and Remote Sensing* 89:741–752. https://doi.org/10.14358/PERS.23-00036R2.

Liu, X., Y. Wang and Q. Liu. 2018. Psgan: A generative adversarial network for remote sensing image pan-sharpening. *25th International Conference on Image Processing*, 7–10 October 2018, Athens, Greece, pp. 873–877. https://doi.org/10.1109/ICIP.2018.8451049.

Lo, E.Y.-M., E.-K. Lin, V. Daksiya, K.-S. Shao, Y.-R. Chuang and T.-C. Pan. 2022. Efficient building inventory extraction from satellite imagery for megacities. *Photogrammetric Engineering and Remote Sensing* 88:643–652. https://doi.org/10.14358/PERS.21-00053R2.

Lu, T., S. Li and W. Fu. 2014. Fusion based seamless mosaic for remote sensing images. *Sensing and Imaging* 15:101. https://doi.org/10.1007/s11220-014-0101-0.

Lu, Y., J. C. Trinder and K. Kubik. 2006. Automatic building detection using the Dempster–Shafer algorithm. *Photogrammetric Engineering and Remote Sensing* 72:395–403. https://doi.org/10.14358/PERS.72.4.395.

Lucas, R., A. Rowlands, A. Brown, S. Keyworth and P. Bunting. 2007. Rule-based classification of multi-temporal satellite imagery for habitat and agricultural land cover mapping. *ISPRS Journal of Photogrammetry and Remote Sensing* 62:165–185. https://doi.org/10.1016/j.isprsjprs.2007.03.003.

Luppino, L. T., F. M. Bianchi, G. Moser and S. N. Anfinsen. 2019. Unsupervised image regression for heterogeneous change detection. *IEEE Transactions on Geoscience and Remote Sensing* 57:9960–9975. https://doi.org/10.1109/TGRS.2019.2930348.

Lv, Z., T. Liu, C. Shi, J. A. Benediktsson and H. Du. 2019. Novel land cover change detection method based on K-means clustering and adaptive majority voting using bitemporal remote sensing images. *IEEE Access* 7:34425–34437. https://doi.org/10.1109/ACCESS.2019.2892648.

Ma, J., H. Shen, P. Wu, J. Wu, M. Gao and C. Meng. 2022. Generating gapless land surface temperature with a high spatio-temporal resolution by fusing multi-source satellite-observed and model-simulated data. *Remote Sensing of Environment* 278:113083. https://doi.org/10.1016/j.rse.2022.113083.

Ma, X., S. Hu, S. Liu, J. Fang and S. Xu. 2019. Remote sensing image fusion based on sparse representation and guided filtering. *Electronics* 8:303. https://doi.org/10.3390/electronics8030303.

Ma, X., Y. Yao, B. Zhang and C. He. 2022. Retrieval of high spatial resolution precipitable water vapor maps using heterogeneous earth observation data. *Remote Sensing of Environment* 278:113100. https://doi.org/10.1016/j.rse.2022.113100.

Maggiori, E., G. Charpiat, Y. Tarabalka and P. Alliez. 2017. Recurrent neural networks to correct satellite image classification maps. *IEEE Transactions on Geoscience and Remote Sensing* 55:4962–4971. https://doi.org/10.1109/TGRS.2017.2697453.

Mao, G., Y. Yuan and L. Xiaoqiang. 2018. Deep cross-modal retrieval for remote sensing image and audio. *10th IAPR Workshop on Pattern Recognition in Remote Sensing*, 19–20 August 2018, Beijing, China, pp. 1–7. https://doi.org/10.1109/PRRS.2018.8486338.

Maxwell, A. E., T. A. Warner and F. Fang. 2018. Implementation of machine-learning classification in remote sensing: An applied review. *International Journal of Remote Sensing* 39:2784–2817. https://doi.org/10.1080/01431161.2018.1433343.

Meng, F., X. Yang, C. Zhou and Z. Li. 2017. A sparse dictionary learning-based adaptive patch inpainting method for thick clouds removal from high-spatial resolution remote sensing imagery. *Sensors* 17:2130. https://doi.org/10.3390/s17092130.

Meng, X., H. Shen, H. Li, L. Zhang and R. Fu. 2019. Review of the pansharpening methods for remote sensing images based on the idea of meta-analysis: Practical discussion and challenges. *Information Fusion* 46:102–113. https://doi.org/10.1016/j.inffus.2018.05.006.

Messina, G., J. M. Peña, M. Vizzari and G. Modica. 2020. A comparison of UAV and satellites multispectral imagery in monitoring onion crop: An application in the 'Cipolla Rossa di Tropea' (Italy). *Remote Sensing* 12:3424. https://doi.org/10.3390/rs12203424.

Mezouar, O., F. Meskine and I. Boukerch. 2023. Automatic satellite images orthorectification using K-means based cascaded meta-heuristic algorithm. *Photogrammetric Engineering and Remote Sensing* 89:291–299. https://doi.org/10.14358/PERS.22-00113R2.

Mou, L., L. Bruzzone and X. X. Zhu. 2019. Learning spectral-spatial-temporal features via a recurrent convolutional neural network for change detection in multispectral imagery. *IEEE Transactions on Geoscience and Remote Sensing* 57:924–935. https://doi.org/10.1109/TGRS.2018.2863224.

Muhammad, S., M. Wachowicz and L.M.T. de Carvalho. 2002. Evaluation of wavelet transform algorithms for multi-resolution image fusion. *Proceedings of the Fifth International Conference on Information Fusion*, 8–11 July 2002, Annapolis, Maryland, pp. 1573–1580. https://doi.org/10.1109/ICIF.2002.1021004.

Nagamani, K., K. Divya, K. Sujatha, K. R. Bonagiri, G. B. Kande and P.S.S. Kumar. 2021. Adaptive histogram equalization of wavelet sub bands for the enhancement of contrast in aerial images. *Materials Today: Proceedings* 52:898–901. https://doi.org/10.1016/j.matpr.2021.10.297.

Nasrollahi, K. and T. B. Moeslund. 2014. Super-resolution: A comprehensive survey. *Machine Vision and Applications* 25:1423–1468. https://doi.org/10.1007/s00138-014-0623-4.

Nazari, A., A. Zehtabian, M. Gribaudo and H. Ghassemian. 2015. Remotely sensed image restoration using partial differential equations and watershed transformation. *Seventh International Conference on Machine Vision*, 19–21 November 2014, Milan, Italy, p. 944520. https://doi.org/10.1117/12.2181817.

Nencini, F., A. Garzelli, S. Baronti and L. Alparone. 2007. Remote sensing image fusion using the curvelet transform. *Information Fusion* 8:143–156. https://doi.org/10.1016/j.inffus.2006.02.001.

Nguyen, H.T.T., T. M. Doan, E. Tomppo and R. E. McRoberts. 2020. Land use/land cover mapping using multitemporal Sentinel-2 imagery and four classification methods—A case study from Dak Nong, Vietnam. *Remote Sensing* 12:1367. https://doi.org/10.3390/rs12091367.

Nichol, J. and M. S. Wong. 2005. Satellite remote sensing for detailed landslide inventories using change detection and image fusion. *International Journal of Remote Sensing* 26:1913–1926. https://doi.org/10.1080/01431160512331314047.

Nie, X., R. Gao, R. Wang and D. Xiang. 2021. Online multiview deep forest for remote sensing image classification via data fusion. *IEEE Geoscience and Remote Sensing Letters* 18:1456–1460. https://doi.org/10.1109/LGRS.2020.3002848.

Nielsen, A. A. 2002. Multiset canonical correlations analysis and multispectral, truly multitemporal remote sensing data. *IEEE Transactions on Image Processing* 11:293–305. https://doi.org/10.1109/83.988962.

Nielsen, A. A. 2007. The regularized iteratively reweighted MAD method for change detection in multi- and hyperspectral data. *IEEE Transactions on Image Processing* 16:463–478. https://doi.org/10.1109/TIP.2006.888195.

Ouma, Y. O., J. Tetuko and R. Tateishi. 2008. Analysis of co-occurrence and discrete wavelet transform textures for differentiation of forest and non-forest vegetation in very-high-resolution optical-sensor imagery. *International Journal of Remote Sensing* 29:3417–3456. https://doi.org/10.1080/01431160701601782.

Palsson, F., J. R. Sveinsson and M. O. Ulfarsson. 2014. A new pansharpening algorithm based on total variation. *IEEE Geoscience and Remote Sensing Letters* 11:318–322. https://doi.org/10.1109/LGRS.2013.2257669.

Pan, S. J., J. T. Kwok and Q. Yang. 2008. Transfer learning via dimensionality reduction. *Proceedings of the 23rd National Conference on Artificial Intelligence*, 13–17 July 2018, Chicago, Illinois, pp. 677–682.

Pan, S. J., I. W. Tsang, J. T. Kwok and Q. Yang. 2011. Domain adaptation via transfer component analysis. *IEEE Transactions on Neural Networks* 22:199–210. https://doi.org/10.1109/TNN.2010.2091281.

Pan, Z., Y. Hu and B. Cao. 2017. Construction of smooth daily remote sensing time series data: A higher spatiotemporal resolution perspective. *Open Geospatial Data Software and Standards* 2:25. https://doi.org/10.1186/s40965-017-0038-z.

Pandit, V. and R. J. Bhiwani. 2015. Image fusion in remote sensing applications: A review. *International Journal of Computer Applications* 120:22–32. https://doi.org/10.5120/21263-3846.

Papasaika, H., E. Kokiopoulou, E. Baltsavias and D. Kressner. 2011. Fusion of digital elevation models using sparse representations. *ISPRS Conference on Photogrammetric Image Analysis*, 5–7 October 2011, Munich, Germany, pp. 171–184.

Papathanassiou, C. and M. Petrou. 2005. Super resolution: An overview. *Proceedings of the IEEE International Geoscience and Remote Sensing Symposium*, 29 July 2005, Seoul, Korea, pp. 5655–5658. https://doi.org/10.1109/IGARSS.2005.1526059.

Pastorino, M., A. Montaldo, L. Fronda, I. Hedhli, G. Moser, S. B. Serpico and J. Zerubia. 2021. Multisensor and multiresolution remote sensing image classification through a causal hierarchical Markov framework and decision tree ensembles. *Remote Sensing* 13:849. https://doi.org/10.3390/rs13050849.

Pohl, C. and J. L. Van Genderen 1998. Multisensor image fusion in remote sensing: Concepts, methods and applications. *International Journal of Remote Sensing* 19:823–854. https://doi.org/10.1080/014311698215748.

Prakash, A. and R. P. Gupta. 1998. Land-use mapping and change detection in a coal mining area—A case study in the Jharia Coalfield, India. *International Journal of Remote Sensing* 19:391–410. https://doi.org/10.1080/014311698216053.

Qin, R. 2017. Automated 3D recovery from very high resolution multi-view satellite images. Presented at the ASPRS Conference, 12–16 March 2017, Baltimore, Maryland.

Qin, R. 2019. A critical analysis of satellite stereo pairs for digital surface model generation and a matching quality prediction model. *ISPRS Journal of Photogrammetry and Remote Sensing* 154:139–150. https://doi.org/10.1016/j.isprsjprs.2019.06.005.

Qin, R., A. Huang, W. Liu and C. Xiao. 2019. Semantic 3D reconstruction using multi-view high-resolution satellite images based on U-Net and image-guided depth fusion. *IEEE International Geoscience and Remote Sensing Symposium*, ,18 July to 2 August 2019, Yokohama, Japan, pp. 5057–5060. https://doi.org/10.1109/IGARSS.2019.8900588.

Qin, R., X. Ling, E. M. Farella and F. Remondino. 2022. Uncertainty-guided depth fusion from multi-view satellite images to improve the accuracy in large-scale DSM generation. *Remote Sensing* 14:1309. https://doi.org/10.3390/rs14061309.

Rajah, P., J. Odindi and O. Mutanga. 2018. Feature level image fusion of optical imagery and synthetic aperture radar (SAR) for invasive alien plant species detection and mapping. *Remote Sensing Applications: Society and Environment* 10:198–208. https://doi.org/10.1016/j.rsase.2018.04.007.

Rao, C. V., J. M. Rao, A. S. Kumar, D. S. Jain and V. K. Dadhwal. 2014. Satellite image fusion using fast discrete curvelet transforms. *IEEE International Advance Computing Conference*, 21–22 February 2014, Gurgaon, India, pp. 952–957. https://doi.org/10.1109/IAdCC.2014.6779451.

Reiche, J., J. Verbesselt, D. Hoekman and M. Herold. 2015. Fusing Landsat and SAR time series to detect deforestation in the tropics. *Remote Sensing of Environment* 156:276–293. https://doi.org/10.1016/j.rse.2014.10.001.

Restaino, R., M. Dalla Mura, G. Vivone and J. Chanussot. 2017. Context-adaptive pansharpening based on image segmentation. *IEEE Transactions on Geoscience and Remote Sensing* 55:753–766. https://doi.org/10.1109/TGRS.2016.2614367..

Rothermel, M., N. Haala and D. Fritsch. 2016. A median-based depthmap fusion strategy for the generation of oriented points. *ISPRS Annals of the Photogrammetry, Remote Sensing and Spatial Information Sciences* III-3:115–122. https://doi.org/10.5194/isprs-annals-III-3-115-2016.

Roy, S. K., A. Deria, D. Hong, B. Rasti, A. Plaza and J. Chanussot. 2023. Multimodal fusion transformer for remote sensing image classification. *IEEE Transactions on Geoscience and Remote Sensing* 61:1–20. https://doi.org/10.1109/TGRS.2023.3286826.

Rumpler, M., A. Wendel and H. Bischof. 2013. Probabilistic range image integration for DSM and true-orthophoto generation. In *Image Analysis: Lecture Notes in Computer Science*, edited by J.-K. Kämäräinen and M. Koskela. Berlin, Germany: Springer, pp. 533–544. https://doi.org/10.1007/978-3-642-38886-6_50.

Salvetti, F., V. Mazzia, A. Khaliq and M. Chiaberge. 2020. Multi-image super resolution of remotely sensed images using residual attention deep neural networks. *Remote Sensing* 12:2207. https://doi.org/10.3390/rs12142207.

Sarker, I. H. 2021. Deep learning: A comprehensive overview on techniques, taxonomy, applications and research directions. *SN Computer Science* 2:420. https://doi.org/10.1007/s42979-021-00815-1.

Scarpa, G., M. Gargiulo, A. Mazza and R. Gaetano. 2018. A CNN-based fusion method for feature extraction from Sentinel data. *Remote Sensing* 10:236. https://doi.org/10.3390/rs10020236.

Scheibenreif, L., J. Hanna, M. Mommert and D. Borth. 2022. Self-supervised vision transformers for land-cover segmentation and classification. *IEEE/CVF Conference on Computer Vision and Pattern Recognition Workshops*, 19–20 June 2022, New Orleans, Louisiana, pp. 1421–1430. https://doi.org/10.1109/CVPRW56347.2022.00148.

Schmitt, M. and X. X. Zhu. 2016. Data fusion and remote sensing: An ever-growing relationship. *IEEE Geoscience and Remote Sensing Magazine* 4:6–23. https://doi.org/10.1109/MGRS.2016.2561021.

Seo, D. K., Y. H. Kim, Y. D. Eo, M. H. Lee and W. Y. Park. 2018. Fusion of SAR and multispectral images using random forest regression for change detection. *ISPRS International Journal of Geo-Information* 7:401. https://doi.org/10.3390/ijgi7100401.

Shajahan, D. A., T. M. Varma and R. Muthuganapathy. 2022. Point transformer for shape classification and retrieval of urban roof point clouds. *IEEE Geoscience and Remote Sensing Letters* 19:1–5. https://doi.org/10.1109/LGRS.2021.3061422.

Shao, Z. and Cai, J. 2018. Remote sensing image fusion with deep convolutional neural network. *IEEE Journal of Selected Topics in Applied Earth Observations and Remote Sensing* 11:1656–1669. https://doi.org/10.1109/JSTARS.2018.2805923.

Shen, H., X. Meng and L. Zhang. 2016. An integrated framework for the spatio–temporal–spectral fusion of remote sensing images. *IEEE Transactions on Geoscience and Remote Sensing* 54:7135–7148. https://doi.org/10.1109/TGRS.2016.2596290.

Shen, H., M. K. Ng, P. Li and L. Zhang. 2008. Super-resolution reconstruction algorithm to MODIS remote sensing images. *Computer Journal* 52:90–100. https://doi.org/10.1093/comjnl/bxm028.

Shen, H. and L. Zhang. 2009. A MAP-based algorithm for destriping and inpainting of remotely sensed images. *IEEE Transactions on Geoscience and Remote Sensing* 47:1492–1502. https://doi.org/10.1109/TGRS.2008.2005780.

Sheykhmousa, M., M. Mahdianpari, H. Ghanbari, F. Mohammadimanesh, P. Ghamisi and S. Homayouni. 2020. Support vector machine versus random forest for remote sensing image classification: A meta-analysis and systematic review. *IEEE Journal of Selected Topics in Applied Earth Observations and Remote Sensing* 13:6308–6325. https://doi.org/10.1109/JSTARS.2020.3026724.

Shi, X., Q. Liu, W. Fan, P. S. Yu and R. Zhu. 2010. Transfer learning on heterogenous feature spaces via spectral transformation. *IEEE International Conference on Data Mining*, 13–17 December 2010, Sydney, Australia, pp. 1049–1054. https://doi.org/10.1109/ICDM.2010.65.

Shingare, P. P., P. M. Hemane and D. S. Dandekar. 2014. Fusion classification of multispectral and panchromatic image using improved decision tree algorithm. *International Conference on Signal Propagation and Computer Technology*, 12–13 July 2014, Ajmer, India, pp. 598–603. https://doi.org/10.1109/ICSPCT.2014.6884944.

Sirguey, P., R. Mathieu, Y. Arnaud, M. M. Khan and J. Chanussot. 2008. Improving MODIS Spatial Resolution for Snow Mapping Using Wavelet Fusion and ARSIS Concept. *IEEE Geoscience and Remote Sensing Letters* 5:78–82. https://doi.org/10.1109/LGRS.2007.908884.

Song, B., H. Yang, Y. Wu, P. Zhang, B. Wang and G. Han. 2024. A multispectral remote sensing crop segmentation method based on segment anything model using multistage adaptation fine-tuning. *IEEE Transactions on Geoscience and Remote Sensing* 62:1–18. https://doi.org/10.1109/TGRS.2024.3411398.

Stucker, C. and K. Schindler. 2020. ResDepth: Learned residual stereo reconstruction. *IEEE/CVF Conference on Computer Vision and Pattern Recognition Workshops*, 14–19 June 2020, Seattle, Washington, pp. 707–716. https://doi.org/10.1109/CVPRW50498.2020.00100.

Su, H., H. Jin and C. Sun. 2022. Deep pansharpening via 3D spectral super-resolution network and discrepancy-based gradient transfer. *Remote Sensing* 14:4250. https://doi.org/10.3390/rs14174250.

Su, R., L. Sun and J. Wang. 2021. Comparison of remote sensing image fusion rules based on the Laplacian pyramid transformation. *IEEE International Conference on Data Science and Computer Application*, 29–31 October 2021, Dalian, China, pp. 670–674. https://doi.org/10.1109/ICDSCA53499.2021.9650282.

Suh, J. W. and W. Ouimet. 2023. Generation of high-resolution orthomosaics from historical aerial photographs using structure-from-motion and lidar data. *Photogrammetric Engineering and Remote Sensing* 89:37–46. https://doi.org/10.14358/PERS.22-00063R2.

Syariz, M. A., B.-Y. Lin, L. G. Denaro, L. M. Jaelani, M. Van Nguyen and C.-H. Lin. 2019. Spectral-consistent relative radiometric normalization for multitemporal Landsat 8 imagery. *ISPRS Journal of Photogrammetry and Remote Sensing* 147:56–64. https://doi.org/10.1016/j.isprsjprs.2018.11.007.

Tan, Y., Y. Shi, Y. Li and B. Xu. 2022. Automatic registration method of multi-source point clouds based on building facades matching in urban scenes. *Photogrammetric Engineering and Remote Sensing* 88:767–782. https://doi.org/10.14358/PERS.22-00069R3.

Tasar, O., A. Giros, Y. Tarabalka, P. Alliez and S. Clerc. 2021. DAugNet: Unsupervised, multisource, multitarget and life-long domain adaptation for semantic segmentation of satellite images. *IEEE Transactions on Geoscience and Remote Sensing* 59:1067–1081. https://doi.org/10.1109/TGRS.2020.3006161.

Theran, C. A., M. A. Álvarez, E. Arzuaga and H. Sierra. 2019. A pixel level scaled fusion model to provide high spatial–spectral resolution for satellite images using LSTM networks. *10th Workshop on Hyperspectral Imaging and Signal Processing: Evolution in Remote Sensing (WHISPERS)*, 24–26 September 2019, Amsterdam, Netherlands, pp. 1–5. https://doi.org/10.1109/WHISPERS.2019.8921269.

Theron, K. J., J. S. Pryke, N. Latte and M. J. Samways. 2022. Mapping an alien invasive shrub within conservation corridors using super-resolution satellite imagery. *Journal of Environmental Management* 321:116023. https://doi.org/10.1016/j.jenvman.2022.116023.

Touati, R., M. Mignotte and M. Dahmane. 2020. Multimodal change detection in remote sensing images using an unsupervised pixel pairwise-based Markov random field model. *IEEE Transactions on Image Processing* 29:757–767. https://doi.org/10.1109/TIP.2019.2933747.

Viana, C. M., I. Girão and J. Rocha. 2019. Long-term satellite image time-series for land use/land cover change detection using refined open source data in a rural region. *Remote Sensing* 11:1104. https://doi.org/10.3390/rs11091104.

Vivekananda, G., R. Swathi and A. Sujith. 2021. Multi-temporal image analysis for LULC classification and change detection. *European Journal of Remote Sensing* 54:189–199. https://doi.org/10.1080/22797254.2020.1771215.

Vivone, G. 2019. Robust band-dependent spatial-detail approaches for panchromatic sharpening. *IEEE Transactions on Geoscience and Remote Sensing* 57:6421–6433. https://doi.org/10.1109/TGRS.2019.2906073.

Vivone, G., R. Restaino and J. Chanussot. 2018. Full scale regression-based injection coefficients for panchromatic sharpening. *IEEE Transactions on Image Processing* 27:3418–3431. https://doi.org/10.1109/TIP.2018.2819501.

Voutilainen, A., T. Pyhälahti, K. Y. Kallio, J. Pulliainen, H. Haario and J. P. Kaipio. 2007. A filtering approach for estimating lake water quality from remote sensing data. *International Journal of Applied Earth Observation and Geoinformation* 9:50–64. https://doi.org/10.1016/j.jag.2006.07.001.

Wan, X., J. G. Liu, S. Li and H. Yan. 2019. Phase correlation decomposition: The impact of illumination variation for robust subpixel remotely sensed image matching. *IEEE Transactions on Geoscience and Remote Sensing* 57:6710–6725. https://doi.org/10.1109/TGRS.2019.2907933.

Wang, J., X. Cai, X. Chen, Z. Zhang and L. Tang. 2019. Classification of forest vegetation type using fused NDVI time series data based on STNLFFM. *IEEE International Geoscience and Remote Sensing Symposium*, 28 July to 2 August 2019, Yokohama, Japan, pp. 6047–6050. https://doi.org/10.1109/IGARSS.2019.8897907.

Wang, X., Z. Shao, X. Huang and D. Li. 2022. Spatiotemporal temperature fusion based on a deep convolutional network. *Photogrammetric Engineering and Remote Sensing* 88:93–101. https://doi.org/10.14358/PERS.21-00023R2.

Wang, Z., Y. Ma and Y. Zhang. 2023. Review of pixel-level remote sensing image fusion based on deep learning. *Information Fusion* 90:36–58. https://doi.org/10.1016/j.inffus.2022.09.008.

Wei, Y., Q. Yuan, H. Shen and L. Zhang. 2017. Boosting the accuracy of multispectral image pansharpening by learning a deep residual network. *IEEE Geoscience and Remote Sensing Letters* 14:1795–1799. https://doi.org/10.1109/LGRS.2017.2736020.

Witharana, C., D. L. Civco and T. H. Meyer. 2013. Evaluation of pansharpening algorithms in support of earth observation based rapid-mapping workflows. *Applied Geography* 37:63–87. https://doi.org/10.1016/j.apgeog.2012.10.008.

Wu, C., L. Zhang and L. Zhang. 2016. A scene change detection framework for multi-temporal very high resolution remote sensing images. *Signal Processing* 124:184–197. https://doi.org/10.1016/j.sigpro.2015.09.020.

Wu, J., H. Huang, Y. Qiu, H. Wu, J. Tian and J. Liu. 2005. Remote sensing image fusion based on average gradient of wavelet transform. *IEEE International Conference Mechatronics and Automation*, 29 July to 1 August 2005, Niagara Falls, Canada, pp. 1817–1821, Vol. 4. https://doi.org/10.1109/ICMA.2005.1626836.

Wu, W., L. Ge, J. Luo, R. Huan and Y. Yang. 2018. A spectral–temporal patch-based missing area reconstruction for time-series images. *Remote Sensing* 10:1560. https://doi.org/10.3390/rs10101560.

Wu, W., X. Sun, X. Wang, J. Fan, J. Luo, Y. Shen and Y. Yang. 2018. A long time-series radiometric normalization method for Landsat images. *Sensors* 18:4505. https://doi.org/10.3390/s18124505.

Wu, X., W. Li, D. Hong, J. Tian, R. Tao and Q. Du. 2020. Vehicle detection of multi-source remote sensing data using active fine-tuning network. *ISPRS Journal of Photogrammetry and Remote Sensing* 167:39–53. https://doi.org/10.1016/j.isprsjprs.2020.06.016.

Xie, Q., G. Yao and P. Liu. 2017. Super-resolution reconstruction of satellite video images based on interpolation method. *Procedia Computer Science* 107:454–459. https://doi.org/10.1016/j.procs.2017.03.089.

Xue, J., Y. Leung and T. Fung. 2017. A Bayesian data fusion approach to spatio-temporal fusion of remotely sensed images. *Remote Sensing* 9:1310. https://doi.org/10.3390/rs9121310.

Yang, B., M. Kim and M. Madden 2012. Assessing optimal image fusion methods for very high spatial resolution satellite images to support coastal monitoring. *GIScience and Remote Sensing* 49:687–710. https://doi.org/10.2747/1548-1603.49.5.687.

Yang, G., K. Zhang, F. Zhang, J. Wang and J. Sun. 2023. Cross-resolution semi-supervised adversarial learning for pansharpening. *IEEE Transactions on Geoscience and Remote Sensing* 61:1–17. https://doi.org/10.1109/TGRS.2023.3271658.

Yang, K., Y. Luo, M. Li, S. Zhong, Q. Liu and X. Li. 2022. Reconstruction of Sentinel-2 image time series using Google Earth engine. *Remote Sensing* 14:4395. https://doi.org/10.3390/rs14174395.

Yang, Z., C. Diao and B. Li. 2021. A robust hybrid deep learning model for spatiotemporal image fusion. *Remote Sensing* 13:5005. https://doi.org/10.3390/rs13245005.

Yanovsky, I. and J. Qin. 2021. Spatio-temporal super-resolution reconstruction of remote sensing data. *IEEE International Geoscience and Remote Sensing Symposium*, 11–16 July 2021, Brussles, Belgium, pp. 2907–2910. https://doi.org/10.1109/IGARSS47720.2021.9553433.

Yao, W., Z. Zeng, C. Lian and H. Tang. 2018. Pixel-wise regression using U-Net and its application on pansharpening. *Neurocomputing* 312:364–371. https://doi.org/10.1016/j.neucom.2018.05.103.

Yin, Z., L. Zou, J. Sun, H. Zhang, W. Zhang and X. Shen. 2021. A nonlinear radiometric normalization model for satellite images time series based on artificial neural networks and greedy algorithm. *Remote Sensing* 13:933. https://doi.org/10.3390/rs13050933.

Yıldırım, D. and O. Güngör 2012. A novel image fusion method using IKONOS satellite images. *Journal of Geodesy and Geoinformation* 1:27–34. https://doi.org/10.9733/jgg.170512.1.

Youssef, R., M. Aniss and C. Jamal. 2020. Machine learning and deep learning in remote sensing and urban application: A systematic review and meta-analysis. *Proceedings of the 4th Edition of International Conference on Geo-IT and Water Resources*, 11–12 March 2020, Al-Hoceima, Morocco, pp. 1–5. https://doi.org/10.1145/3399205.3399224.

Yu, C., L. Chen, L. Su, M. Fan and S. Li. 2011. Kriging interpolation method and its application in retrieval of MODIS aerosol optical depth. *19th International Conference on Geoinformatics*, 24–26 June 2011, Shanghai, China, pp. 1–6. https://doi.org/10.1109/GeoInformatics.2011.5981052.

Yu, H., Z. Lin, G. L. Chai, C. H. Yan and N. Raman. 2008. A DCT-based change detection method for multi-temporal SAR images. *IEEE International Geoscience and Remote Sensing Symposium*, 7–11 July 2008, Boston, Massachusetts, p. III-166–III-169. https://doi.org/10.1109/IGARSS.2008.4779309.

Yuan, D. and C. D. Elvidge. 1996. Comparison of relative radiometric normalization techniques. *ISPRS Journal of Photogrammetry and Remote Sensing* 51:117–126. https://doi.org/10.1016/0924-2716(96)00018-4.

Yuan, F., K. E. Sawaya, B. C. Loeffelholz and M. E. Bauer. 2005. Land cover classification and change analysis of the Twin Cities (Minnesota) metropolitan area by multitemporal Landsat remote sensing. *Remote Sensing of Environment* 98:317–328. https://doi.org/10.1016/j.rse.2005.08.006.

Zeng, C., H. Shen and L. Zhang. 2013. Recovering missing pixels for Landsat ETM+ SLC-Off imagery using multi-temporal regression analysis and a regularization method. *Remote Sensing of Environment* 131:182–194. https://doi.org/10.1016/j.rse.2012.12.012.

Zeng, L., Y. Du, H. Lin, J. Wang, J. Yin and J. Yang. 2021. A novel region-based image registration method for multisource remote sensing images via CNN. *IEEE Journal of Selected Topics in Applied Earth Observations and Remote Sensing* 14:1821–1831. https://doi.org/10.1109/JSTARS.2020.3047656.

Zeng, Q., H. Li, T. Zhang, J. He, F. Zhang, H. Wang, Z. Qing, Q. Yu and B. Shen. 2022. Prediction of radar echo space-time sequence based on improving TrajGRU deep-learning model. *Remote Sensing* 14:5042. https://doi.org/10.3390/rs14195042.

Zeng, Q., H. Qin, X. Yan and T. Yang. 2020. Fourier domain anomaly detection and spectral fusion for stripe noise removal of TIR imagery. *Remote Sensing* 12:3714. https://doi.org/10.3390/rs12223714.

Zerrouki, N., A. Dairi, F. Harrou, Y. Zerrouki and Y. Sun. 2022. Efficient land desertification detection using a deep learning-driven generative adversarial network approach: A case study. *Concurrency and Computation: Practice and Experience* 34:e6604. https://doi.org/10.1002/cpe.6604.

Zhang, F., K. Zhang, J. Sun, J. Wang and L. Bruzzone. 2023. DRFormer: Learning disentangled representation for pan-sharpening via mutual information-based transformer. *IEEE Transactions on Geoscience and Remote Sensing*. https://doi.org/10.1109/TGRS.2023.3339650.

Zhang, H., Y. Song, C. Han and L. Zhang. 2021. Remote sensing image spatiotemporal fusion using a generative adversarial network. *IEEE Transactions on Geoscience and Remote Sensing* 59:4273–4286. https://doi.org/10.1109/TGRS.2020.3010530.

Zhang, J. 2010. Multi-source remote sensing data fusion: Status and trends. *International Journal of Image and Data Fusion* 1:5–24. https://doi.org/10.1080/19479830903561035.

Zhang, J., M. K. Clayton and P. A. Townsend. 2015. Missing data and regression models for spatial images. *IEEE Transactions on Geoscience and Remote Sensing* 53:1574–1582. https://doi.org/10.1109/TGRS.2014.2345513.

Zhang, J., H. Sun, D. Gao, L. Qiao, N. Liu, M. Li and Y. Zhang. 2020. Detection of canopy chlorophyll content of corn based on continuous wavelet transform analysis. *Remote Sensing* 12:2741. https://doi.org/10.3390/rs12172741.

Zhang, K., G. Yang, F. Zhang, W. Wan, M. Zhou, J. Sun and H. Zhang. 2023. Learning deep multiscale local dissimilarity prior for pansharpening. *IEEE Transactions on Geoscience and Remote Sensing* 61:1–15. https://doi.org/10.1109/TGRS.2023.3303336.

Zhang, K., F. Zhang, W. Wan, H. Yu, J. Sun, J. Del Ser, E. Elyan and A. Hussain. 2023. Panchromatic and multispectral image fusion for remote sensing and earth observation: Concepts, taxonomy, literature review, evaluation methodologies and challenges ahead. *Information Fusion* 93:227–242. https://doi.org/10.1016/j.inffus.2022.12.026.

Zhang, X., P. Xiao, X. Feng and M. Yuan. 2017. Separate segmentation of multi-temporal high-resolution remote sensing images for object-based change detection in urban area. *Remote Sensing of Environment* 201:243–255. https://doi.org/10.1016/j.rse.2017.09.022.

Zhang, Y., S. De Backer and P. Scheunders. 2009. Noise-resistant wavelet-based Bayesian fusion of multispectral and hyperspectral images. *IEEE Transactions on Geoscience and Remote Sensing* 47:3834–3843. https://doi.org/10.1109/TGRS.2009.2017737.

Zhang, Z., C. Wang, J. Song and Y. Xu. 2022. Object tracking based on satellite videos: A literature review. *Remote Sensing* 14:3674. https://doi.org/10.3390/rs14153674.

Zheng, S., W. Shi, J. Liu and J. Tian. 2008. Remote sensing image fusion using multiscale mapped LS-SVM. *IEEE Transactions on Geoscience and Remote Sensing* 46:1313–1322. https://doi.org/10.1109/TGRS.2007.912737.

Zhong, J., B. Yang, G. Huang, F. Zhong and Z. Chen. 2016. Remote sensing image fusion with convolutional neural network. *Sensing and Imaging* 17:10. https://doi.org/10.1007/s11220-016-0135-6.

Zhou, C., G. Zhang, Z. Yang and J. Zhou. 2022. A novel image registration algorithm using wavelet transform and matrix-multiply discrete Fourier transform. *IEEE Geoscience and Remote Sensing Letters* 19:1–5. https://doi.org/10.1109/LGRS.2020.3031335.

Zhou, K., X. Meng and B. Cheng. 2020. Review of stereo matching algorithms based on deep learning. *Computer Intelligence and Neuroscience* 2020:e8562323. https://doi.org/10.1155/2020/8562323.

Zhou, T., H. He, Y. Wang and Y. Liao. 2023. Improved gated recurrent units together with fusion for semantic segmentation of remote sensing images based on parallel hybrid network. Under review. https://doi.org/10.21203/rs.3.rs-3400980/v1.

Zhou, W., A. Troy and M. Grove. 2008. Object-based land cover classification and change analysis in the Baltimore metropolitan area using multitemporal high resolution remote sensing data. *Sensors* 8:1613–1636. https://doi.org/10.3390/s8031613.

Zhu, H., W. Song, H. Tan, J. Wang and D. Jia. 2016. Super resolution reconstruction based on adaptive detail enhancement for Zy-3 satellite images. *ISPRS Annals of the Photogrammetry, Remote Sensing and Spatial Information Sciences* III-7:213–217. https://doi.org/10.5194/isprsannals-III-7-213-2016.

Zhu, H., X. Tang, J. Xie, W. Song, F. Mo and X. Gao. 2018. Spatio-temporal super-resolution reconstruction of remote-sensing images based on adaptive multi-scale detail enhancement. *Sensors* 18:498. https://doi.org/10.3390/s18020498.

Zhu, T., J. Shen and F. Sun. 2022. Long short-term memory-based simulation study of river happiness evaluation—A case study of Jiangsu section of Huaihe River Basin in China. Heliyon 8:e10550. https://doi.org/10.1016/j.heliyon.2022.e10550.

Zhu, X., F. Cai, J. Tian and T.K.-A. Williams. 2018. Spatiotemporal fusion of multisource remote sensing data: Literature survey, taxonomy, principles, applications and future directions. *Remote Sensing* 10:527. https://doi.org/10.3390/rs10040527.

Zhuang, H., K. Deng, Y. Yu and H. Fan. 2017. An approach based on discrete wavelet transform to unsupervised change detection in multispectral images. *International Journal of Remote Sensing* 38:4914–4930. https://doi.org/10.1080/01431161.2017.1331475.

SUSTAINING MEMBERS

Applanix
Richmond Hill, Ontario, Canada
http://www.applanix.com
Member Since: 7/1997

Ayres Associates
Madison, Wisconsin
www.AyresAssociates.com
Member Since: 1/1953

Dewberry
Fairfax, Virginia
www.dewberry.com
Member Since: 1/1985

Digital Mapping, Inc.(DMI)
Huntington Beach, California
www.admap.com
Member Since: 4/2002

Environmental Research Incorporated
Linden, Virginia
www.eri.us.com
Member Since: 8/2008

GeoCue Group
Madison, Alabama
http://www.geocue.com
Member Since: 10/2003

GeoDyn GmbH
Munich, Germany
www.geodyn.com/index
Member Since: 3/2024

Geographic Imperatives LLC
Centennial, Colorado
Member Since: 12/2020

GPD Group
Columubs, Ohio
https://gpdgroup.com/
Member Since: 7/2024

GPI Geospatial Inc.
Orlando, Florida
www.aca-net.com
Member Since: 1/1994

Halff Associates, Inc.
Richardson, Texas
https://halff.com/
Member Since: 8/2020

Keystone Aerial Surveys, Inc.
Philadelphia, Pennsylvania
http://www.kasurveys.com
Member Since: 1/1985

Kucera International
Willoughby, Ohio
www.kucerainternational.com
Member Since: 1/1992

L3Harris Technologies
Broomfield, Colorado
www.l3harris.com
Member Since: 6/2008

Leica Geosystems AG
Heerbrugg, Switzerland
https://leica-geosystems.com/en-us/
Member Since: 1/1990

Merrick & Company
Greenwood Village, Colorado
www.merrick.com
Member Since: 4/1995

Miller Creek Associates
SeaTac Washington
www.mcamaps.com
Member Since: 12/2014

NV5 Geospatial
Sheboygan Falls, Wisconsin
www.quantumspatial.com
Member Since: 1/1974

Pickett and Associates, Inc.
Bartow, Florida
www.pickettusa.com
Member Since: 4/2007

PixElement
Belmont, Michigan
https://pixelement.com
Member Since: 2/2017

Riegl USA, Inc.
Orlando, Florida
https://www.rieglusa.com
Member Since: 11/2004

Sanborn Map Company
Colorado Springs, Colorado
www.sanborn.com
Member Since: 10/1984

Surdex Corporation
(a Bowman company)
Chesterfield, Missouri
www.surdex.com
Member Since: 12/2011

Surveying And Mapping, LLC (SAM)
Austin, Texas
www.sam.biz
Member Since: 12/2005

T3 Global Strategies, Inc.
Bridgeville, Pennsylvania
https://t3gs.com/
Member Since: 6/2020

Towill, Inc.
San Francisco, California
www.towill.com
Member Since: 1/1952

U.S. Dept. of Commerce/NOAA/NOS/ National Geodetic Survey
Chesapeake, Virginia
https://www.ngs.noaa.gov/
Member Since: 7/2009

U.S. Geological Survey
Reston, Virginia
https://www.usgs.gov/
Member Since: 4/2002

Woolpert LLP
Dayton, Ohio
www.woolpert.com
Member Since: 1/1985

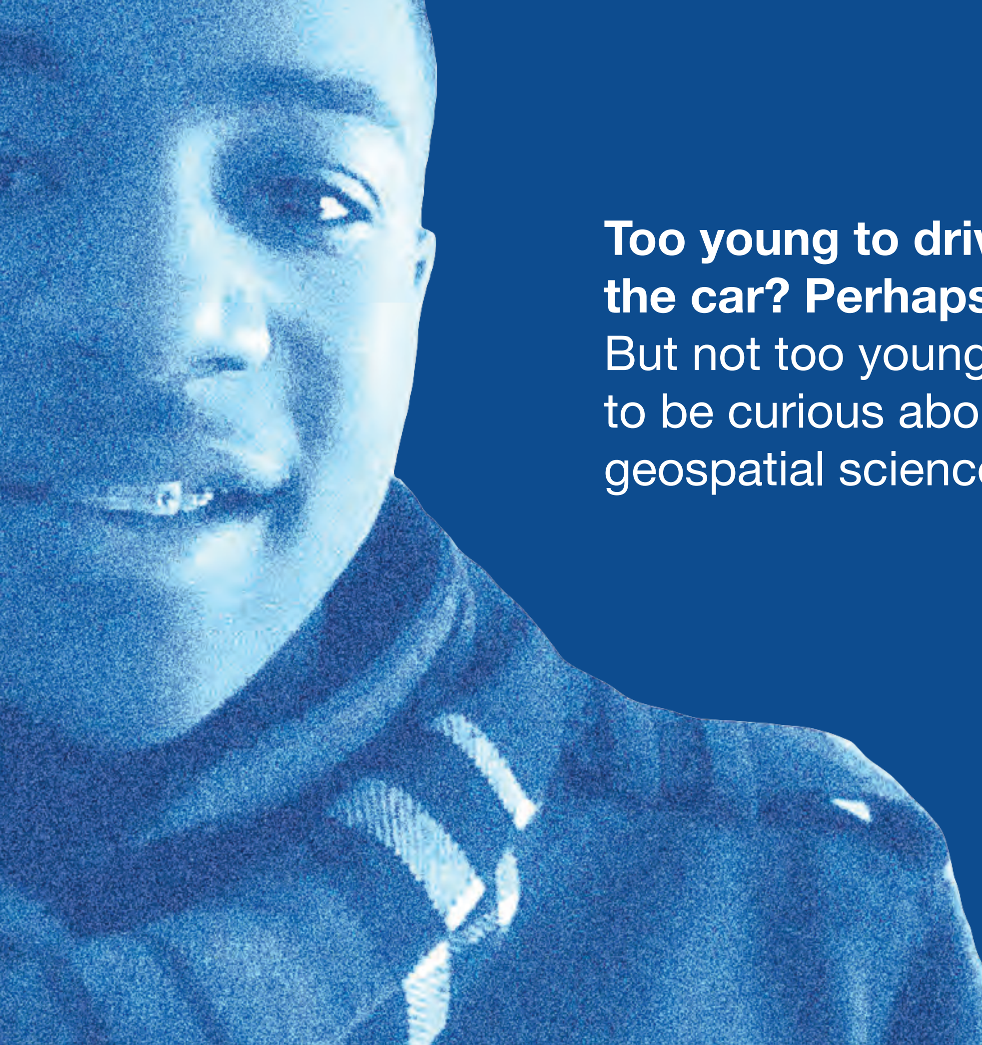

asprs
FOUNDATION